POLITECNICO DI TORINO

Dipartimento di Ingegneria Meccanica e Aerospaziale

Master of science degree in
Automotive Engineering

Master Thesis

Studies on brake blending and developing of braking control strategies to maximize performances and energy efficiency for a Formula SAE electric vehicle

Supervisor/s
Prof. Andrea Tonoli

Candidate
Mario Migliorucci

Academic Year 2020-2021

Alla mia famiglia

Abstract

The present thesis comes from the interest on electric vehicles that was born from my experience in Formula Student team of Politecnico di Torino for seasons 2018/2020. Electric vehicles are becoming more and more widespread as car companies are investing on them. Part of the investment comes from the need to redesign some important systems of the ICE vehicles. The braking system is one of them since the braking ability of the vehicle is now shared between the friction and electric systems. This work has the aim to search the best way to implement regenerative braking in coexistence, also called blending, with friction braking and get a better understanding regarding to what extent a regenerative brake system can recover energy and how it will affect vehicle stability and manoeuvrability along with changes for the typical brake systems.

To do so, the thesis first focuses on ideal brake studies to understand the principles of brake system design and the duality between ideal performance and real system performance. The effects of unbalanced braking and braking out of ideal conditions is so studied by also the presentation on typical systems used to increase brake efficiency along with more modern systems like ABS and EBD. These studies are important to understand the effect of regenerative and the need for increasing efficiency that require the forces to be away from ideal line, a requirement that is opposite to brake balance and shortest brake distance. Regenerative braking is presented by the analysis on its characteristics and limitations coming from the other, eventual, elements inside electric powertrains. The way the regenerative braking and friction braking can coexist are presented by first division upon legislation definitions and then addressed by presenting two different layouts, based on the level of technology present in vehicles and the respective logics to blend the braking effects are explained. Results are finally collected based on the analysis on typical brake power and energy used in WLTP and NEDC test procedures that are standard used for automotive in Europe. These studies let understand the eventual impact and performance windows required in braking and the pros and cons of each hybrid braking system. Finally, the same approach is presented on the formula SAE vehicle of Squadra Corse PoliTO that, being a formula vehicle, presents new design constraints and needs that are mostly focused on performance but on the other side, present higher forces and accelerations that could lead to higher regenerative efficiency. The regenerative impact is studied based on typical Formula Student events data, and the target values are developed along with a deep study on the eventual use of regenerative strategy on accelerator pedal, following what is typically called “Single pedal control”.

Acknowledgments

I would like to express my gratitude to Professor Andrea Tonoli, for his valuable advice and feedbacks during the development of this thesis work and, as faculty advisor for Squadra Corse PoliTO, for allowing me to participate to a great project, really important to improve my engineering skills.

Then, I would like to thank my colleagues of Squadra Corse PoliTO for the support during these months and for the great times we shared together and most importantly I would like to thank Alberto and Lorenzo with which I grew professionally, with continuous exchange of ideas, and personally, with the time spent with them.

Last but not least important, I would like to express my deepest gratitude to my parents Antonio and Antonella, my brothers Francesco and Pompeo and the rest of my family for their great support during the years, away from home.

Table of contents

List of figures

List of tables

Thesis outline

The aim of this thesis is to study the coexistence of traditional, friction braking, and electric brake forces applied by the electric powertrains that will represent the future of urban mobility. This study comes from the need to understand the impact of the new technology on vehicle topology and to outline the principles to maintain braking performances and safety but also to introduce the need for more efficient powertrains to lower CO_2 emissions. The input and interest on this subject comes from my experience in Squadra Corse PoliTO for the season 2018/19 and 2019/2020 where, thanks to the resources made us available by Politecnico di Torino and FCA, our squad was able to design and realize a fully electric vehicle prototype. The vehicle of season 2018/2019 will be the reference in the later part of this work since Covid-19 pandemic didn't let us finish the vehicle for season 2019/20. Working with electric vehicle presents new challenges but also opens to new way to see vehicles.

The thesis work is covering the subject in four steps: Chapter 1 is dedicated to the theory review of ideal braking and braking systems characteristics along with what will imply to brake away from ideal line. This is needed to understand what the introduction of regenerative braking is doing to braking. Chapter 2 introduces the new challenges related to electric braking and what are the main differences with respect to friction braking. Moreover, it will introduce a way to analyse the braking power and energy needed during a drive cycle and which cycle is best to use for such analysis. Finally, the systems that allow electric braking and friction braking cooperation will be explained. Chapter 3 is focused on the explanation of the simulator used in this work and the explanation of the choices used to model the vehicle subsystems like battery pack and electric motors and the logics for brake blending. In Chapter 4, it will be exposed the differences in performances between the already introduced in Chapter 2 parallel and series systems.

Chapter 5 is focused on conducting the already used studies on the vehicle of Squadra Corse for the season 2018/2019, SC19. In this last chapter the focus will be on seek performances in conditions that are totally different from urban driving, presented in first chapters.

1 Braking theory

Driving a vehicle, involves, among other things, braking. Fortunately, when we apply brakes in our vehicles, most of the times, we brake very softly, far from the braking performance limit. Most drivers, perhaps, never need to experience the limit braking performance of their car in everyday traffic. However, engineers must know very well the mechanics of braking a vehicle, to allow it to stop as soon as possible in case of emergency or, by means of the introduction of electric powertrains inside our everyday vehicles, how to manage the interaction between the two worlds that have different and sometimes opposite requirements as will be highlighted in the following work.

After all, braking performance and balance remain very important topics in a vehicle and in the future of mobility.

Whereas braking performance is easily understood since can be explained by "stopping the vehicle in the shortest distance", brake balance means how much to brake front wheels with respect to rear wheels and involves considerations about tire-ground grip, weight distribution and brake line construction.

1.1 Vehicle models for braking manoeuvres

When a complex and nonlinear system like a vehicle must be studied during a dynamic manoeuvre, it is used a simpler model to get data and understanding of the phenomena going on. Just an example at system level: when braking, a load shift will take place from the rear to the front axle that will imply sprung mass movements along with suspension movements and change of wheel angle with respect to the ground, affecting so the grip. On the other side also ground conditions will change in non-ideal word. All this and much more is taking place all at once, dynamically changing instant by instant and representing a challenging system to be modelled and studied in its completeness. A very complicated, high-number degrees of freedom model, will certainly give values much closer to reality and giving important data that can be used for the design at component level but, at cost o slightly errors on the magnitude of the phenomena, it is possible to use simpler models for much clearer understanding.

By following what treated in [1], the starting case for braking analysis is a rigid, two axles vehicle in a pure braking condition where it is possible to assume that no lateral forces, no yaw moment, and no lateral load transfers is happening. By assumption for the mass to be symmetrical with respect to *xz* plane, also all loads will be equally symmetrical and wheels on the same axle equally loaded.

Being the suspensions and the compliance of tires neglected the motion is descried by a single equation of a point mass in longitudinal direction:

$$m\ddot{x} = \sum_{\forall i} F_{xi} \tag{1.1}$$

This model is quite coarse because, when accelerating, several rotating masses must be accelerated as well or that the vehicle will never travel under symmetrical conditions, particularly when it will follow non straight lines and so it is not accurate to describe braking-in-turn manoeuvres, but it is enough to get understanding of basic principles governing braking.

1.2 Ideal braking

From the model used and represented in Figure 1.1, it is possible to write the equilibrium equations of forces and moments. This procedure will be treated by writing down the most significant equations and not explaining in detail where they come from since are extensively explained in every book of vehicle dynamics like [1].

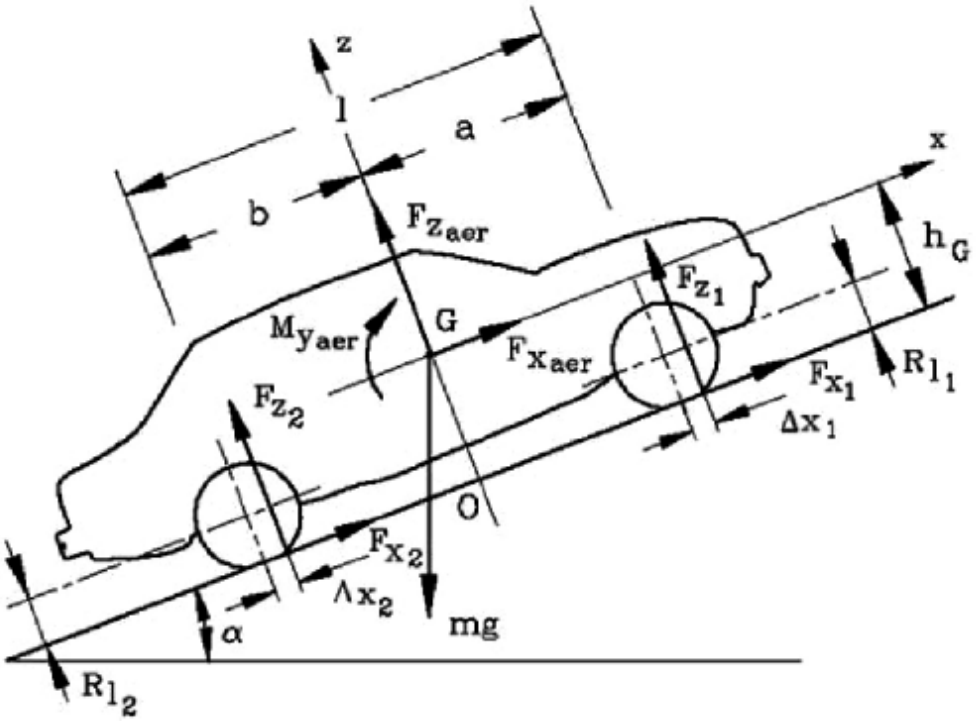

Figure 1.1 Forces acting on a vehicle on inclined road

From vertical force equilibrium:

$$F_{z1} = mg\frac{(b-\Delta x_2)\cos\alpha - h_g\sin\alpha - K_1V^2 - \dot{V}\frac{h_g}{g}}{l+\Delta x_1-\Delta x_2} \tag{1.2}$$

$$F_{z2} = mg\frac{(a+\Delta x_1)\cos\alpha + h_g\sin\alpha - K_2V^2 + \dot{V}\frac{h_g}{g}}{l+\Delta x_1-\Delta x_2} \tag{1.3}$$

In equations (1.2) and (1.3), Δx values are representing the centre of contact patch of the tire on the ground that in case of non-rolling tire is different from its centre. Moreover, the ground inclinations α is firstly considered but will later be eliminated to simplify the analysis. The term K_iV^2 is the aerodynamic effect in vertical direction on the i^{th} axle. To simplify the calculations the aerodynamic drag and lift will be neglected in the following because they will only modify the curves to an extent that for most of everyday urban vehicle is negligible.

$$\frac{dV}{dt} = \frac{\sum_{\forall i}\mu_x F_{zi} - \frac{1}{2}\rho V^2 S C_x - f\sum_{\forall i}F_{zi} - mg\sin\alpha}{m} \tag{1.4}$$

The equation concerning the total amount of forces acting in longitudinal direction is the (1.4). In this equation we consider negligible the aerodynamic drag effect and rolling resistance term $f\sum_{\forall i}F_{zi}$ because rolling resistance is much smaller than braking forces (Moreover, citing what written in [1], "rolling resistance can be considered more as causing a braking moment on the wheel than a braking force directly on the ground").

Therefore, with all hypotheses stated before, we remain with the formulas (1.5), (1.6) and (1.7):

- For the maximum deceleration possible, due to grip limits

$$\frac{dV}{dt} = g\mu_x \tag{1.5}$$

- For vertical forces on the axle:

$$F_{z1} = \frac{m}{l}\left[gb - h_g\frac{dV}{dt}\right] \tag{1.6}$$

$$F_{z2} = \frac{m}{l}\left[ga + h_g\frac{dV}{dt}\right] \tag{1.7}$$

By manipulating the previous formulas also by using the relations between longitudinal and vertical forces $F_x = \mu_x F_Z$, relation (1.8) will result:

$$(F_{x1} + F_{x2})^2 + mg\left(F_{x1}\frac{a}{h_g} - F_{x2}\frac{b}{h_g}\right) = 0 \tag{1.8}$$

Equation 1.8 is representing the locus of all values of $F_{x1}$and $F_{x2}$for which ideal braking is obtained.

With only geometrical values and the mass of the vehicle, by means of (1.8) is possible to represent the parabola in Figure 1.2:

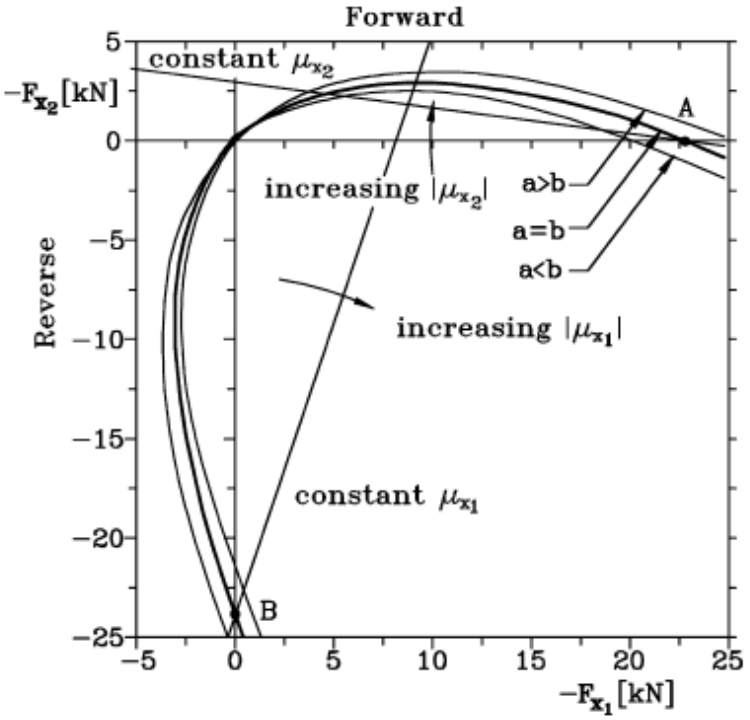

Figure 1.2 Locus of all forces in ideal braking

In our case, since we chose a model with longitudinal direction being positive from rear to front, we are only interested in forward braking and negative values of $F_{x1}$and F_{x2}, being the first quadrant with negative forces on *x* and *y* axis.

1.3 Actual braking

The relationship between the braking moments at the rear and front wheels is in practice different from those stated to comply with the conditions for ideal braking and is imposed by the parameters of the braking system of the vehicle. A braking system can develop a certain torque on front and rear axle that depends on the mechanical elements used and is possible to use a parameter to define the relationship between them (1.9).

$$K_b = \frac{M_{b1}}{M_{b2}} \tag{1.9}$$

By assuming that both front and rear axles have same radius in loaded conditions (which in its turn is a more difficult condition since it is depending on a lot of parameters; from tire pressure to tire load itself), equation (1.9) will also become a ratio between front and rear forces on the axle.

So, K_b is depending on the actual layout of the brake system, whether it is using drum or disk brakes, or the presence and behaviour of valves used in the pressure line. In practical terms, and for what concerns our analysis is enough to understand that this coefficient will define the coefficient of a line passing from 0 on the ideal braking plot and whose interception is defining the condition for which the actual system will perform ideally. In this point, here called A, the definition of $K_b$is (1.10). This equation is coming from the substitution in (1.9) of (1.6) and (1.7) where $\frac{dV}{dt} = -\mu_x^* \, g$.

$$K_b = \frac{b + h_g|\mu_x^*|}{a - h_g|\mu_x^*|} \tag{1.10}$$

In the following analysis will be used the parameters listed in the Table 1.1 below, representing a generic urban vehicle:

Table 1.1 Vehicle characteristics

	Unit	Values
Vehicle mass	kg	1500 (Laden) 1250 (Unladen)
Aerodynamic drag coefficient		0.3
Frontal area	m^2	2.2
Wheelbase	m	2.7
Distance from gravity centre to front wheel centre	m	1.25
Gravity centre height	m	0.6

Fully loaded and unladen vehicle's, ideal, braking line (red and blue lines in Figure 1.3) should be defined in the first steps, representing the two limit conditions for the braking system. The brake system characteristic of the vehicle is also represented (black in Figure 1.3) where the K_b value is the one which will brake in ideal conditions for accelerations of 0.9g, defined by the point A for the laden condition in Figure 1.3 (why such a value is considered will be explained in Chapter 2). For the unladen condition the optimum value, B in Figure 1.3, is different and allowing a minimum deceleration of 0.7g(considering that the acceleration lines are shown only for the mass of a laden vehicle in Figure 1.3) without going over the line.
Moreover, if a braking line efficiency is defined as the ratio between the actual performances of the brake line with respect to the ideal performances dictated by mass shift during braking (1.11), point A

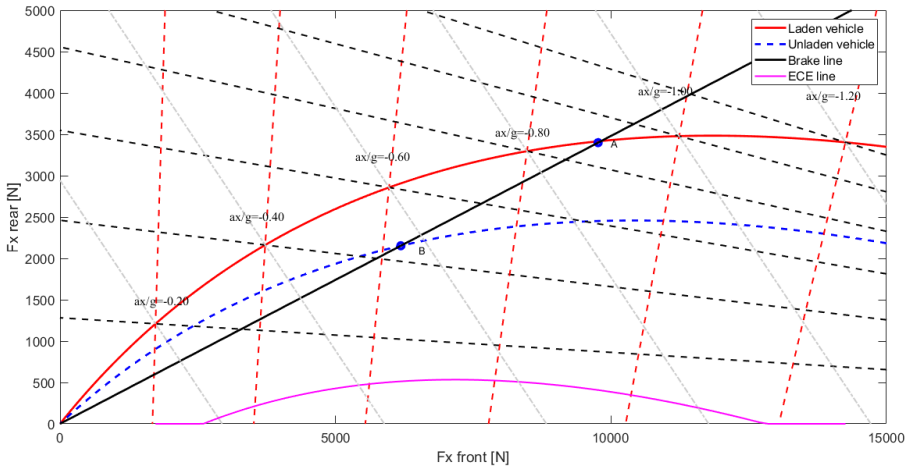

Figure 1.3 Ideal, brake system and ECE line representation

represents the most efficient spot for the braking system where is possible to obtain the ideal deceleration with those forces. Every point before and after it will have a lower deceleration than the ideal one, like represented in Figure 1.4.

$$\mu_b = \frac{(dV/dt)_{actual}}{(dV/dt)_{ideal}} = \frac{(dV/dt)_{actual}}{\mu_x g} \tag{1.11}$$

1.4 Braking in non-ideal conditions

The following analysis assumes no ABS or ESC operation. If wheel lock does not occur, the braking force generated at each tyre/road interface (in the longitudinal direction) is determined by the specification of the brake system that equally splits, ideally, the respective forces on the axle. As will be discussed in the section dedicated to tires, wheel lock will occur if the magnitude of the longitudinal brake force on any wheel exceeds the maximum that the tyre/road interface can sustain. Maximum brake force is developed just at the critical point (A and B in Figure 1.3), so it follows that for the maximum vehicle deceleration or rate of braking to be achieved on any given road surface, all wheels must simultaneously approach the point of locking. In practice, if the wheels on one axle will lock and the driver continues to increase the pedal effort, the unlocked wheels will deliver increased brake force until those wheels also lock, and then the driver would notice a further reduction in the vehicle deceleration because the coefficient with the ground results to be smaller than the previous case.
The braking distribution defined by K_b for the vehicle presented before is 75/25 to front wheels and gives reasonably good braking efficiency between $0.40<\mu<0.80$ for the unladen vehicle, and between $0.65<\mu<1$ for the laden vehicle, as represented in Figure 1.4; these values would be considered enough by carmakers [2]. Since the maximum rate of braking a_x/g cannot exceed the coefficient of adhesion μ, this means that this vehicle would have reasonably good braking efficiency under higher deceleration conditions on good road surfaces. But on lower adhesion surfaces the braking efficiency is lower, which means that the driver effort would need to be higher to achieve the same deceleration than if the braking efficiency were higher.
If the vehicle is facing low deceleration values, thus we are on the left of the point A in Figure 1.3, the rear wheel brake less than required for ideal braking. If a limit condition occurs in this zone, which can happen because of poor conditions of the road, front wheel will lock first. On the other hand, working on the right side of A will imply having higher rear forces than the needed ones and if the limit condition is reached, rear wheels will lock first.

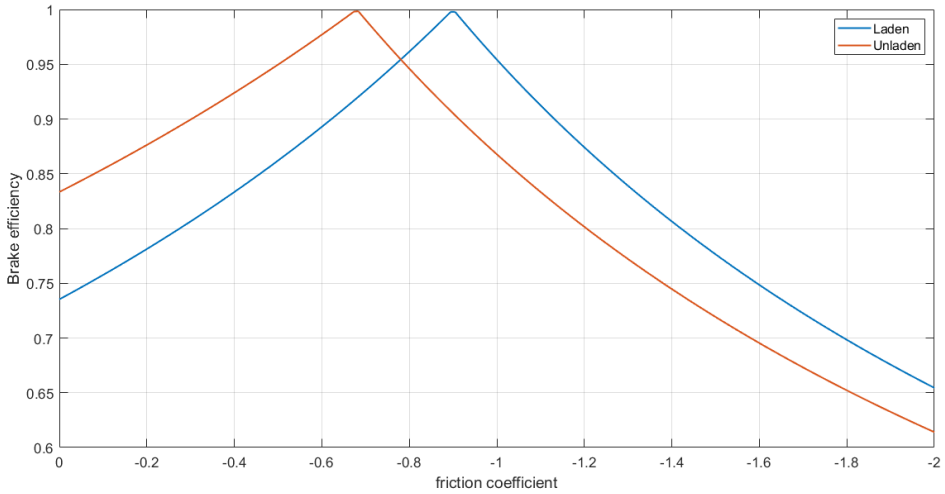

Figure 1.4 Braking efficiency over friction coefficients

Last condition must be avoided because it brings directional instability with it. This is because when wheels lock, they lose their capability to generate side forces; if it happens to the rear, it might start to slide sideways with body slip angle increasing as well as the slip angle of front tires which causes more lateral forces on that axle. Moreover, the arm between the centre of gravity and the front axle will increase, increasing also the total moment about the centre of gravity itself and leading to more sideways movement and the cycle repeats.

When the same condition happens to front wheels, the lateral movement is rapidly corrected by the moment acting because of the arm created by centre of gravity and the rear axle, reducing body slip and consequently lateral forces. This is called lack of directional control but is a stable condition and for this reason the brake system characteristic should lie always under the ideal line [1].

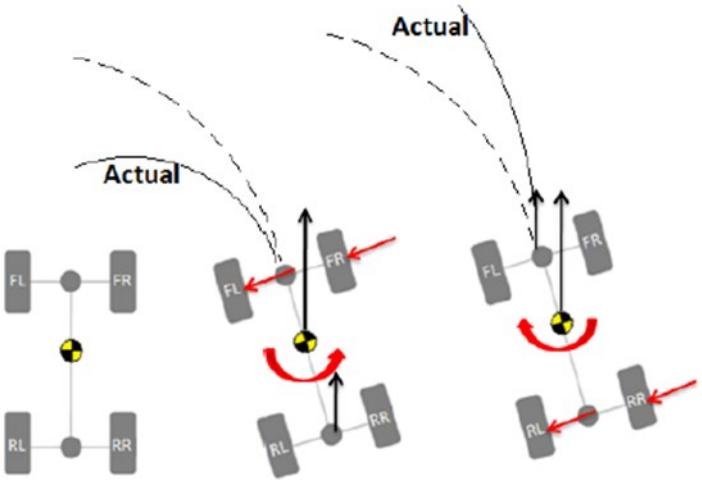

Figure 1.5 Representation of instability and lack of directional control

1.4.1 Methods to improve braking efficiency

Road vehicles generally cannot achieve an acceptable compromise between stability and efficiency with a fixed braking distribution (K_b) so in order to improve the braking efficiency over a greater range of vehicle loading and usage conditions, the braking ratio needs to be designed to be variable.

By adopting appropriate measures, however, the actual braking force can be changed to approximate more closely to the ideal braking force (no wheel lock-up) as represented in Figure 1.6 by the black line labelled as "3" that is steeper on the first part and then flattens out to reach point 4. A distinction is made between static or dynamic pressure regulating valves, and pressure limiting valves. Quoting [2]: "With a pressure regulating valve, the rate of pressure increase for the rear brakes is less than that for the front brakes upwards of a specific pressure (changeover pressure or changeover point). Static pressure regulating valves regulate the brake pressure according to a fixed characteristic, while dynamic pressure regulating valves do so on the basis of a regulating ratio that depends on the vehicle load or the rate of deceleration. Pressure regulating valves must be designed in such a way that under practical conditions, the braking force is distributed at a level well below the ideal level". Moreover, always on pressure regulating valves: "The effect of variations in the frictional coefficient of the road surface, the engine braking torque and the tolerance limits of the pressure regulating valve must also be taken into account in order to prevent rear-wheel lock-up. The pressure limiting valve prevents the brake pressure to the rear wheels rising any further once a specific level (shut-off pressure) has been reached" [2]. In the following, there will be briefly treated the most used solutions: Fixed-setting pressure regulating valve, load-dependent pressure regulating valve, deceleration-dependent pressure regulating valve, and pressure limiting valve.

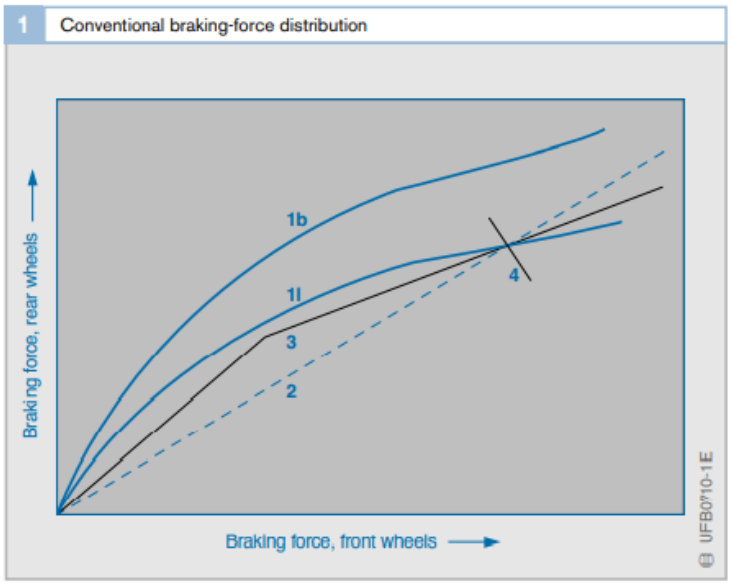

Figure 1.6 Fixed and varying Kb lines for brake circuits for laden and unladen vehicles [2]

Fixed-setting pressure regulating valve. The pressure regulating valve (Figure 1.7) is fitted in the rear-axle brake circuit. The valve body (8 in Figure 1.7) encloses a graduated piston (7) with an integral valve (9). The output pressure is reduced relative to the input pressure in proportion to the ratio of the effective areas of the annular chambers (2, 5). Shortly before the changeover pressure is reached, the pressure acting on the annular-chamber effective area (2) pushes the graduated piston to the right as far as the stop so that the valve (9) closes off the channel to the outlet port (4). As the pressure continues to increase, the graduated piston moves rapidly back and forth, opening and closing the valve (9) accordingly, thereby regulating the output pressure in proportion to the ratio of the effective areas (2, 5). Once the braking sequence ends, the pressure at the outlet port (4) pushes the graduated piston (7) against the compression spring (6) until the excess pressure in the annular chambers (2, 5) has reduced. Figure 1.7 shows the valve elements on the left and pressure curves on the right with no-regulation line (1) and regulated line (3) after the changeover point (5) [2].

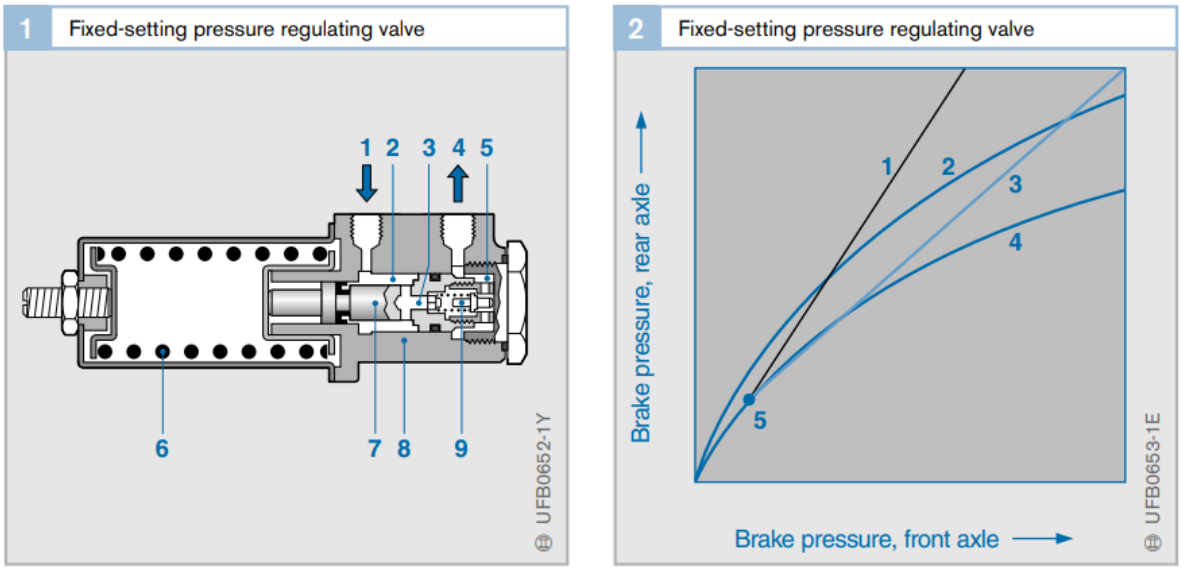

Figure 1.7 Fixed-setting pressure regulating valve elements(left) pressure curve (right) [2]

Load-dependent pressure regulating valve. Vehicles whose payload can alter significantly from one journey to the next require so-called load-dependent pressure regulating valves (Figure 1.8) so that the braking forces can be adjusted according to the weight being carried. This type of pressure regulating valve is attached to the bodywork and connected to the vehicle's rear axle (6) by means of a rod linkage (5). The relative movement between suspension and body as the springs are compressed is transmitted to the graduated piston (1). The piston then compresses the control springs (2) according to the amount of suspension travel, thereby altering the changeover point. This achieves an adaptive response of the rear-axle brake pressure relative to the weight of the vehicle payload that is represented by all the parallel lines on the right image in Figure 1.8 [2].

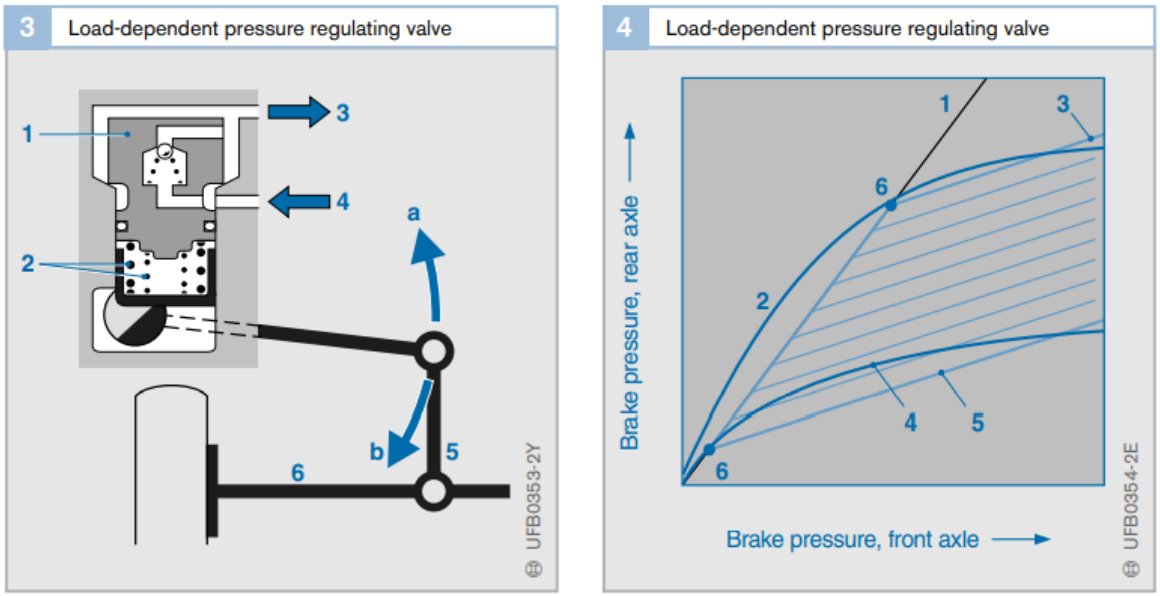

Figure 1.8 Load-dependent pressure regulating valve elements (left) pressure curve (right) [2]

Deceleration-dependent pressure regulating valve. This type of pressure regulating valve must be fitted in the rear-axle brake circuit and set at an angle, α, to the vehicle's horizontal axis in such a way that when the vehicle is stationary, the ball (4 in Figure 1.9 left) rests at the back of the valve away from the stepped piston (2, Figure 1.9 left). As the brake pressure required to obtain a given rate of deceleration depends on the weight being carried by the vehicle, this type of valve is load-dependent as

well as deceleration-dependent. As soon as the rate of deceleration under braking reaches a certain level, the inertia of the ball causes it to roll up the inclined plane – assisted by the pressure from the inlet port (9) – and close off the channel (8) through the stepped piston (2). This point represents the first changeover point (1 or 3, Figure 1.9 on the right) because further increase of pressure at the inlet port (9) cannot initially be passed through to the rear-axle brake circuit (pressure limiter function). As the pressure at the inlet port (9) continues to increase, however, the stepped piston (2) is pushed forwards against the action of the leaf spring (7) towards the outlet port (1) and away from the ball. At that stage, the second changeover point (2 or 4) has been reached. The piston channel (8) has been opened again and the passage of fluid between the two ports (9 and 1) is possible again. The pressure in the rear-axle brake circuit can now rise again at a reduced rate (pressure regulating function). Figure 1.9, on the right, shows the changeover points of a deceleration-dependent pressure regulating valve for an unladen (1-2 line) and a fully laden vehicle (3-4 line) [2].

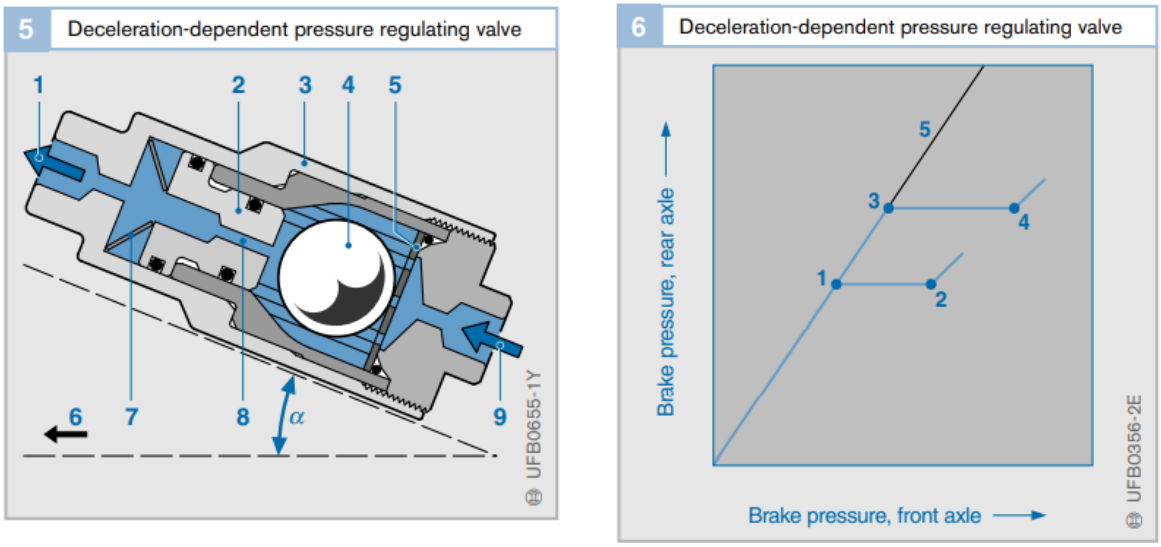

Figure 1.9 Deceleration-dependent pressure regulating valve elements(left) pressure curve(right)

Braking-force limiter. The braking-force limiter (Figure 1.10) is fitted in the rear-axle brake circuit and prevents the rear-axle brake pressure rising beyond its shut-off pressure. At that point, the valve piston (6) compresses the compression spring (5) and brings the valve cone (4) into contact with the valve seat (8) so that no further pressure increase at the outlet port (9) is possible. When the braking sequence comes to an end, the valve opens and releases the pressure. Figure 1.10 also shows the forces plot after an eventual pressure limitation in point B [2].

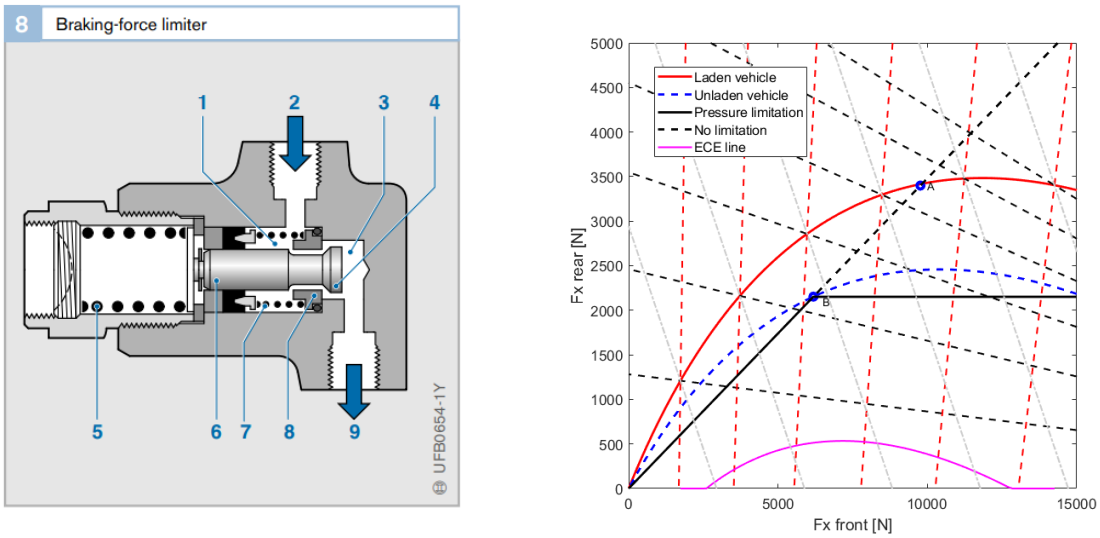

Figure 1.10 Braking-force limiter elements (left) and force plot (right)

1.4.2 ABS and EBD impact on braking

1.4.2.1 ABS systems

In recent years, technology has driven the development of vehicles towards increasing level of electronics to improve safety in normal operating conditions and performances of all the systems inside the vehicle. One of the most famous and important systems implemented for braking is the ABS. The antilock braking system (ABS) detects if one or more wheels are about to lock up under braking and if so, makes sure that the brake pressure remains constant or is reduced. By so doing, it prevents the wheels from locking up and as a consequence, the driver can stop the vehicle quick and safe, and the vehicle can have still some steering capability.

The ABS braking system is based on the components of the conventional system that are: Brake pedal, brake booster, master cylinder reservoir brake lines and hoses and brakes. In addition, there are also wheel speed sensor, hydraulic modulator and a dedicated control unit.

The speed of rotation of the wheels is an important input variable for the ABS control system. Wheel-speed sensors detect the speed of rotation of the wheels and pass the electrical signals to the control unit that uses that information to calculate the degree of slip (1.12) that indicates the degree to which the wheel's circumferential speed, v_r, lags behind the vehicle's linear speed (road speed), v_f and therefore detects whether any of the wheels is about to lock up (brake slip λ=100%).

$$\lambda = \frac{v_f - v_r}{v_f} 100\% \tag{1.12}$$

In Figure 1.11 is represented the circuit of ABS modulator for a single wheel and whose explanations and materials are taken from [2] where the reader should refer for a full explanation that is out of the purposes of this work. The hydraulic modulator incorporates a series of solenoid valves that can open or close the hydraulic circuits between the master cylinder and the brakes. In addition, it can connect the brakes to the return pump. Solenoid valves with two hydraulic connections and two valve positions are used (2/2 solenoid valves). The inlet valve between the master cylinder and the brake controls pressure application, while the outlet valve between the brake and the return pump controls pressure release. There is one such pair of solenoid valves for each brake.

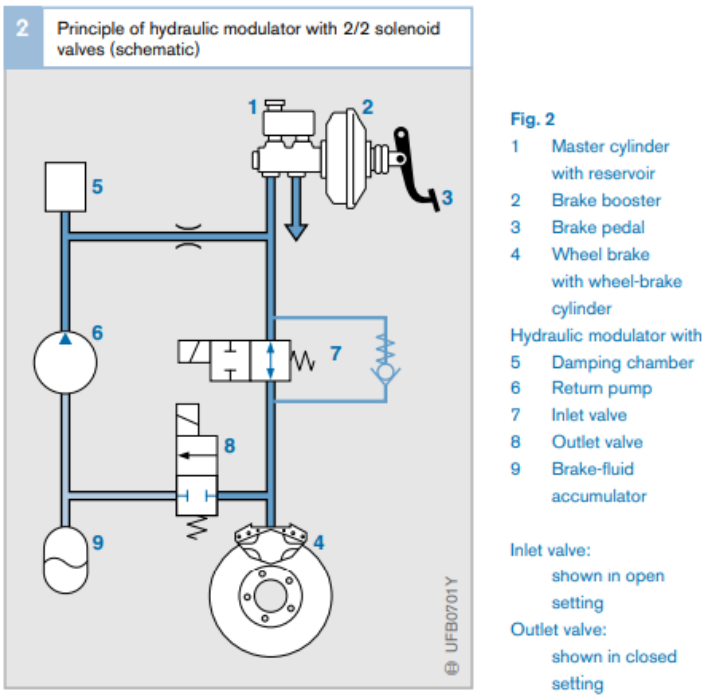

Figure 1.11 Hydraulic modulator for ABS systems [2]

Under normal conditions, the solenoid valves in the hydraulic modulator are at the "pressure application" setting. That means the inlet valve is open. The hydraulic modulator then forms a straight-through connection between the master cylinder and the brakes. Consequently, the brake pressure generated in the master cylinder when the brakes are applied is transmitted directly to the brakes at each wheel.

As the degree of brake slip increases due to braking on a slippery surface or heavy braking, the risk of the wheels locking up also increases. The solenoid valves are then switched to the "maintain pressure" setting. The connection between the master cylinder and the brakes is shut off (inlet valve is closed) so that any increase of pressure in the master cylinder does not lead to a pressure increase at the brakes. If the degree of slip of any of the wheels increases further despite this action, the pressure in the brake(s) concerned must be reduced. To achieve this, the solenoid valves are switched to the "pressure release" setting. The inlet valve is still closed, and in addition, the outlet valve opens to allow the return pump integrated in the hydraulic modulator to draw brake fluid from the brakes concerned in a controlled manner. The pressure in the relevant brake is thus reduced so that wheel lock-up does not occur.

1.4.2.2 EBD systems

As anticipated, the ABS is an important step toward regulation of pressure on brake to prevent tire lock in critical situations. But this work is focused on normal driving conditions where ABS should not work and therefore now it will be presented another system that comes from "natural evolution" of ABS systems. This system is the Electronic Braking-force Distribution (**EBD**) and has the purpose to improve braking in all normal driving situations in order to ensure always the best performances for the brake systems. It relies on the existing ABS system's hydraulics, sensors and electronics, but with modified valves and software, to allows the braking force at the rear wheels to be reduced. For the Electronic Braking-force Distribution (EBD) function, only the rear-brake valves of the ABS system are activated, the return pump motor in the hydraulic modulator unit remains de-energized.

The vehicle is designed in such a way that without a proportioning valve, the fixed braking-force distribution curve intersects the ideal braking-force distribution curve (1 in Figure 1.12) at a point P at a lower overall braking force, e.g. 0.5g. The ECU continuously calculates the slip difference (1.12) between the front and rear wheels in all driving situations. If the ratio of front to rear wheel slip exceeds a defined stable-handling threshold when braking, the ABS pressure inlet valve for the appropriate rear wheel is closed. This prevents further increase of brake pressure at that wheel. If the driver then further increases the force applied to the brake pedal, and therefore the brake pressure, the degree of slip at the

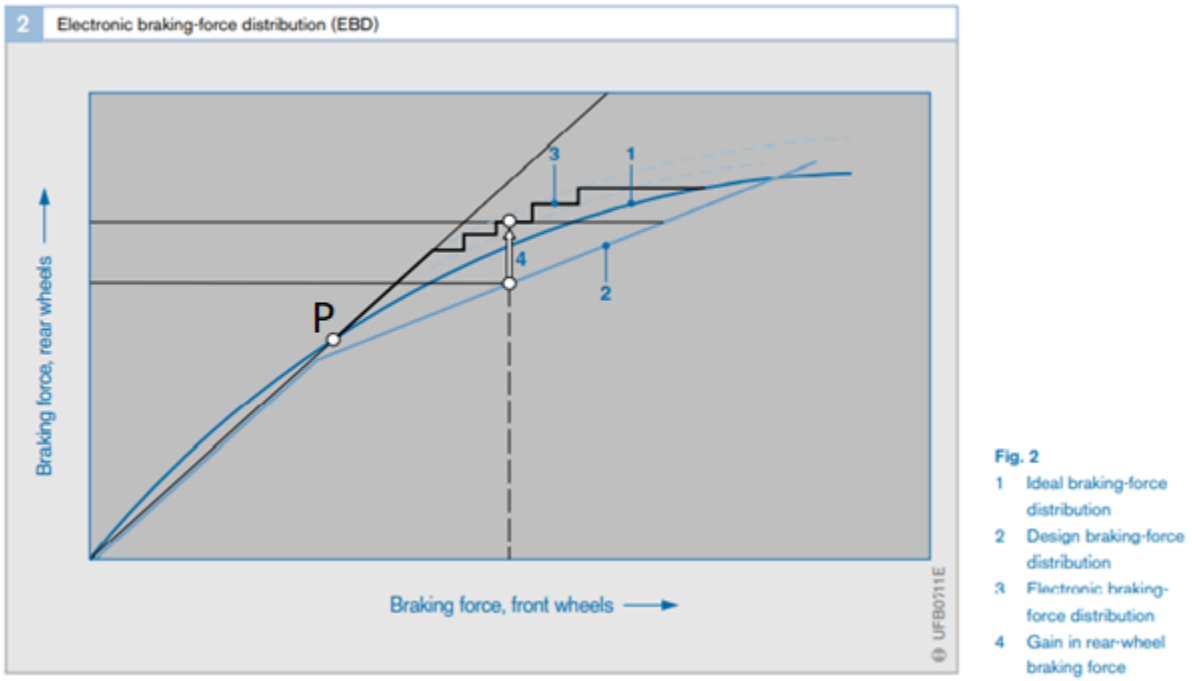

Figure 1.12 EBD braking force distribution plot [2]

front wheels also increases. The difference between front and rear wheel slip diminishes and the pressure inlet valve is opened again so that the pressure at the rear wheel rises once more. This process may then be repeated a number of times depending on the brake pedal force and the manoeuvre being performed. With the just written actions, the EBD brake distribution curve takes on a staircase appearance (curve 3 in Figure 1.12) which approximates to the ideal braking-force distribution curve and that has much more degrees of freedom with respect to a conventional pressure regulating valve.

The characteristics of the EBD system outlined above provide the following advantages: Optimized vehicle handling stability under all payload conditions and in all cornering situations, on uphill or downhill gradients, and in any drivetrain status (clutch engaged/ disengaged, automatic transmission), no need for conventional proportioning valves or limiting valves, reduced thermal stresses on the front brakes, even wear between front and rear brake pads, better vehicle deceleration with the same pedal force, constant braking-force distribution patterns over the entire life of the vehicle, only minor modifications to existing ABS components are required.

1.5 Regulation on braking requirements for braking systems

A third line is present in Figure 1.3, and it is the one, in purple colour, representing forces distribution stated by ECE regulation [3] for passenger cars regard to braking, that dictates the limits for braking line design and especially the case when, to be safe and having the K_b line under the ideal, the designer exaggerates, reducing too much the utilization of road adhesive capability. That is, when front wheels are locked, and rear wheels are not.

The regulation states that:

- For all states of load of the vehicle, the adhesion utilization curve of the rear axle shall not be situated above that for the front axle for all braking rates between 0.15 and 0.8
- For decelerations between 0.2 and 0.8 the minimum vehicle deceleration is:

$$\frac{a_x}{g} \geq 0.1 + 0.85 * (\mu - 0.2) \tag{1.13}$$

The physical meaning of equation (1.13) is that when the front wheels are locked, the rear braking force must be large enough to make the vehicle yield a deceleration rate not smaller than the value dictated.

1.6 Tire behaviour during braking and cornering limitations

When talking about the model used for braking, it has been mentioned that pure braking is considered and all lateral forces, yaw moment and lateral load transfers are null. This hypothesis helps to simplify the problem also from tire limit point of view but on the other side a brief explanation is needed since it will help in future assumptions.

The mechanism of build-up of forces in tires has been extensively studied because they represent the interface between the vehicle and the road thus influencing the vehicle behaviour. Yet, tires are a very complex components that behave in particular way and need to be studied separately from the vehicle for a full understanding.

1.6.1 Tire modelling

When there is the need to introduce tires into a study or models, there are different choices on how to consider them, depending on the model used or wanted level of complexity.

These models can vary from totally empirical, based on ad-hoc tyre tests from which extrapolate parameters, to theoretical, describing the tire in greater detail and very complex physical models. Whenever the study is not focused on tires and there is the need for a good estimation yet quick

evaluation of tire limits, the Pacejka model is used. Figure 1.13 gives an idea about the various type of models from full empirical to theoretical as presented in [4].

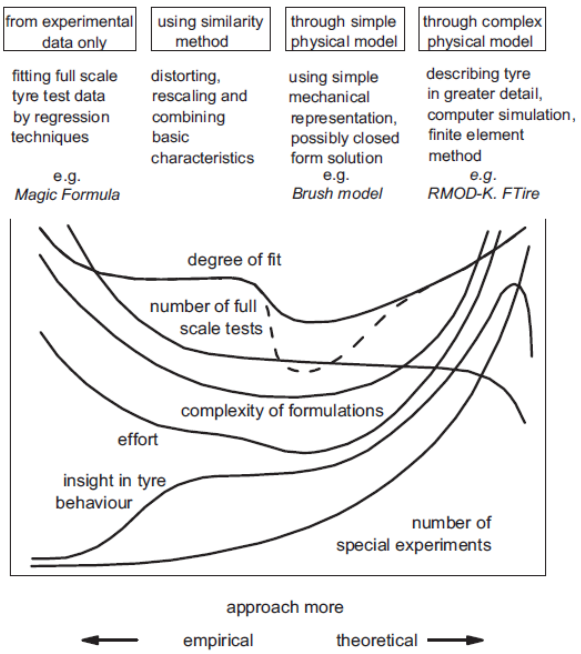

Figure 1.13 Tire models classification from full empirical to theoretical

Pacejka model, or Magic Formula, is a semi-empirical model that, as the name suggests, combines physical and empirical modelling philosophies. The models can either have one specific property being modelled using physical equations or can have empirical relationships modified on the basis of phenomena observed from physical models. It consists of several parameters whose weight in the formula derives from data fitting of ad-hoc tests performed on the tires under study. Of course, there can be different levels of complexity for the formula and the parameters implied in the description of a single characteristic like the longitudinal force developed. The real advantage is that they require less computation capability than simple physical models since the underlying definition is purely mathematical.

Formula 1.14 is an example of Pacejka model formula for 2006 version [4] where the output quantity y, is function of input quantity x and several coefficients: B is the stiffness factor, C the shape factor, D the peak value, E is the curvature factor and S the vertical shift. Coefficients are depending on all quantities related to the developing of forces and their geometrical meaning is shown in Figure 1.14.

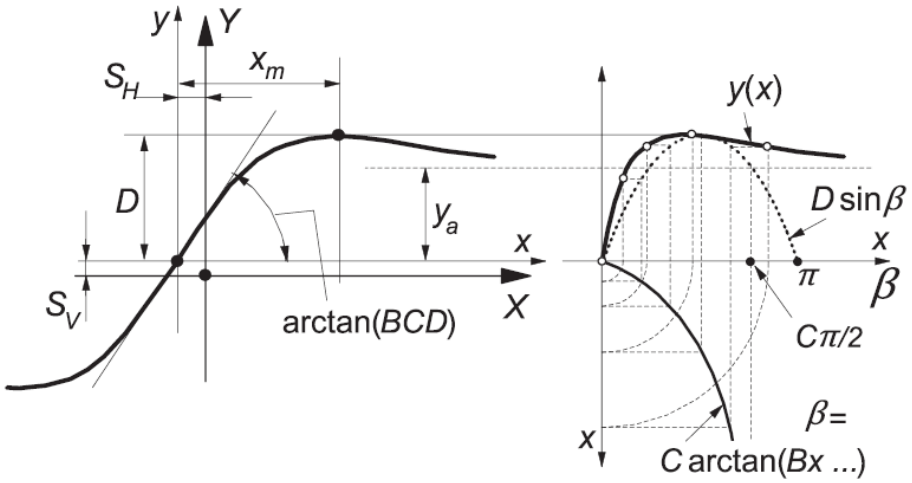

Figure 1.14 Curve produced by formula 1.14 with geometrical parameter representation

The y quantity could be longitudinal force or lateral force with related input quantities (κ for longitudinal and α for laterlal) and respective scaling factors. The full description of formulas can be found in Chapter 4 of [4].

$$y = D\sin\{C\arctan[B(1-E)x + E\ \arctan(Bx)]\} + S_v \tag{1.14}$$

1.6.2 Tire forces and slip quantities

The description of forces on tires could be simplified by means of the hypothesis of linear behaviour and small quantities to get a simplified form of the force equations, like in Formula 1.15, 1.16 and 1.17 where linear coefficients $C_{F\kappa}$, $C_{F\alpha}$ and $C_{M\alpha}$ are assumed to describe the slope of the respective force curves as function of the slip components.

$$F_x = C_{F\kappa}\kappa \tag{1.15}$$

$$F_y = C_{F\alpha}\alpha + C_{F\gamma}\gamma \tag{1.16}$$

$$M_z = -C_{M\alpha}\alpha + C_{M\gamma}\gamma \tag{1.17}$$

Forces exchanged with ground are influenced by the so-called slip components and loads, following the reference system in Figure 1.16. Slip quantities will be briefly explained here, following the text [4].

First slip quantity κ, or longitudinal slip, is the result of application of torque to a free rolling wheel and is defined as the difference from the rotational speed of a free rolling wheel and the actual speed of the wheel when torque is applied.

$$\kappa = -\frac{V_x - r_e\Omega}{V_x} \tag{1.18}$$

The difference between the two speeds is present because tires are not rigid bodies and subject to deformations when loads are applied so that also the radius changes. These deformations are also responsible for the developing of forces as reaction forces. During braking, the fore-and-aft slip becomes negative; in case of wheel lock, this coefficient would be equal to -1.

The second slip quantity is the side sleep and is defined as the ratio of the lateral and the forward velocity of the wheel. The relative angle, sideslip angle, is the difference from the direction of speed vector of the wheel and the mid plane of the wheel. This difference gives rise to deformation in lateral direction and developing of lateral forces.

$$\tan\alpha = -\frac{V_y}{V_x} \tag{1.19}$$

In Figure 1.15 are represented the forces developed by tires as function of slip angle and different brake slip and vice versa.
The third and last slip quantity is the so-called spin which is due to rotation of the wheel about an axis normal to the road. Both the yaw rate resulting in path curvature when α remains zero and the wheel camber γ (as represented in Figure 1.16) of the wheel plane about the x axis, contribute to the spin and thus influencing lateral force and moment about the vertical plane of the wheel.

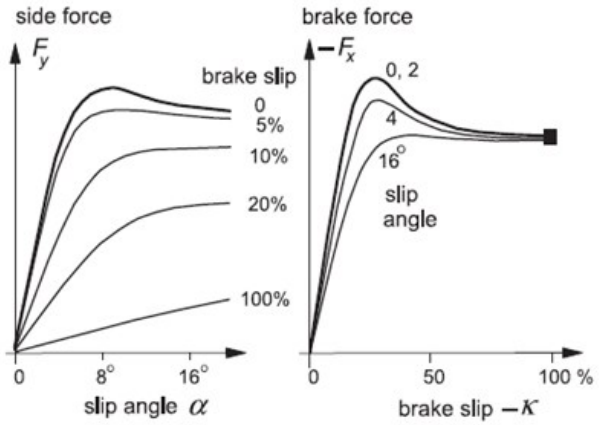

Figure 1.15 Lateral (on the left) and longitudinal (on the right) forces as function of side slip angle and longitudinal slip

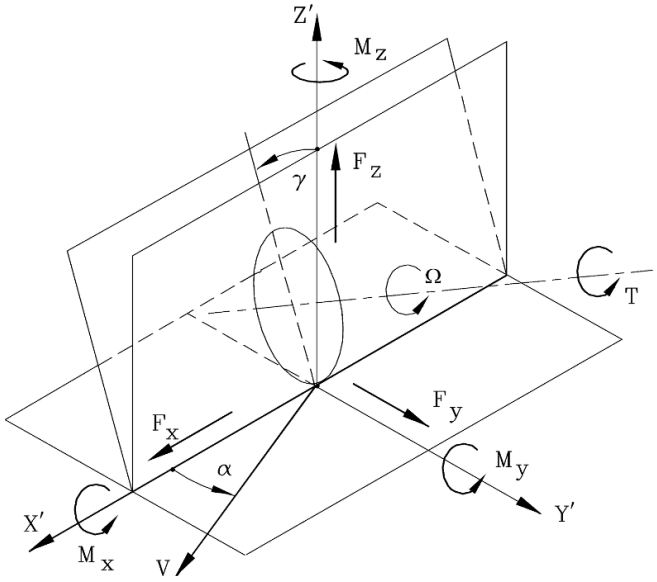

Figure 1.16 Reference system used to study forces exchanged between tire and ground. Definition of positive direction of forces, moments and slip angles

1.6.3 Grip factor and combined forces effect on tire forces

A very important concept is that tires do have a limited amount of force that can build and consequently transmit, and it depends on many tire construction parameters and working conditions. When a force is considered, it can be defined the so-called friction coefficient μ (1.20) that expresses how much force is developed by the tire, normalized to the vertical force applied. This friction coefficient or grip factor is also depending on ground conditions. If the forces applied on the tire is higher than what the grip with ground could fulfil, the tire will experience a macro and complete slip of the contact patch over the ground surface. Typical values assumed for road cars on dry asphalt are μ =0.8-0.9 and 0.3-0.4 on wet [5]. These values, representing the maximum grip achievable by the tires on a determined surface will be assumed in the following work.

$$\mu_{x,y}=\frac{F_{x,y}}{F_z} \tag{1.20}$$

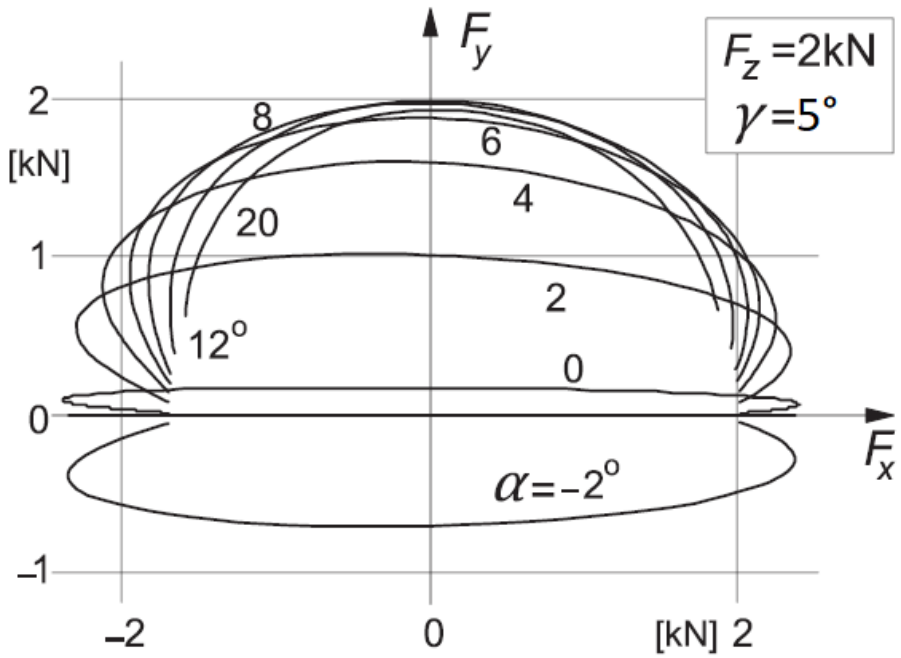

Figure 1.17 Grip parabola, function of vertical load and camber angle

In the real world is not possible to have forces applied in only one direction, there is always a small error and more often the tires are always in the case of developing thrust and lateral forces simultaneously when driving a vehicle. In this last condition, when forces have combined directions, tires cannot develop the same amount of force they would if stresses in a single direction. The locus of all points defining the maximum for the tires in each condition is the so-called grip parabola, represented in Figure 1.17. This parabola characterizes a tire and the behaviour in the combined lateral and longitudinal direction. A single parabola is function of the vertical load and defines the limit conditions so tires can be in any of the points under the parabola.

This introduction to tires was crucial because it will help to define some limit conditions in this work. This work starts with ideal braking condition but when generalizing the case or setting some limits to longitudinal forces it will also be done considering that the real capability of the tires will be limited by the presence of also some lateral forces. This is particularly useful when talking about “following the braking system line that is not ideal” and that, in other terms, applies more braking force on an axle with respect to ideal cases. Approaching these limits will increase the risk to trigger sliding on the axle and loss of controllability for the vehicle.

2 Electric powertrains and regenerative braking

In this chapter there will be an introduction to electric powertrains, mostly on their characteristics involving braking and their capacity to regenerate. These aspects influence the way we can think about stopping our vehicles and they also require a more in-depth study on the topology to use on already established braking systems.

2.1 Electric powertrains characteristics

One of the most important features of EV, HEVs, and fuel cell vehicles (FCVs) is their ability to recover significant amounts of braking energy. The electric motors can be controlled to operate as generators to convert the kinetic or potential energy of vehicle mass into electric energy that can be stored in the energy storage elements and then reused. Thus, these elements will affect the design of the braking system for a vehicle that must always meet the distinct demand of quickly reducing vehicle speed and maintaining vehicle direction controllable by the steering wheel with a further goal to now increase energy efficiency of the powertrain. The first goal requires the braking system to be able to supply sufficient braking torque on all wheels. The second requires proper braking force distribution on all wheels, as discussed in previous chapter and the third will be here introduced and then studied in following chapters.

Besides the advantage of energy recuperation in braking, electric powertrains have also other advantages with respect to IC engines and friction systems:

1. Torque generation of an electric motor is very quick and accurate. This is an essential advantage. The electric motor's torque response is several milliseconds, 10-100 times as fast as that of the internal combustion engine or hydraulic braking system. This enables fast responsive feedback control and hence vehicle characteristics can be changed without any change in characteristics from the driver and adapt to every situation.

2. A motor can be attached to each wheel or both axles and independently develop torque. Small but powerful electric motors installed into each wheel can generate even the anti-directional torques on left and right wheels. Distributed motor location can enhance the performance of Vehicle Stability Control (VSC) such as Direct Yaw Control (DYC).

3. Motor torque can be measured easily. There is much smaller uncertainty in driving or braking torque generated by an electrical motor compared to that of an IC engine or hydraulic brake. It can be known from the motor current. Therefore, a simple 'driving force observer' can be designed and it can easily estimate the driving and braking force between tire and road surface in real time.

4. An electric machine has a characteristic of torque over rotor speed that is known to be much better for traction purposes with respect to an internal combustion engine because of all torque ready from lowest speed, yet it presents limitations at higher speeds where it enters the constant power portion and torque must decrease.

Since now, we have been talking about benefits of electric powertrains and their abilities to better control vehicle behaviour but there are also some drawbacks.

Regenerative braking has no great limitations for what concerns the electric machine itself other than its characteristics and the efficiency of its working condition, but limitations come when we observe the entire powertrain and in particular the energy storage element and drivetrain efficiencies.

1. It is difficult to regenerate at low speed because of low electromotive force generated at low motor rotational speed. This limit is varying depending on the drivetrain efficiency. In the

following work, a motor with characteristics and a regenerative cut off at 800 rpm like in Figure 2.1 has been used.

2. Unlike friction brakes, regenerative torque depends on the speed of the motor and in negative way when braking, since it is lower for higher speeds.

3. Another kind of limitation on the regenerative torque quantity comes from the energy storage conditions that will be briefly treated in the following paragraph.

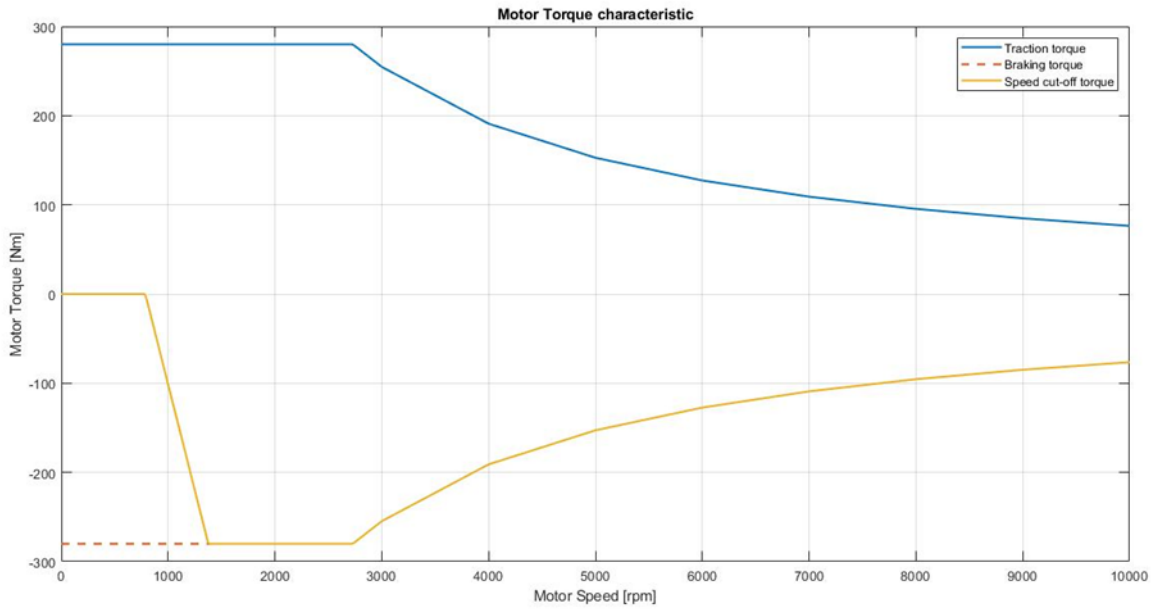

Figure 2.1 Motor torque VS speed characteristic in traction and braking

2.2 Energy storage states that affect regenerative braking

Cell states that will influence the amount of regenerative torque will mainly be SoC, temperature and charge rate. These limits are stated to save the cells form critical conditions concerning safety or the aging of the cell itself to preserve the health throughout their service life.

2.2.1 SoC influence

State of charge is not a limit by itself, it basically indicates the amount of charge remaining inside the cell with respect to the maximum that can be stored. The rated capacity or the capacity at the beginning of life is commonly used as the reference value. Usually, a level of 80% of SoC is the limit at which we can have the regenerative effect. This is mostly done to avoid that for high charging currents a single cell hits too high voltage [6]. This is done because excessive overcharging can entail gas evolution and overpressure inside the cell.

On the other side, we do not want the SoC to be under 20% that will imply high discharge stress a low discharge efficiency.

Moreover, when talking about battery pack and not about single cells, SoC detects the overall state of the battery pack where not all cells discharge in the same way as we would expect in an ideal word. This condition also limits to further extent the available, overall charge because the failure of a single cell can lead to failure of the whole battery pack, in particular if the cells are connected in series.

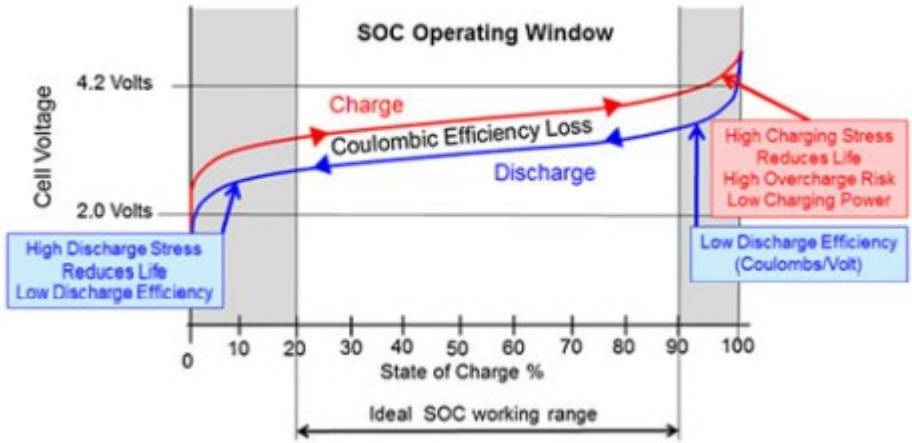

Figure 2.2 Cell voltage VS state of charge

2.2.2 Temperature influence

Most of the temperature effects are related to chemical reactions occurring in the batteries and materials used in the batteries. Regarding chemical reactions, the relationship between the rate of chemical reactions and reaction temperature follows Arrhenius equation, and temperature variation can lead to the change of electro-chemical reaction rate in batteries. Besides chemical reactions, the ionic conductivities of electrodes and electrolytes are also affected by temperature. For example, the ionic conductivity of lithium salt-based electrolytes decreases at low temperatures [7].

The study [7] tried to highlight the effect of higher temperature on Li-ion batteries. The first effect is that passing from the rated temperature of 25°C to 55°C there was an increase of 20% on maximum storage capacity. But even though the capacity increases at first place, the degradation rate at higher temperature increases such as passing from -3.3% after 200 cycles at 25°C to -10% at 55°C. This has been mostly ascribed to the degradation of electrodes, where the phase change and surface modification were aggravated at high temperature.

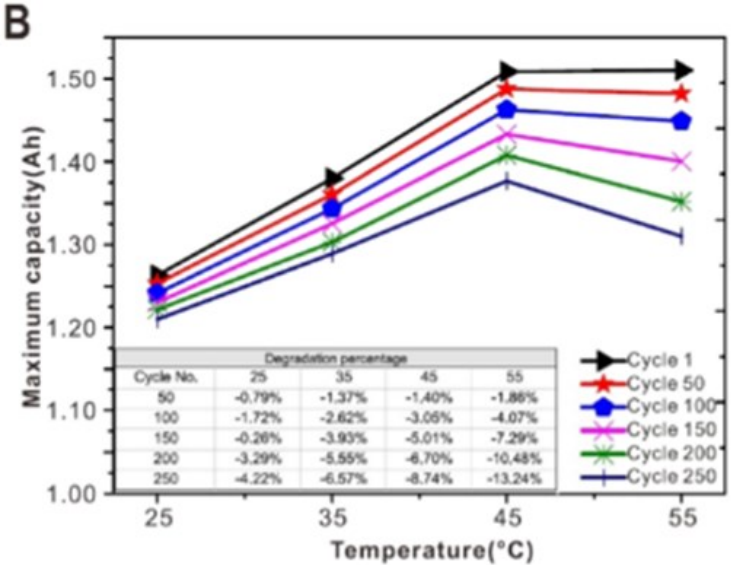

Figure 2.3 Maximum capacity dependence on temperature and number of cycles

2.2.3 Charge rate effects

A high-rate charge pulse can lower the surface lithium concentration to the point at which irreversible phase change can occur. At high enough currents, the overpotential for direct lithium reduction becomes

negative and lithium deposition starts to compete with intercalation for the incoming Li+ flux. This plated lithium decreases the inventory of cyclable Li+ in the cell, and chemically reduces surrounding electrolyte species.

Figure 2.4 coming from [6], illustrates the effect of C-rate on the battery capacity fade and also reveals the proportion of different attributes, ranging from kinetic hindrance (including: polarization and the other Li ion transport problems) to loss of lithium inventory and active material, in the capacity fade of a {LiMn1/3Ni1/3Co1/3O2 + LiMn2O4} composite positive electrode-based Li-ion cell as a function of the number of cycles under 2C cycle aging regime. This study's authors [8] concluded that the cell degradation takes place in two steps. In the first step, the capacity fade is shown to be linear during the first 500 cycles (Figure 2.4). In this step, capacity fading arises from the loss of lithium inventory caused in turn by parasitic reactions, forming the SEI (solid electrolyte interphase) film on the electrode surfaces. As a subsequent implication, less amounts of Li+ come back to the negative electrode during charging regime. In the second step, because the SEI layer proceeds to grow on the electrode surfaces, it restrains interfacial kinetics causing active material loss in the electrodes which expedites the capacity fading.

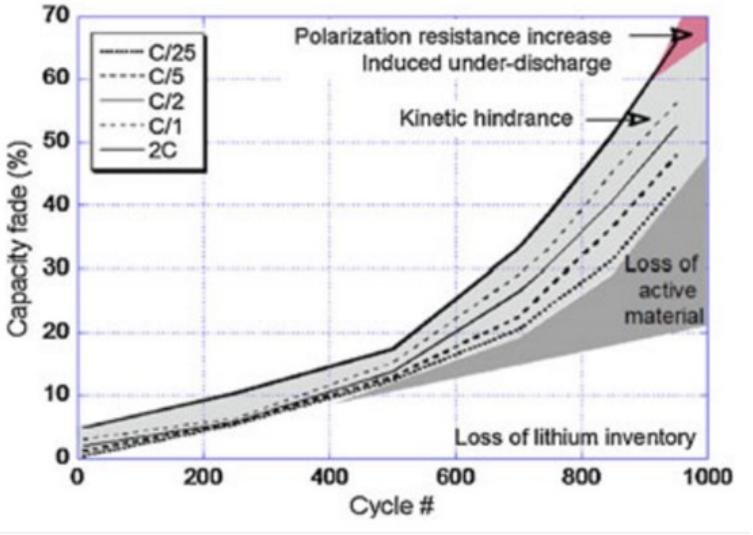

Figure 2.4 Capacity fade due to charge rate

2.2.4 Energy conversion efficiency

Finally, as in all systems where energy is converted, there are also efficiencies. Efficiency values for electric vehicles are more difficult to be stated than ICE vehicles and they drastically depend on the technologies used but usually much greater than 25-35% that ICE can give.

The energy transformation path starts from conversion of chemical energy of battery to electrical energy. This step has and efficiency that depends on the type of battery cells and on the states of the battery pack. Typically, for high temperatures and C-rates the process is more inefficient and could be of 80-90% for Li-ion cells.

In most of the electric motor applications for vehicles on the market, the electric energy must be converted from DC to AC by means of power electronic converters and then motor controllers will command the motor actuation. This process implies energy dissipation and efficiency has usually high values, higher than 90% [9].

Electric energy is converted into mechanical in motors. Their efficiency depends on the working point, typically at optimum when working at 75% of rated load and drastically dropping if used underloaded. A very great effect comes also by the quality of the machine and the insulation class [10].

With presence of a mechanical transmissions mechanical energy is dissipated even more but typical values are greater than 95% even because with electric motor there is no need for gearboxes.

2.3 *Braking energy exploited in urban driving*

If the braking torque required during normal driving conditions, in almost any driving cycles used for vehicle testing, is analysed, it is possible to see that the maximum required braking torque is much larger than the torque the electric motor can usually produce. Moreover, electric motors torque depends on speed, dropping when this last parameter increases. These conditions make necessary to have also mechanical brakes to fully cover high power braking conditions and coexist with regenerative brakes for what is called brake blending.

The urban driving cycles that will be considered in this work are the NEDC (Figure 2.5) and WLTP (Figure 2.6) [11]. Even though WLTP is by far more important in Europe since it has been created to represent better the driving behaviour of a vehicle in different driving conditions, NEDC is taken into considerations to have a comparison on obtained results.

In the following, the vehicle characteristics present in Table 1.1 are used with a fully loaded vehicle.

At first analysis, in a urban cycle, the intensity of decelerations are quite small, far from 0.7g that represent a heavy/emergency brake case. It is possible to also see that when a vehicle is driving in a stop-and-go pattern in urban areas, a significant amount of energy is dissipated by frequent braking that could account for about 30% of the total traction energy. Successful design of the hybrid braking system for recovering as much of the braking energy as possible requires a full understanding of braking behaviour and its characteristics with respect to vehicle speed, braking power, deceleration rate. The following table gives a rapid understanding of important parameters right listed and comparing them between the presented cycles.

Table 2.1 Cycles characteristics concerning braking

	WLTP	**NEDC**
Maximum speed [km/h]	131	120
Average speed [km/h]	46.52	33.6
Maximum deceleration [g]	0.15	0.14
Average deceleration [g]	0.06	0.08
Travelling distance per cycle [km]	23	11
Traction energy [kWh]	3.14	1.27
Braking energy [kWh]	0.85	0.37
Percentage of braking energy to total traction energy [%]	27.1	29.1

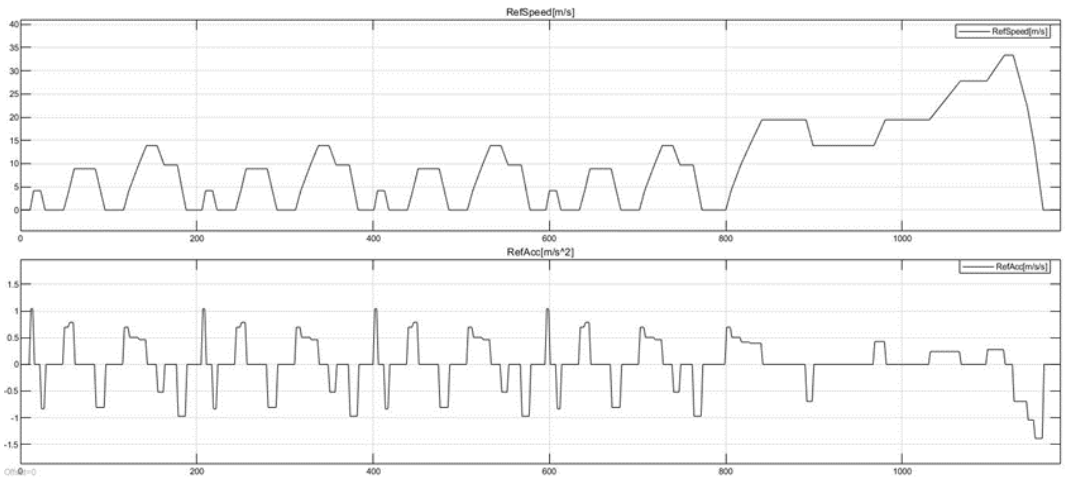

Figure 2.5 NEDC cycle- Speed profile(top) acceleration profile(bottom)

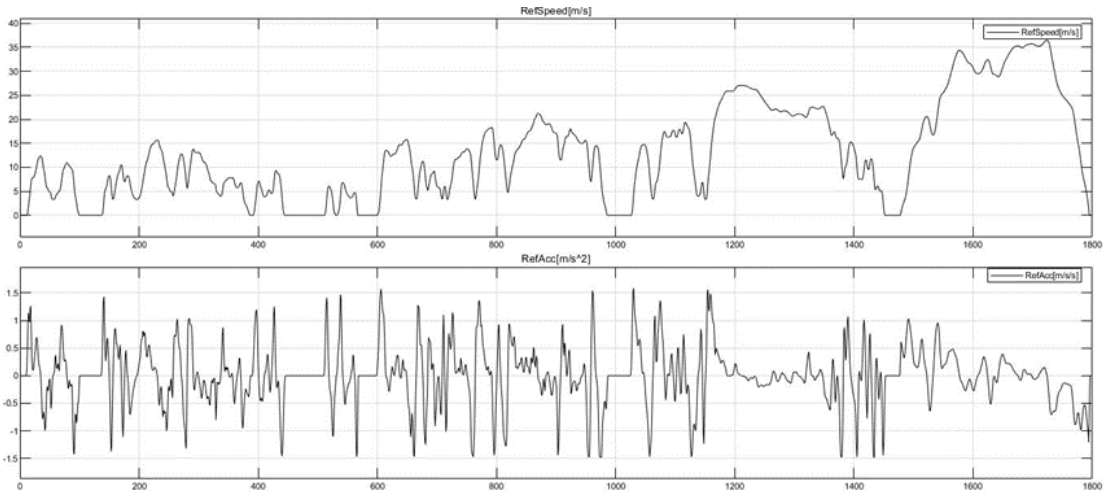

Figure 2.6 WLTP cycle- Speed profile(top) acceleration profile(bottom)

2.4 Braking power versus vehicle speed

2.4.1 WLTP cycle analysis

By the analysis of driving cycles, also presented by the authors of [12] in Chapter 14, it is possible to extract some data to choose the right powertrain and design the regenerative capability of the system. From Figure 2.7 is possible to see how much of braking energy is used under a certain speed. This plot is useful since is possible to see that under a speed of 15 km/h, only 4% of the total braking energy is used, that also means that for low speed we can deactivate the recovery because of low electromotive forces but we only waste 5% of the total braking energy.

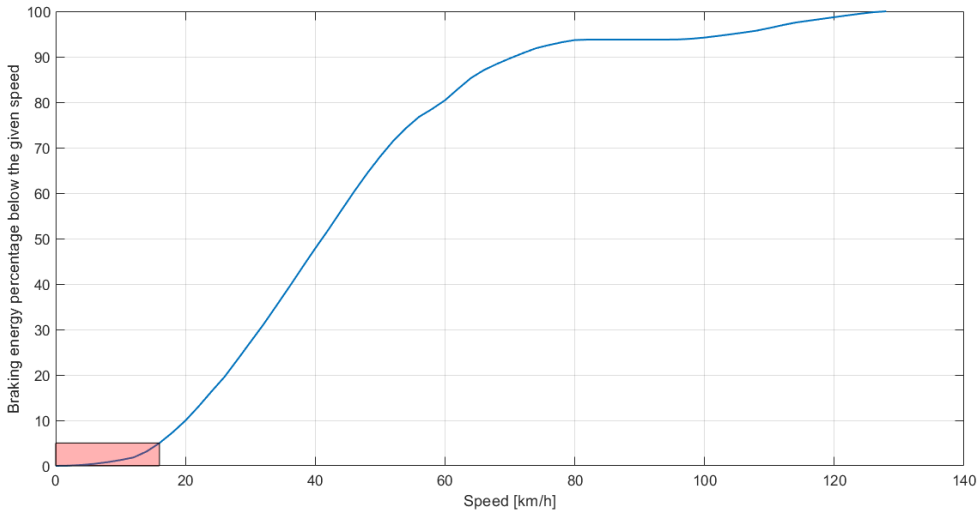

Figure 2.7 WLTP-Braking energy below a given speed

Moreover, it is possible to synthetize the information like in Figure 2.8 where the percentage of mechanical energy in braking and braking power are related in how much energy percentage is not covered by a braking power, greater than the one indicated on the axis. This helps for the choice about motor power and the achievable energy recuperation that also bring together decision about cost, space and weight. From this plot is possible to see that for what concerns urban mobility the mechanical power request is small and could be fulfilled also by low power motors, for example a 15-kW motor would waste less than 10 % of braking energy available for the recuperation. A 30-kW motor would cover the

power request during braking of the WLTP duty cycle and could represent a valid choice for modern vehicle mobility without the need to increase power.

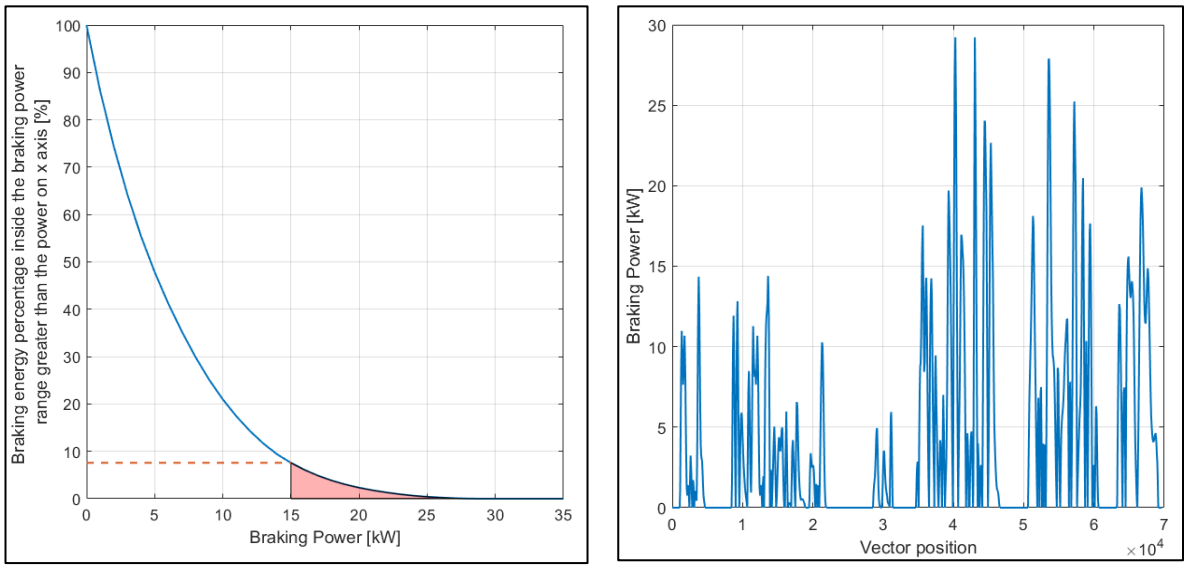

Figure 2.8 WLTP-Braking energy percentage under a given power(left) braking power during the cycle(right)

For our analysis, braking power distribution over vehicle speed can also be useful as in Figure 2.9. The bars in Figure 2.9 represent the maximum braking power in the analysed drive cycle, at specified vehicle speeds. The solid lines represent the supposed motor speed-power profiles that would cover 90% (red line) and 100% (black line) of the braking energy. The braking power versus vehicle speed profiles naturally match the power–speed characteristics of the motor, in which the power is proportional to the speed from zero speed to base speed (constant torque) and is constant beyond the base speed. Thus, electric motors do not need a special design and control for regenerative braking purposes.

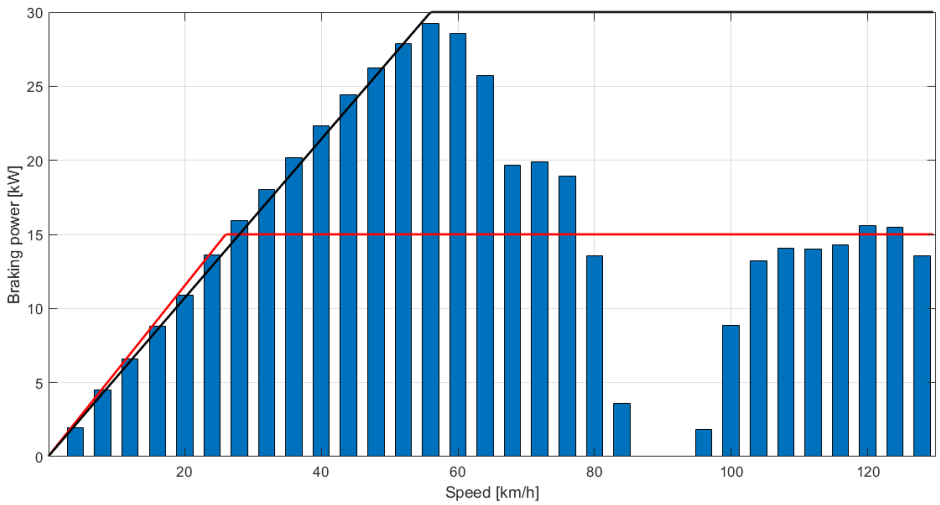

Figure 2.9 WLTP- Braking power as function of speed and motor power characteristic

2.4.2 NEDC cycle analysis

To see how the powertrain would perform in other conditions we can perform the same analysis also for NEDC that is only slightly different but still gives good information. The same 15 and 30 kW are imposed on Figure 2.10 but, in this case, the 30kW motor would result to be more than needed. A 15 kW power motor would be enough to cover more than 90% of total braking energy, same for WLTP. By turning off the regenerative at 15 km/h and going on Figure 2.12, 12% of energy in braking would be lost; much greater than the 5% of WLTP.

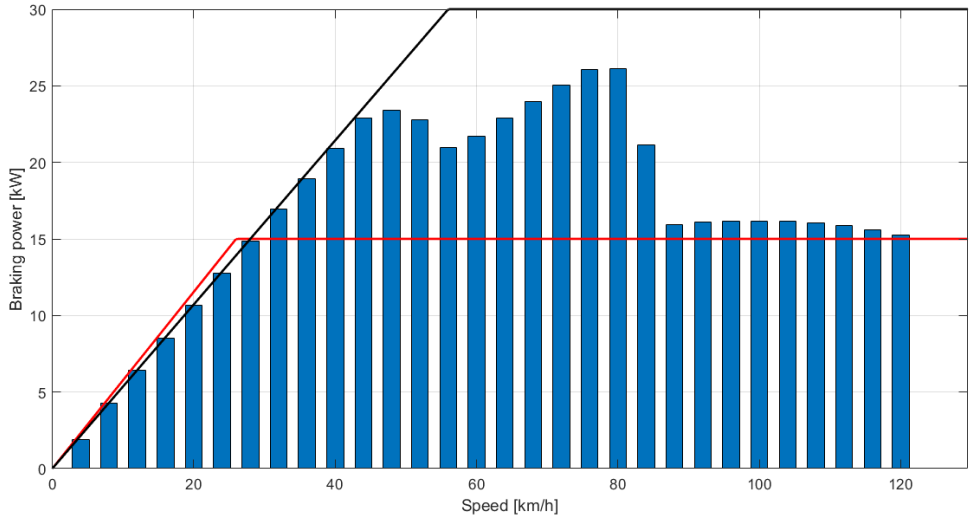

Figure 2.10 NEDC- Braking power as function of speed and motor Power characteristic

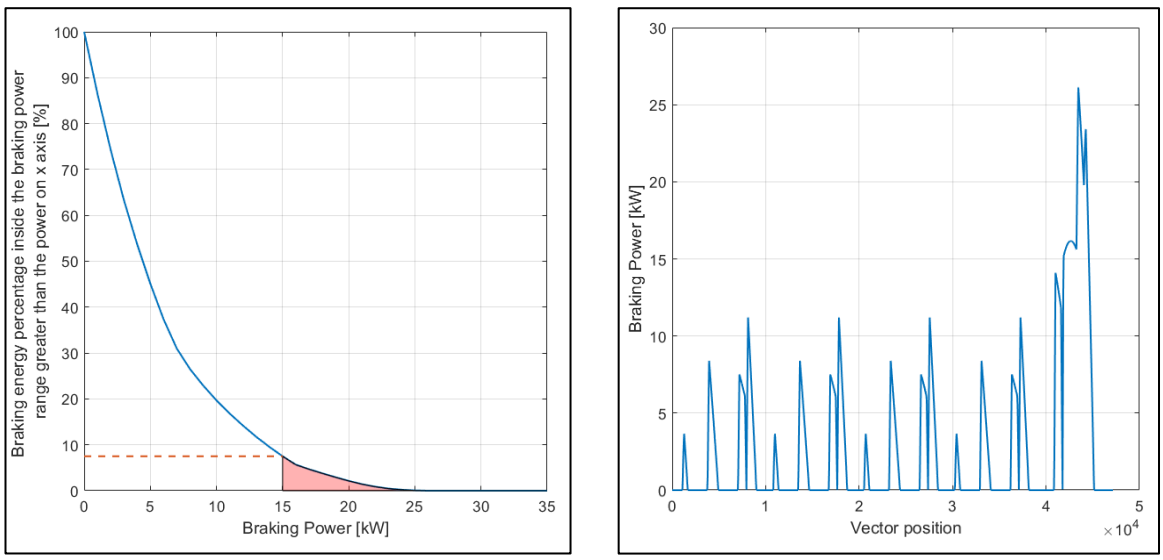

Figure 2.11 Braking energy percentage under a given power(left) braking power during the cycle(right)

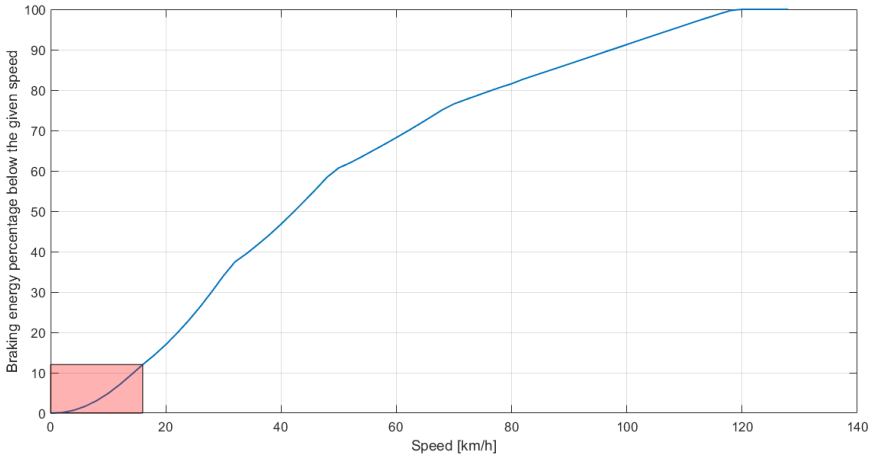

Figure 2.12 NEDC-Braking energy below a given speed

2.4.3 Final considerations of driving cycles

The analysis of cycles gives a good starting point to understand the energies and power involving braking and emphasizes the impact on efficiency of the propulsion system on how the vehicle is driven. Another information that can be extracted is that low power electric motors, in the order of 30 kW, would be enough to brake vehicles in urban cycles. Moreover, if compared to traction power for the WLTP cycles in Figure 2.13, the same 30 kW motor would limit the performances to a negligible extent; for example, a 15 kW motor would be impossible to be used in this case because it would limit the performances of the vehicle too much as showed in Figure 2.13. What discussed here does not consider inefficiencies and the fact that 30 kW in braking or traction for the vehicle would require a greater power motor, but it points out the importance right powertrain for the right application. This is because electric powertrains have a very good advantage with respect to IC engines: that is working with higher efficiency and regenerative braking also increases the overall. Moreover, if the average usage of vehicles is considered like the Figure 2.14 representing the annual usage of vehicles in UK [14], only 18% of total miles per year is coming from motorways and therefore going out of what a urban driving cycle can represent or optimize for electric vehicles. The best thing seems to be, changing urban mobility and vehicles toward specialization for urban driving and sensibilization of customers to use less powerful and heavy vehicles to improve electric powertrain performances. This will give the possibility to design more efficient powertrains for a smarter and greener mobility for the upcoming years.

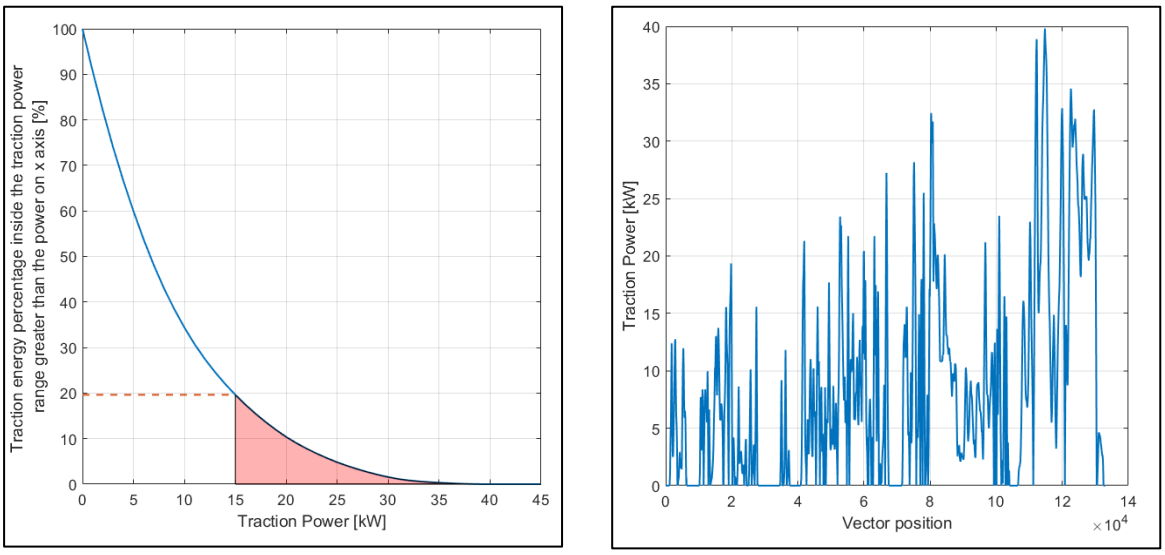

Figure 2.13 WLTP-Traction energy percentage under the power(left) traction power over the cycle

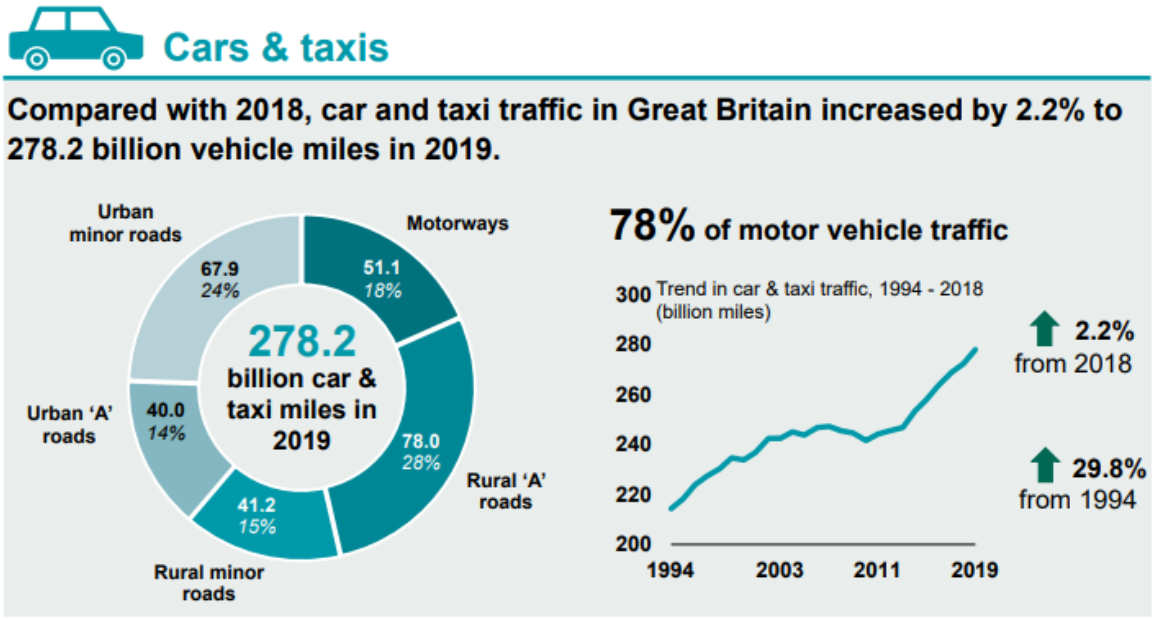

Figure 2.14 Road traffic estimates-Great Britain 2019 [14]

2.5 Regulations on braking and category divisions

The driving factors for braking and regenerative braking have already been listed but another requirement has also to be taken into account, legal regulations. The European Union regulations regarding the braking systems in passenger vehicles are described by two documents:

1) European regulation (EC) No 661/2009 [15],

2) ECE Regulation 13H and 13.11 [3].

These regulations are largely similar in terms of vehicles with conventional propulsion systems but differ concerning the requirements for H/EVs, which are given in the ECE Regulation 13H and 13.11. The Regulations 13H and 13.11 divide the braking systems equipped with a regenerative braking mode into two categories; A and B, where the category B is split further into two systems; non-phased and phased.

- Category A – describes the braking systems in which the regenerative braking system is not a part of the main braking system. Such systems use the regenerative braking only for throttle-off braking.
- Category B, non-phased – includes the braking systems in which the regenerative braking exists as a part of the main braking system. The regenerative braking torque can be delivered together with the friction braking torque or slightly after an activation threshold – parallel braking strategy.
- Category B, phased – the regenerative braking is a part of the main braking system. However, in this category the regenerative braking torque can be deployed before the braking torque generated by the friction brakes.

Category A brake systems require throttle-by-wire systems and cannot be used for strong braking since, talking of safety, an active and safe braking manoeuvre must be separated by the throttle pedal. This type of braking systems suite to emulate engine braking and to tune the level according to the need or driver feelings.

Category B systems will now be studied more in detail since they offer the possibility for brake blending and achieve very good levels of regenerated energy.

2.6 Brake blending layouts

The last part of the chapter is dedicated to the analysis of different layouts of category B systems and how regenerative braking and conventional friction braking can coexist in a vehicle, that is literally said brake blending.

Regenerative braking introduces some complexity to the braking system design. Two basic questions arise: how to distribute the total required braking forces among regenerative braking and frictional braking to recover as much braking energy as possible and how to distribute the total braking forces on the front and rear axles to achieve stable braking performance. These two requirements are opposite to each other since going far from the ideal braking line means for sure leaving braking performance and stability. On the other side if we want to maximize forces on one axle, we should leave the ideal line and in the following part it will be explained how.

This chapter introduces two configurations of hybrid brake systems and their corresponding design and control principles for the vehicle presented in Table 1.1. One is the parallel hybrid brake system, which has a simple structure and control and retains all the major components of conventional brakes also mentioned in Chapter 1. The other is a fully controllable hybrid brake system which can fully control the braking force for each individual wheel, explained for the EBD case in Chapter 1, thus greatly enhancing the vehicle's braking performance on all types of roads.

2.6.1 Parallel systems

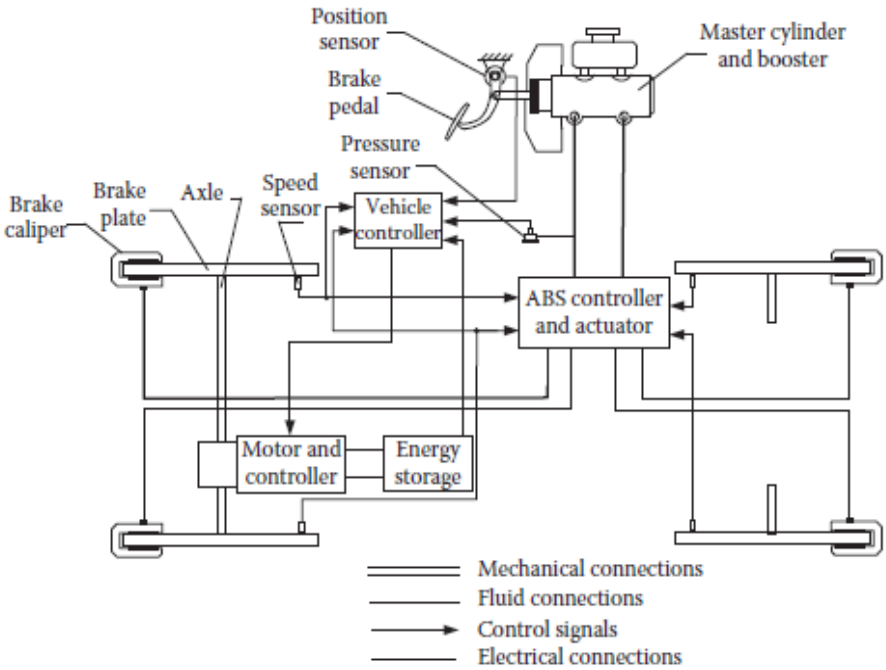

Figure 2.15 Possible parallel system layout

Perhaps the simplest system that is closest to conventional pure mechanical brakes (hydraulic or pneumatic) is the parallel hybrid brake system, which retains all the major components of conventional mechanical brakes and adds electric braking on the most convenient axle or where it is available, like represented in Figure 2.15. The mechanical brake system consists of a master cylinder and booster. It may or- may not have an ABS controller and actuator but has a brake calliper and brake disks. The electric motor directly applies its braking torque to the axle and is controlled by the vehicle controller, based on vehicle speed and brake pedal position signals, which represents the desired braking strength and braking control strategy embedded in the vehicle controller. The feature of the parallel hybrid brake system is that only the electric braking force (torque) is electronically controlled, and the mechanical

braking force (torque) is controlled by the driver through the brake pedal before the ABS starts its function.
Besides the actual friction braking system used, that is not part of this work, the interesting part is how to develop an effective regenerative strategy with a parallel layout. In the configuration of vehicle used, the friction part is represented in Figure 2.16 by the black line with respect to the ideal line and the ECE regulation already explained in Chapter 1.
This friction brake system is designed to work in ideal conditions when the grip offered by tire-ground contact has a value of 0.9. This would allow good efficiency over the working range but most of all, guarantee that also for emergency braking conditions (ax/g>0.7 [13]) front wheel will lock before rear ones, preserving so the stability during braking.

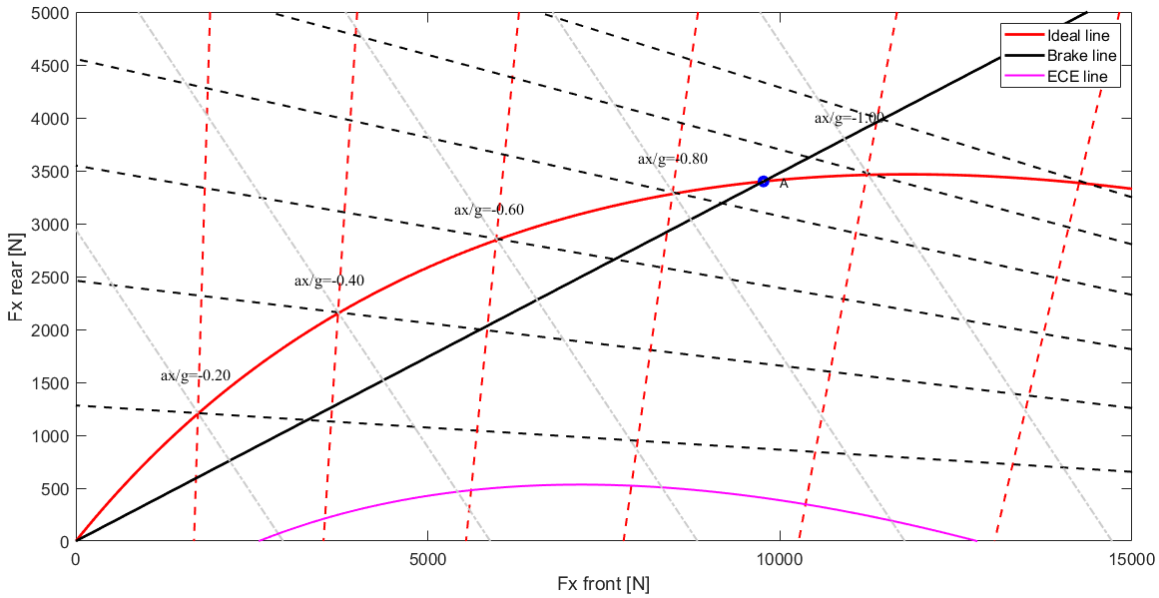

Figure 2.16 Friction system characteristic

The analysis on drive cycles explained before has been used to decide the amount of regenerative braking in parallel with the friction line. To give an idea of how forces and thus torque will be distributed in parallel, Figure 2.17 is used.

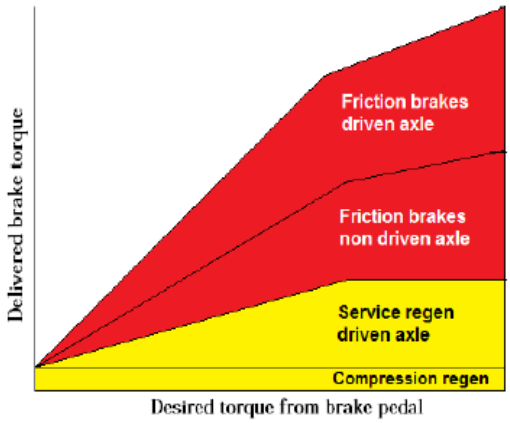

Figure 2.17 Generic parallel brake torque division

2.6.1.1 Parallel system-Regenerative force allocation

The allocation of regenerative portion for parallel systems will be done by following some constraints, coming from the previous analysis on the drive cycle, braking safety and driver feeling [13]:

- Maximum deceleration where only regenerative forces are allowed <= 0.1g: For decelerations less than 0.1 g, representing the vast majority of decelerations in urban drive cycle, regenerative can be used alone, emulating the effect of engine braking for conventional vehicles. For deceleration higher than 0.1g also the friction system will contribute to braking. In between 0.1 and 0.7 g (see the second point), regenerative braking is effective and can be distributed over the axles. In this analysis, front regenerative braking has been preferred since it represents a good share of market where motors are mounted on front axles using the assets of ICE placement on already designed and established platforms that represent very high cost for every OEM and because it represents a limit case for braking stability.
- Limit deceleration where regenerative is allowed = 0.70 g: Since decelerations>0.7g represents emergency braking [13], only friction braking will be allowed from 0.7g on, to enhance safety.
- Maximum regenerative force obtainable from motor characteristics: the maximum braking torque coming from the motors (and calculated at ground) has to be considered as constraint because it is usually greater than average braking forces but could be lower than strong braking forces.
- Minimize force compensation effect on brakes when regenerative decreases: This constraint has been set because a sudden loss of regenerative effect or also a drop of available regenerative force because of SoC or motor rpm would cause a sharp fade of force and thus deceleration. This effect will cause the driver action on the brakes to compensate for that loss of forces. This effect is conditioned by the difference in slope of the parallel line (blue) and hydraulic line (black) in Figure 2.18. The greater the force applied, the bigger the difference between blue and black line and the greater the required action by the driver with uncomfortable sensations. Force fade due to regeneration must carefully evaluated and stated when presenting the vehicle to tests for homologations, but it is not really limited. In this work the 3500 N limit has been set so that the difference is always under the equivalent of 0.25g of deceleration.

2.6.1.2 Different regenerative forces allocation on parallel systems

In Figure 2.18 are presented different parallel system lines superimposed to the ideal braking line (red line) and the hydraulic system line (black line). All the lines will have different amount of regenerative action on front axle, fraction of the maximum front axle force at 0.1g. The different front axle regenerative allocation can be seen in Figure 2.19, but it is straightforward that the greater the force coming from motors with respect to brake line, the higher will be the efficiency of the braking manoeuvre. Therefore, being 0.1g judged safe to let regenerative brake alone, the reference system will be the blue line in Figure 2.18, also represented in Figure 2.21 alone.

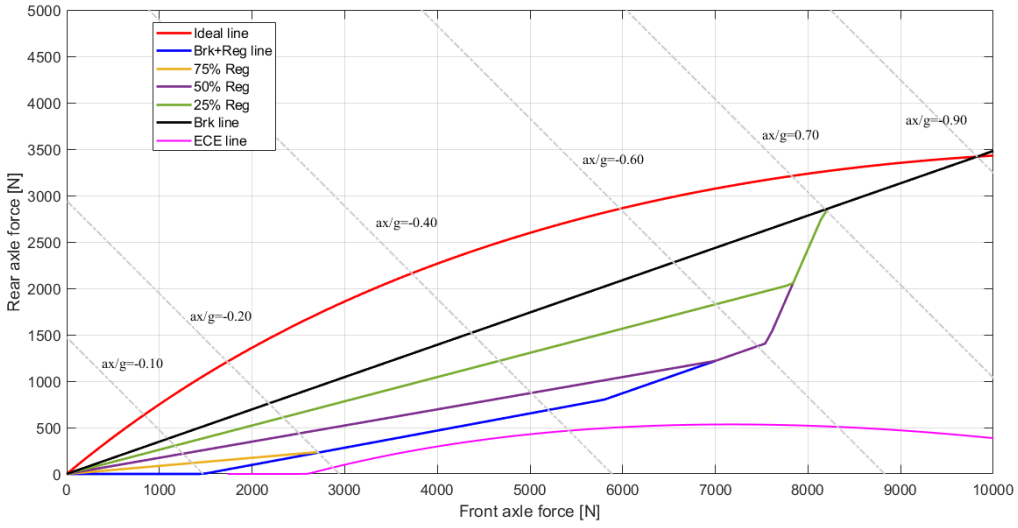

Figure 2.18 Different parallel system lines

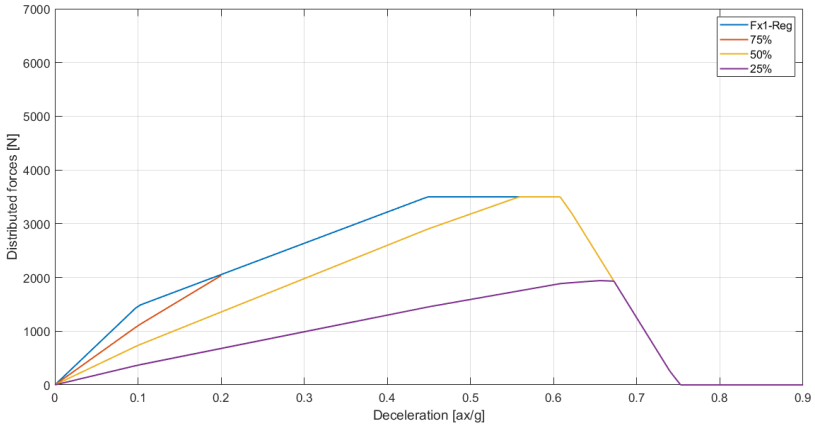

Figure 2.19 Different regenerative force allocation for parallel systems over deceleration rates

2.6.1.3 Reference parallel system behaviour-Maximizing regenerative effect

The parallel system that will be adopted in this works as reference, and represented in Figure 2.21, utilizes only front forces developed by electric motors until 0.1g and is always over the ECE regulation. Moreover, to maximize the amount of regenerative force, electric braking is increasing up to 0.6 g and then set to go to 0 Nm at 0.70 g so that the last part, with more aggressive braking manoeuvres, is left to friction braking. This behaviour can be also seen from Figure 2.20 where the different forces are distributed from regenerative to friction on the different axles depending on the acceleration. At the same time, it reaches the maximum of 3500 N at about 0.45 g in order to limit the force compensation on the brakes as written before.

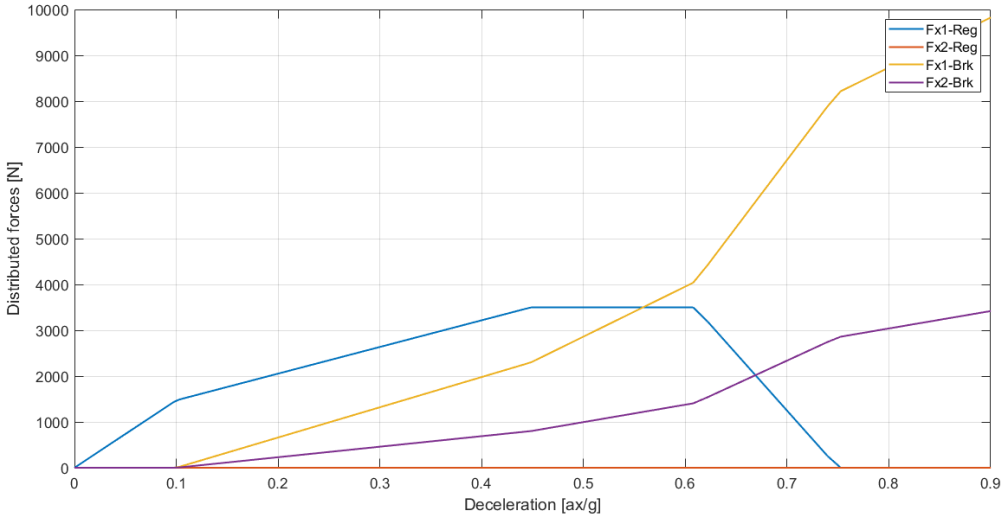

Figure 2.20 Parallel system forces over deceleration rates

With this strategy, with a deceleration such as 0.4g it will happen what described in Figure 2.21. The total line, blue in Figure 2.21, meets the total force requirement of 4g's with the front axle force=5226 N and rear axle force=660 N. Since the systems are in parallel a certain force will be applied by the friction braking that form the same graph it will be a force of 1900N on front axle and 660N on the rear. This means that the total regenerative force applied on front axle is Fx1_reg=5226-1900=3326 N which represents the 60% of total braking force on front axle and 56% of total force.

In the case of lower decelerations, e.g. 0.15g (see Figure 2.22), 2097 N on front axle will be necessary and from this system layout, 320 N will be applied by the friction braking system on the front and 110 N on rear, meaning that regenerative forces will account for (2097-320)/2207 =80% of total braking force.

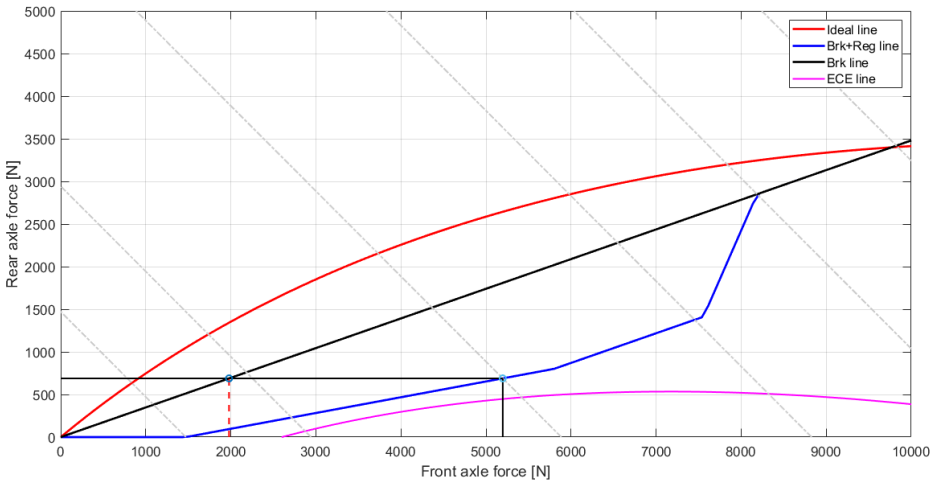

Figure 2.21 System behaviour under 0.4 g of acceleration

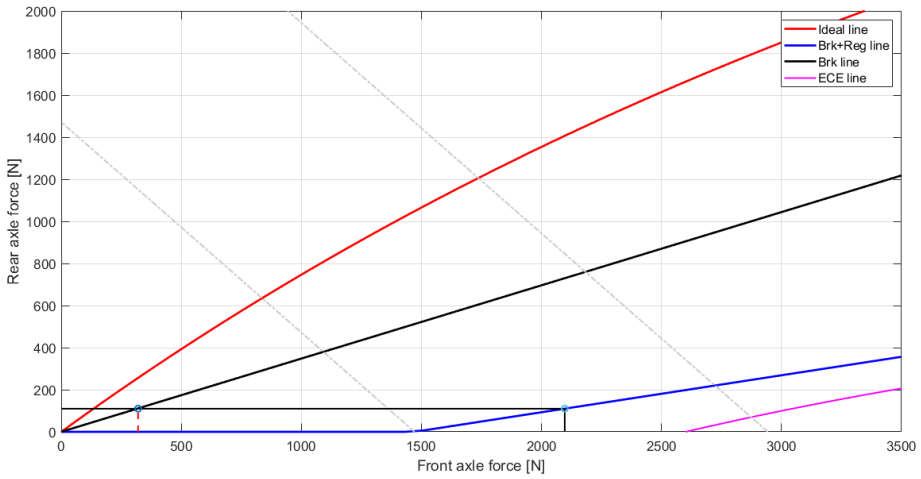

Figure 2.22 System behaviour under 0.1 g of acceleration

2.6.2 Series systems

In recent years, more advanced braking systems have emerged that allow to control the braking force on each wheel independently. Hydraulic-electronic brake systems (H-EBSs, represented in Figure 2.23) and mechanical electric brake systems are two typical examples. A Hydraulic-electronic brake system consists mainly of a brake pedal and its position sensor, a master cylinder, an electrically operated and controlled brake actuator, electrically controlled three-port switches, a fluid accumulator, and a pressure sensor [16]. The mechanical braking torque applied on each wheel is independently produced by the corresponding brake actuator, which is commanded by the H-EBS controller. The torque command to each wheel is generated in the H-EBSs, based on the pressure signal from the pressure sensor, the brake pedal stroke signal from the brake pedal position sensor, wheel speed signal from the wheel speed sensor, and the embedded control rule in the H-EBS controller. One of the key problems in this system is how to control the mechanical and electric braking torques to obtain acceptable braking performance and recover as much of the available regenerative braking energy as possible. With the possibility to change pressure inside the mechanical braking system it is also safe to let the electric motor supply also all the necessary torque needed. This means that is also possible to follow the ideal braking line with very high performances as already explained in Chapter 1 when the EBD was explained.

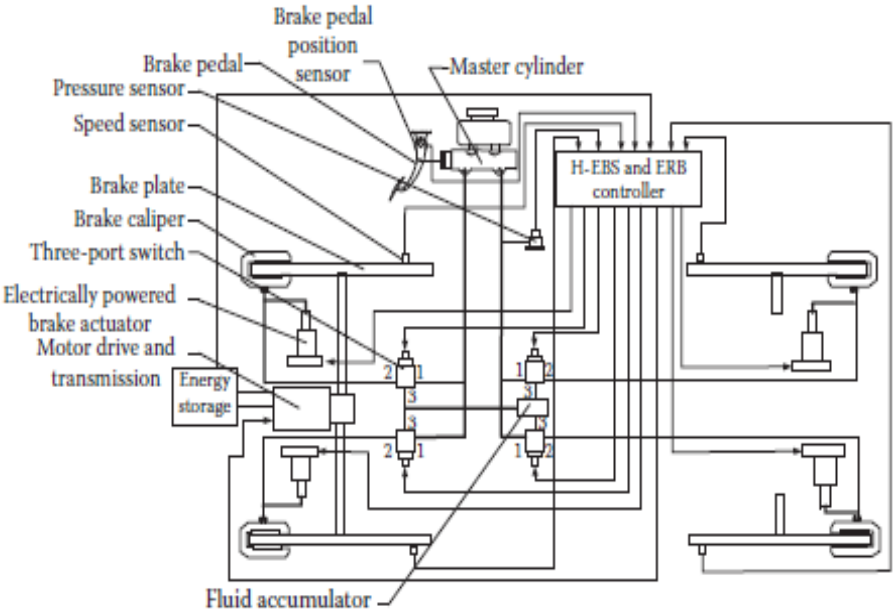

Figure 2.23 Series system-possible layout

The series system logic, generalized in Figure 2.24, will divide the force between friction and electric brakes always giving priority to regenerative but also following the ideal curve. If the needed braking force is higher than what the motor can give in that condition (considering SoC value and speed) the remaining part of the torque will be supplied by the friction brakes. The problem that was encountered with parallel systems concerning the acceleration gap by force fade due to regeneration does not represent a problem in series systems. This is because the division between regenerative and friction forces are split time by time and adjusted and where the input from the driver sets the maximum values. The only limit to this system is the speed of the hydraulic circuit to build up the pressure after the control unit input but remains hundreds of times faster than humans.

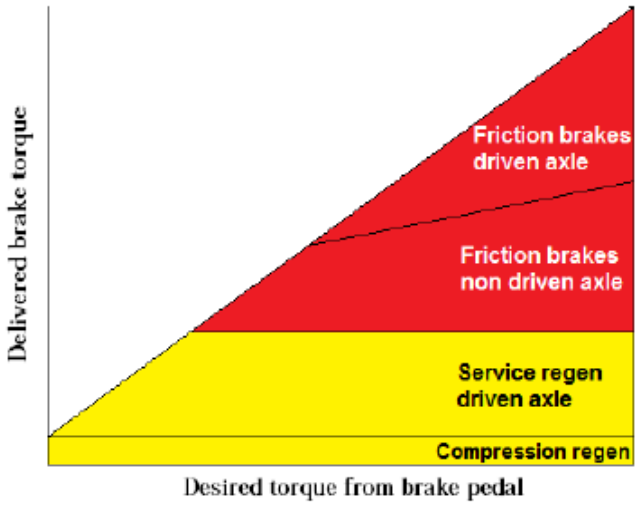

Figure 2.24 Generalized series systems

2.6.2.1 Modification to series systems logic

The need to modify this logic is coming because of the gap that is present in regenerative forces if the ideal line is followed. This can be seen in Figure 2.25; If it is assumed that electric motors can apply much higher forces than what needed to decelerate the vehicle at 0.1 g rate, it is possible to see that the force that would be applied on front axle by following the ideal line is always lower than the one corresponding to 0 N applied on rear axle at equal deceleration, that would represent the parallel system described in 2.1.6.3. This means that the total force is divided by front and rear to have a balanced braking, but regenerative forces are sacrificed and consequently this logic will be less effective with respect to parallel systems.

If 4WD was used there would have been no need to change the ideal line but in case of front/rear wheel drive, where there is a waste due to friction brake on the axle where motors are not acting, has been decided to use full regenerative under 0.1g deceleration as indicated by "FWD line" in Figure 2.25.

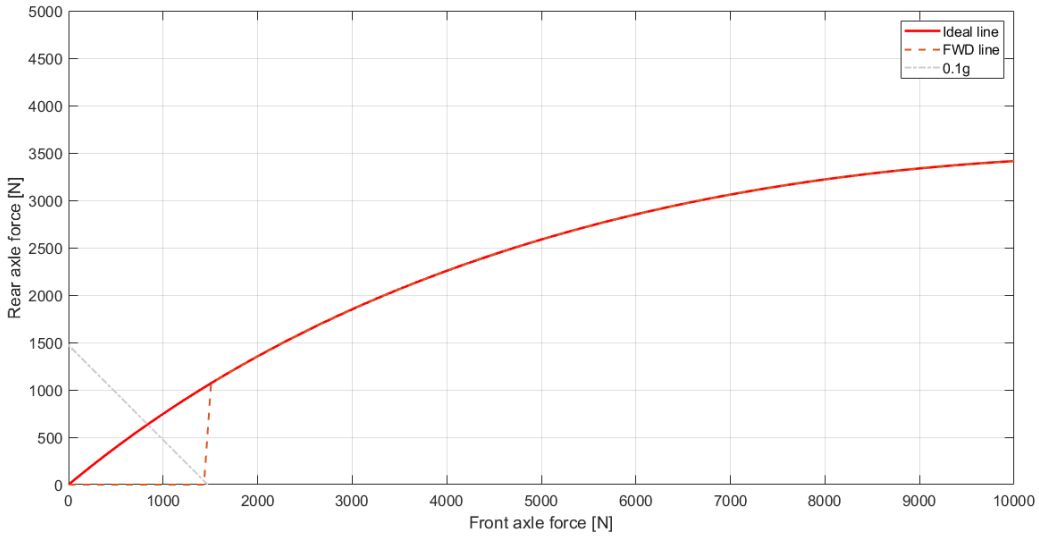

Figure 2.25 Series system-Ideal line and full front regenerative line (FWD)

2.6.2.2 Full regenerative series logic

What discussed in the previous paragraph opens to a more general logic that will go away from ideal line to maximize regenerative forces. It is represented in Figure 2.26, and it will use regenerative always in the limits of the red area, between ideal (red line) and ECE line (purple line). The principle of its functioning is explained in Figure 2.26 and Figure 2.27. When the maximum regenerative force is higher

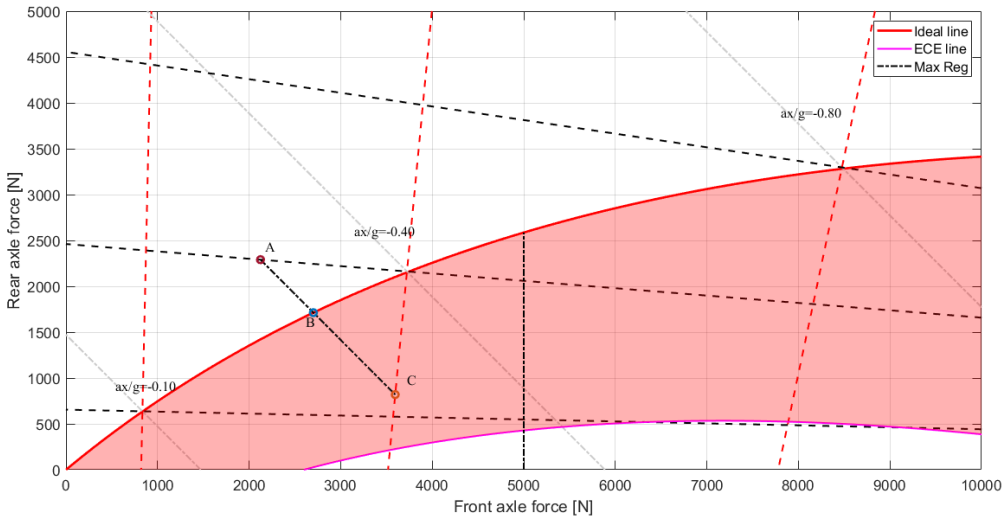

Figure 2.26 Series system optimized strategy behaviour with low force request

than the maximum needed for braking (considering a front wheel-drive electric vehicle), all force is going on the front/regenerative with the only limit of following ECE line that means to decrease the force on the front and apply friction on the rear. This is limited also by the grip factor μ that in Figure 2.26 is 0.4 (simulating wet conditions).

In the case represented, an acceleration of 0.3g is requested that would be fulfilled by the line $\overline{AC}$. This limit is coming from the friction available of 0.4 that sets the maximum force repartition before rear, point A, and front, point C will slip. In this situation the series system used will brake at point C that is 3500 N on front and 820 N on rear instead of braking at point B. Thanks to this logic the braking forces will be less balanced, but the portion of forces covered by regenerative braking will be higher.

In Figure 2.27 the grip is higher, set to 0.8 like good dry ground but also the request of braking forces is higher. In this case the maximum regenerative force is lower than the requested and represented by the vertical line in Figure 2.27, This logic will apply the maximum regenerative torque and will add friction braking to front and rear to follow the ideal line. It means that for the case of 0.7g represented in Figure 2.27, since the maximum regenerative force is 5000 N to be expressed on front axis and the point C cannot be reached with only regenerative, the hydraulic circuit will provide 2200N on front and 3090N on rear to reach point B on ideal braking line.

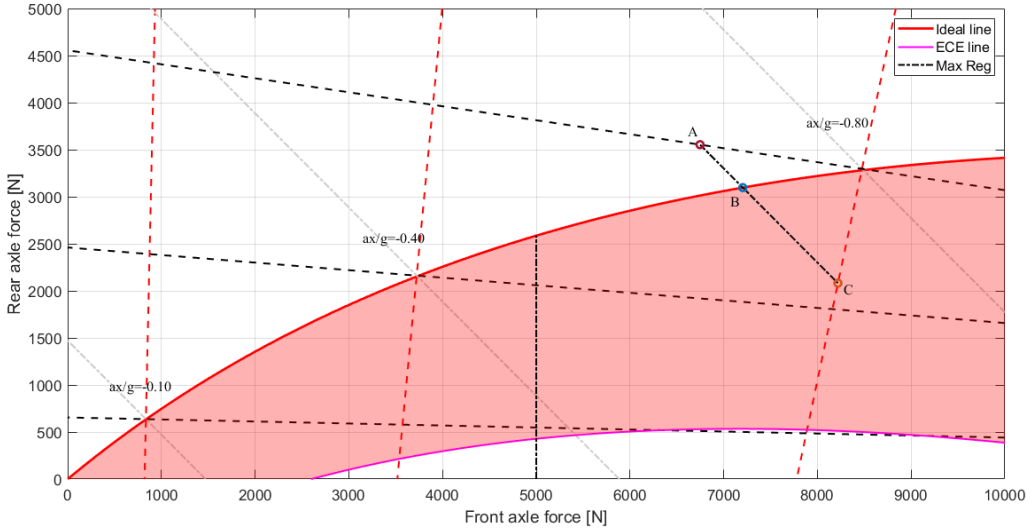

Figure 2.27 Series system optimized strategy behaviour with high force request

2.6.3 Examples on the different behaviour in braking

The main characteristics of the two systems have been presented in last paragraphs; from constructional point of view, parallel systems are closer to mid-low budget vehicles and maintain the well-established braking line structure with the addition of regenerative action, controlled separately. Series systems imply new hardware like brake by wire or more sophisticated pressure lines now only used in high-end vehicles. In Figure 2.28 are reported the entity and the distribution between friction and regenerative forces.

Series systems:

For the first part of the braking manoeuvre there is no need for system to apply front friction forces because the torque available at motors is enough but at the same time it will apply a rear brake force because the acceleration is higher than 0.1g.

When the motor torque cannot be used anymore because of low speed, only friction force will be applied and, in this situation, will be only at the front, following the FWD in Figure 2.25 curve, under 0.1g.

Parallel systems:

The parallel system is obliged to use front and rear friction force when the motor cannot provide all the force in that instant (being the deceleration greater than 0.1g) and the friction forces will follow the K_b line (or repartition) of the system.

In the second part of the brake there is the same split, following the curve of the reference system of Figure 2.21.
It is possible to see that force and so pressures are different and whereas the series system applies the optimum force depending on the ideal line, parallel systems can only apply the established forces by the brake line construction.

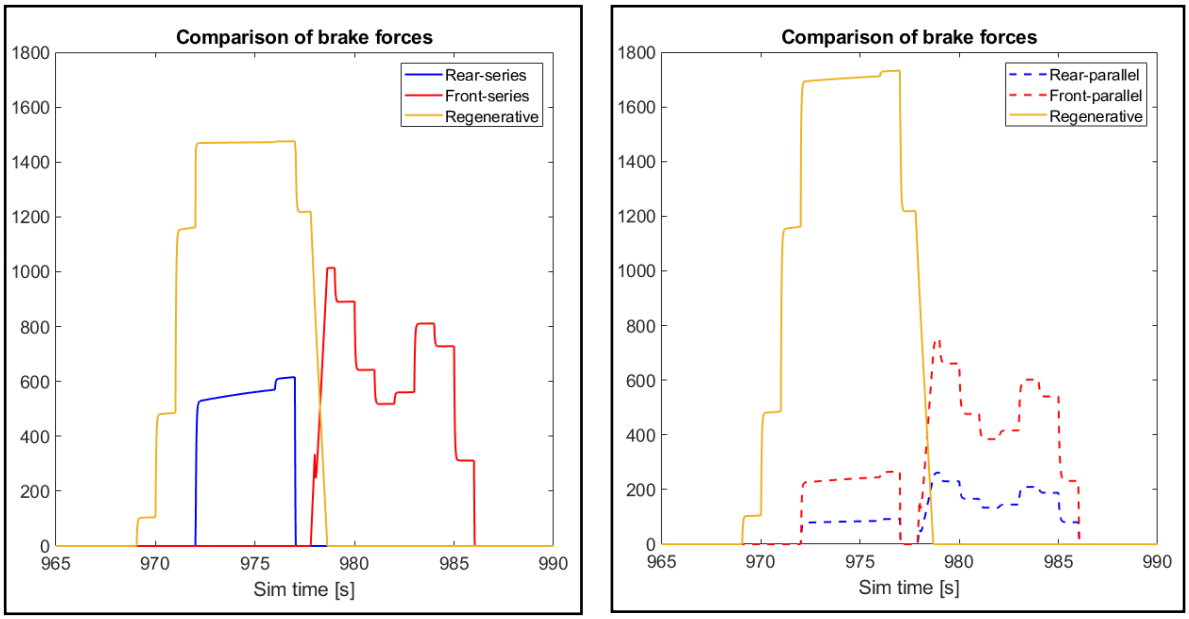

Figure 2.28 Brake forces comparison between series(left) and parallel(right) systems

The fact that the system is in parallel also brings other differences that are highlighted in Figure 2.29. The command applied by the driver on the brakes is substantially different. On the left the series system is represented and is much more constant looking at its peaks.
On the right of Figure 2.29 is possible to see that the command for parallel systems is not constant and this is due to the change in available torque from motors. A change in available torque means different requirements to the driver to maintain the wanted deceleration with the now only available friction system. This translates to changing feeling during braking and challenging situations for drivers used to only friction brakes.

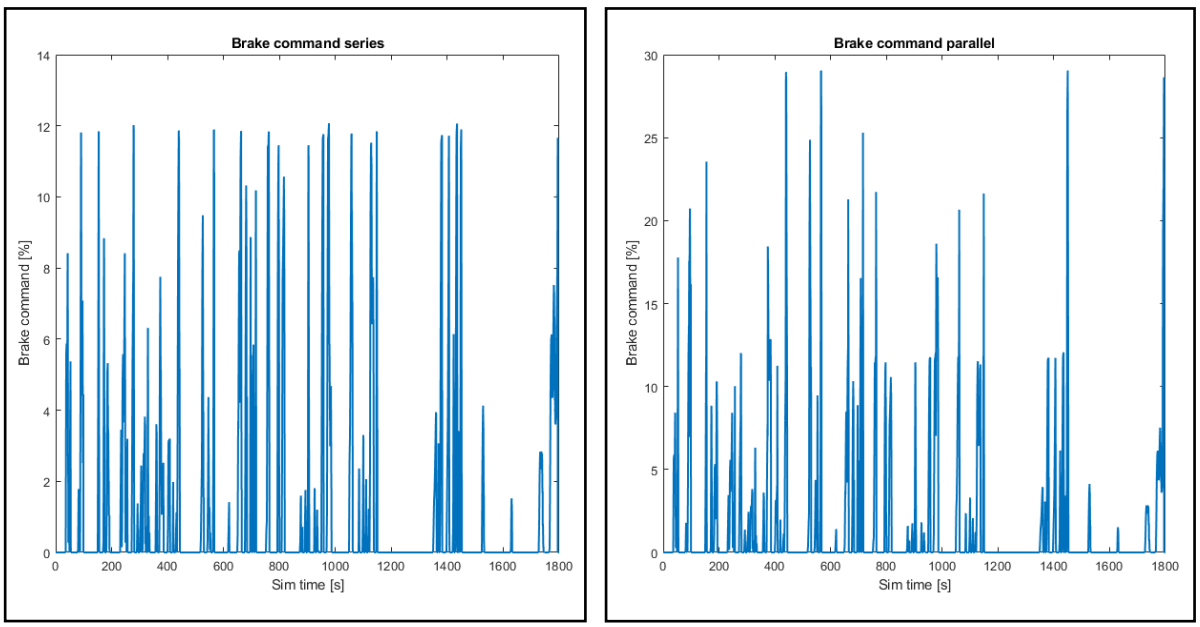

Figure 2.29 Brake pedal input comparison between series(left) and parallel(right) systems

3 Vehicle model simulator

Chapter 3 is about an explanation of the MATLAB model used in this work along with the considerations done and the performance analysis of the different brake blending control.

3.1 Overall layout

The model in Figure 3.1 is based on the BEV model by MATLAB that can be found in MATLAB Central [17] and opportunely modified with the data used for this work and by substituting or modifying some subsystems. This is composed by a brake system subsystem, motor subsystem, driveline and battery model and the final vehicle model represented by point mass, that as explained in the previous chapters is enough to represent brake cycles to a very good extent. Once the speed profile followed by the vehicle has been computed, the driver, represented by PID controller decides whether to brake or accelerate and at which extent.

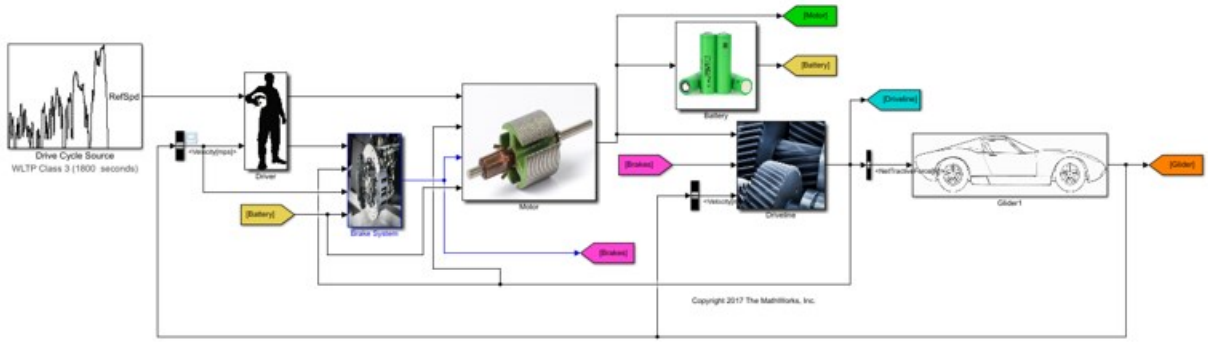

Figure 3.1 Simulator layout

3.2 Battery subsystem

One of the first steps of battery modelling is to decide, what is the purpose of the modelling itself. Every application of the model requires slightly different approaches and parameters. There is no strict rule, how to categorize battery models, same models can belong to more than one class.

There are different perspectives of modelling, to:

- Electrochemical models, electrical models, thermal models, mechanical models, molecular models, o combinations of interdisciplinary models (electro-thermal, etc.),
- Different depth of modelling: for system level, pack level, stack and module level, full cell level, material level
- Different techniques or approaches: physical based models (Electrochemical), empirical models, analytical or mathematical model, equivalent electrical circuit models, stochastic models, hybrid models
- Different time scales of the models: short term (dynamic behaviour, partial charge, discharge), medium term (full cycle), long term (multiple cycles, complete lifetime).

In this work, an electrical circuit-based model has been used. It models the equivalent electrical circuits to capture the characteristics of batteries by using the combination of voltage and current sources, capacitors, and resistors. Some of these models can also track the SoC and predict the runtime of the batteries by using sensed currents and/or voltages. The electrical circuit models are good for codesign and cosimulation with other electrical circuits and systems. However, the existing electrical circuit models do not integrate battery nonlinear capacity behaviours, leading to an inaccurate prediction of remaining battery capacity and operating time.

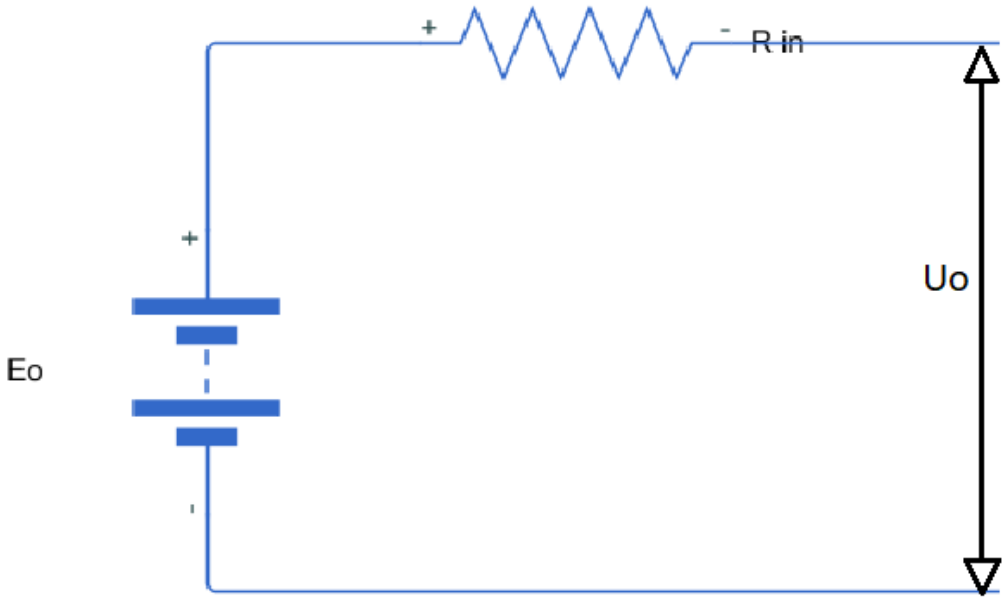

Figure 3.2 Battery equivalent circuit model-Open circuit voltage and internal resistance

This model is the simplest and the most approximate equivalent circuit model. It consists of an ideal battery with open-circuit voltage E_0 and constant internal resistance R_{in} (Figure 3.2) Both values can be obtained from open-circuit measurements and measurements with connected load when battery is fully charged.

The pack is modelled using as reference the battery pack of a vehicle in production with:

Table 3.1 Vehicle battery pack configuration

Total capacity	40 kWh
Number of modules (configuration of the module)	24 (4s2p)
Rated voltage	3.65 V
Rated discharge capacity	56.3 Ah

The choice on this model comes from evaluations of possible drawbacks. Dynamic behaviour of current, voltage or dependence on temperature values have not been considered because there has not been used a motor and power controller model that could use that and because this work has not the goal to investigate on the dynamic behaviour of electrical components but to guide to the choice at system level of the regenerative braking.

In fact, talking about regenerative braking and system level it has been considered maximum charge and discharge limits to avoid the problems on battery cells explained in previous chapters and a power management algorithm is also present to limit the torque request (Figure 3.3 and Figure 3.4).

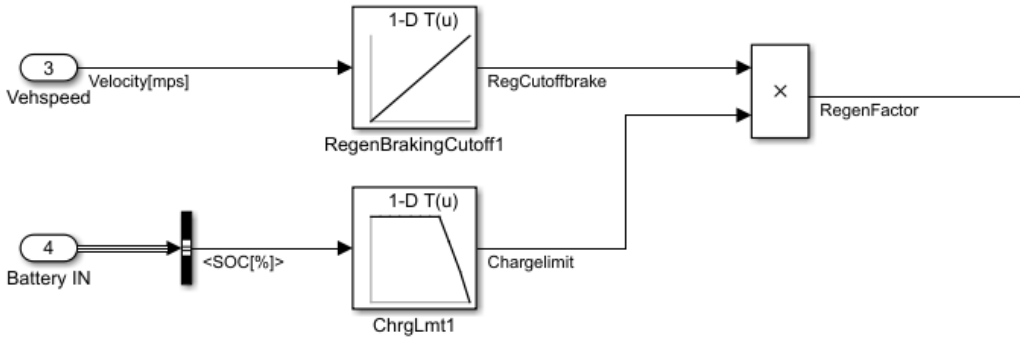

Figure 3.3 Regenerative braking cut-off due to speed and SoC level

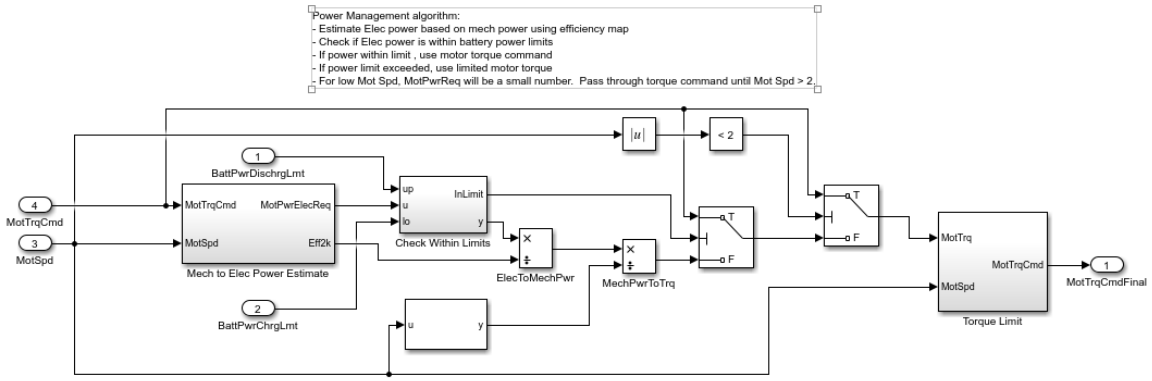

Figure 3.4 Electric powertrain power management system

3.3 Powertrain-Motors subsystems

The configuration used in the model is a pure electric vehicle that has its motor mounted on the front. Moreover, there is the possibility to switch between forward, rear and all-wheel but front wheel drive will be preferred since it covers the greatest piece of market configuration for urban vehicles.

The motor used is the one in the Figure 3.5 and is an 80kW motor capable of 280 Nm and limited to 10000 rpm that with 1250 kg of curb mass will enter among the 64 kW/t vehicles. That amount of torque is not enough for traction purposes neither to brake with today's performances. Thus, a final ratio of 7 is used on the transmission so that is possible to achieve good torque values and the final speed of at least 150 km/h.

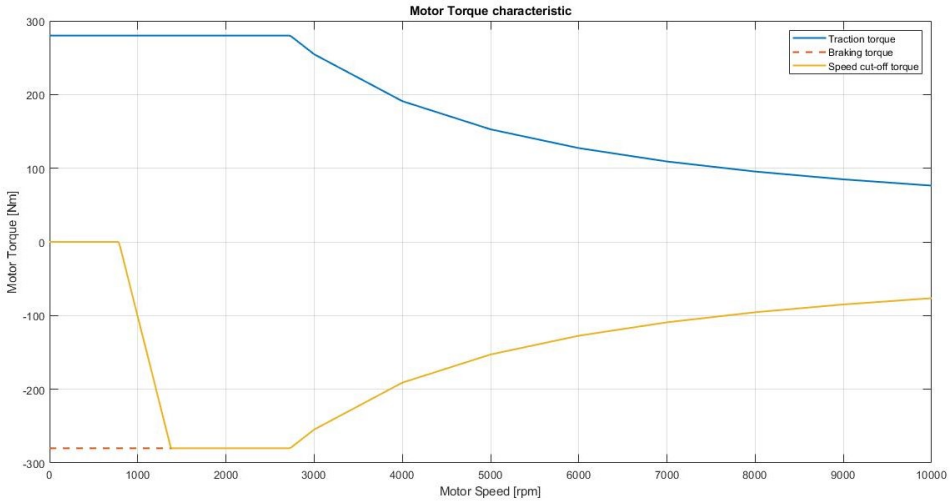

Figure 3.5 Motor torque characteristics in traction and braking

Finally, also the powertrain efficiency is considered by means of the efficiency map illustrated in Figure 3.6. In the efficiency map represented are considered power converter efficiency, usually very high, mechanical efficiency of powertrain and efficiency for the motors that is usually the bottleneck as least efficient element.

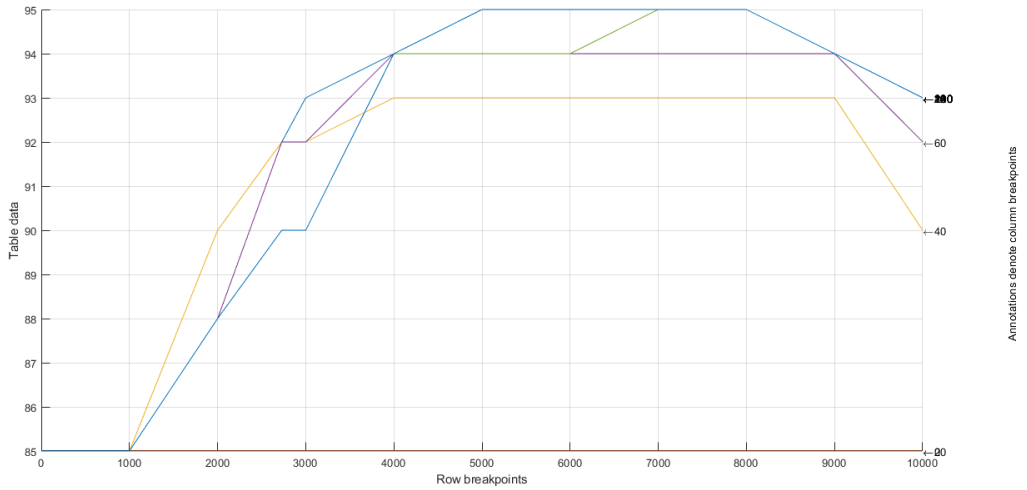

Figure 3.6 Motor and converter efficiency look-up table

3.4 Glider model

In the glider subsystem is present the model used to describe the motion of the vehicle. A point mass vehicle is used; acceleration is determined by the total available tractive force at which are subtracted the aerodynamic drag, rolling resistance and forces due to grade like represented by the formula 3.1 and 3.2.

$$a_x = \left(\frac{F_{tr} - F_{drag} - F_{grade} - F_{RR}}{m_{tot}}\right) \tag{3.1}$$

Where:

-F_{tr} is the total traction force available from powertrain point of view

-F_{drag} is the aerodynamic drag acting against the vehicle motion

-F_{grade} is the force due to grade of the road that must be presented but it is neglected in urban duty cycles like WLTP and NEDC

-F_{RR} is the rolling resistance force defined as in formula (3.2) where typical values are assumed based on data coming from literature. [1]

$$F_{RR} = -f\ F_z \tag{3.2}$$

Where:

$$f = f_0 + KV^2 \tag{3.3}$$

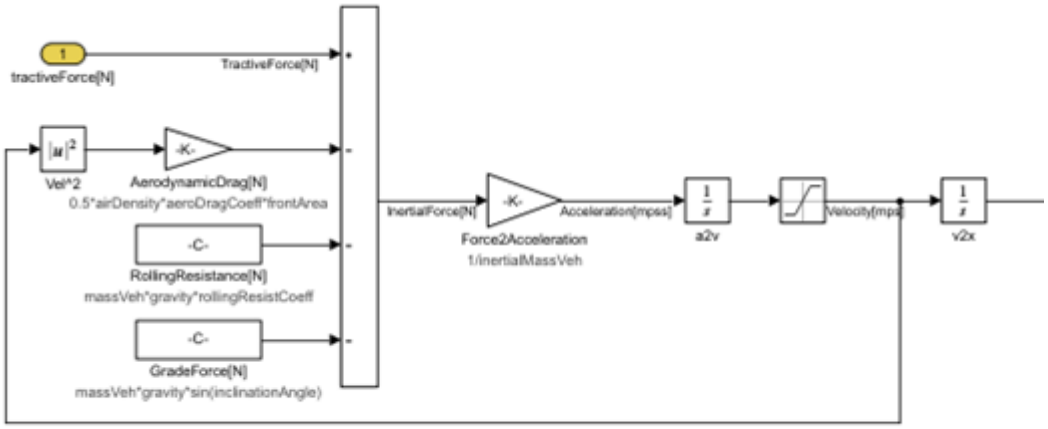

Figure 3.7 Vehicle dynamics model for straight traction/braking

3.5 Brake subsystem

The brake subsystem is the hearth of the study. Here is possible to switch between series or parallel braking and change so the strategy according to what explained in previous chapters.

The friction brakes are modelled on disc brakes by choosing the values for the brakes of a generic vehicle and setting the maximum pressure inside the line; all that will be subject to the driver decision on how much brake is needed.

Assuming disc brakes, the torque generated by a single brake (3.4) would be dependent on the friction coefficient μ, the total actuation area of the hydraulic piston(s) A_e actuating the pad times the number of pads, the hydraulic actuation efficiency, and the effective radius to generate braking torque:

$$\text{Torque}=\text{Pressure}*(\mu * A_e * R_e * \text{num\_pads} * \eta) \tag{3.4}$$

In this work are assumed the following values that are typical values in urban vehicles [1]:

-Friction coefficient=0.4

-Hydraulic actuation efficiency=0.95

The computed brake torque is compared to the maximum torque the electric motor can give according to speed and successively lowered by SoC limits and cut off due to low speed.

The way it is compared and distributed from rear to front and friction and regenerative depends on the strategy we decide to use. A more general definition of the logic that will be defined right after is the one in Figure 3.8 where it is represented a flowchart with the main things to look for and check. In practice, if the SoC value does not allow regeneration, only friction braking will be present. If the values of SoC allow regeneration, the force is divided according to the series or parallel system installed on the vehicle that have been explained in Chapter 2. The logic used will divide the braking request to friction brakes and regenerative brakes. This request will then pass through the subsystems already explained in previous sections.

Figure 3.8 Flowchart for brake blending

3.5.1 Parallel system model

According to the previously seen study, the maximum amount of regenerative is already stated as well as the behaviour of the friction line that in this case is fixed since it is directly dependent on brake pedal actuation. The maximum force request is subdivided into the friction and regenerative according to some look up tables as in Figure 3.9 defined according to the studies of Chapter 2. Only the regenerative force is compared with the maximum level available as in Figure 3.10 and lowered according to the conditions of the powertrain, i.e. speed and SoC. If the level of regenerative is lowered, the only choice is to depress more the brake pedal to gain that from mechanical brakes.

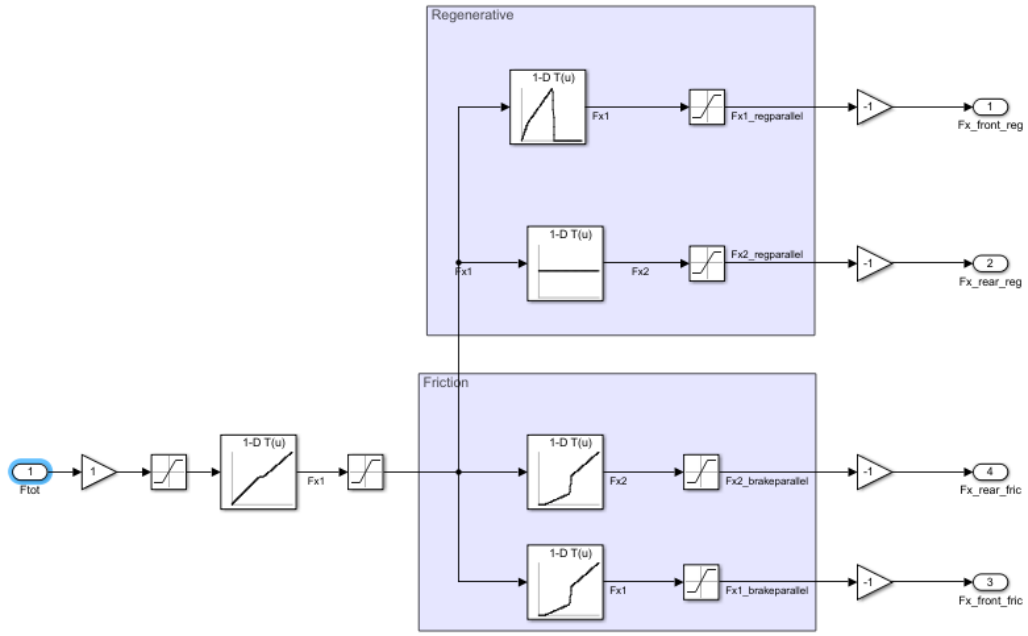

Figure 3.9 Parallel blending-Assignment of braking and regenerative forces

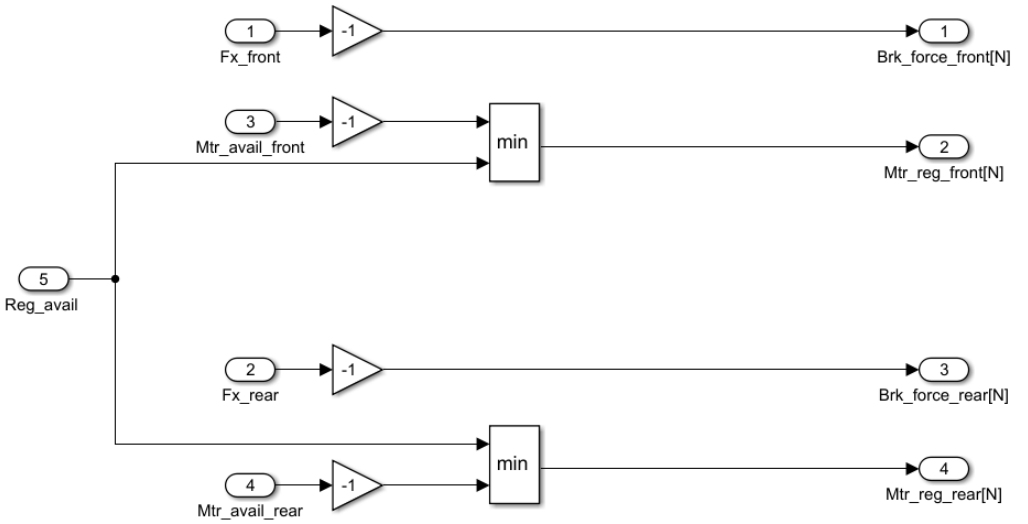

Figure 3.10 Parallel blending-Comparison between needed and available regenerative torque

3.5.2 Series system model

The first step is to break down the total brake force into front and rear forces following the ideal braking line as in Figure 3.11.

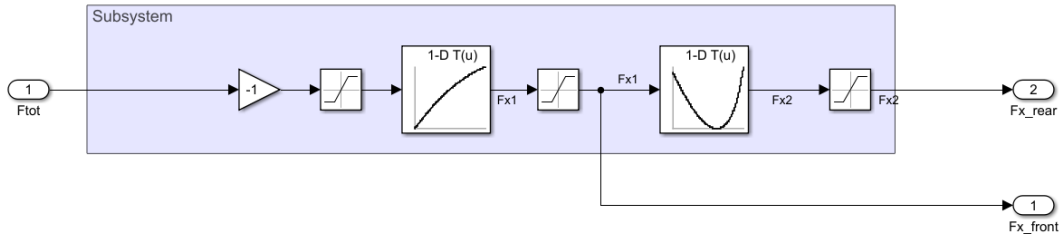

Figure 3.11 Series blending- Definition of ideal braking line

As second step there is the division between friction brake and regenerative force depending on if the regenerative braking can cover all the needed force. If so, friction line will not receive any signal to build up pressure and then force. If the available torque at the motor is not enough, the difference will be covered by the friction line, as represented in Figure 3.12. In this way, the amount of regenerated energy can be maximized in all conditions, even for strong braking.

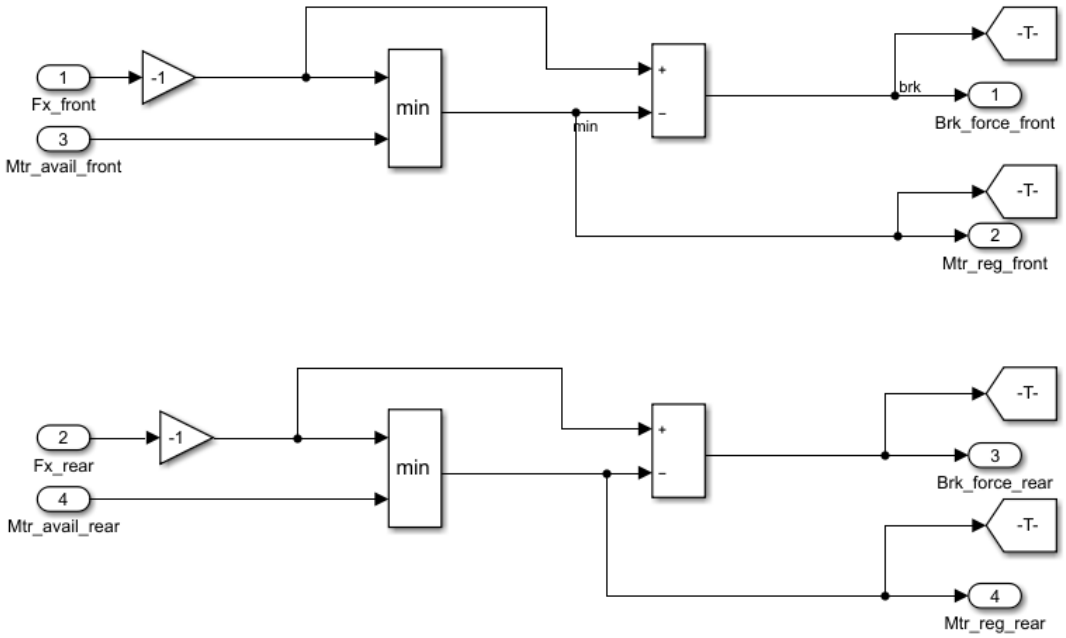

Figure 3.12 Series Blending-Assignment of braking and regenerative forces

4 Results

In the following chapter the results will be evaluated to see the difference between the two main strategies, parallel and series and their impact on energy recovery.

4.1 Main evaluation indexes for regenerative braking and energy recovery

Several parameters are tracked to analyse the effect of the different strategies to understand their effectiveness [18].

- A first parameter will be the amount of torque/force asked to the motors by the controller with respect to the force of the friction brakes, this gives an idea of the difference between the approach of the two strategies.
- SoC level will also be used to better highlight the differences and impact on the range even though it is a qualitative kind of information; quantitative assumptions could be done in presence of more sophisticated battery model.
- Regenerative braking efficiency will be also used. This KPI is defined as in formula (4.1)

$$\eta_b = \frac{Regenerated\ energy(E_b)}{Total\ baking\ energy(E_k)} = \frac{\int U_b I_b dt}{\frac{1}{2} m({v_b}^2 - {v_0}^2)} \tag{4.1}$$

Where the regenerated energy E_b is the effective recovery capacity of the braking energy and is calculated by using the charging current, voltage and sampling time of the battery pack during braking phase.

In the equation:

U_b-The voltage at the battery terminals when braking

I_b-Current at battery terminals when the vehicle is braking

Where E_k, is the total energy consumed during the braking phases and:

V_b-speed at the start of braking phase

V_0-speed at the end of braking phase

- Last indicator is represented by direct ratio between the total energy consumed by the battery and the regenerated energy that represents the percentage of regenerated energy in formula (4.2)

$$\xi_{reg} = \frac{Regenerated\ energy(E_b)}{Total\ used\ energy(E_{tot})} = \frac{\int U_b I_b dt}{\int U\ I\ dt} \tag{4.2}$$

Where:

U_b-The voltage at the battery terminals when braking

I_b-Current at battery terminals when the vehicle is braking

U and *I* are the voltage and current at battery level throughout the whole cycle.

4.2 *Braking at constant speed and different maximum deceleration*

One way to test the differences between the logics before seeing what happens in normal city driving is by means of the study on their performances at different deceleration, all starting at same speed so that there are no differences on the maximum torque the motor can exert.

The model will try to follow the input in speed in Figure 4.1 that will correspond to the accelerations displayed on the same plot (red line) where are tested four different decelerations of different intensity, -0.4, -0.3, -0.2 and -0.1g all starting at same initial speed of 60 km/h (blue line in Figure 4.1).

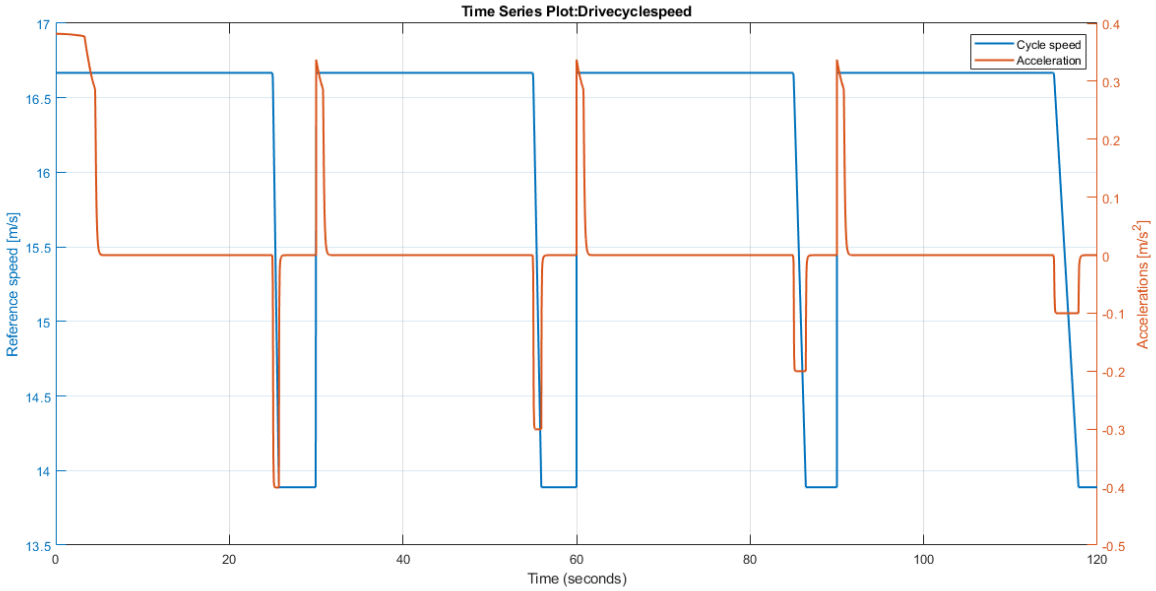

Figure 4.1 Pure braking at different intensities. Speed (blue) and acceleration(red) profiles

The first difference can be seen in motor torque amount at different accelerations as in Figure 4.2.

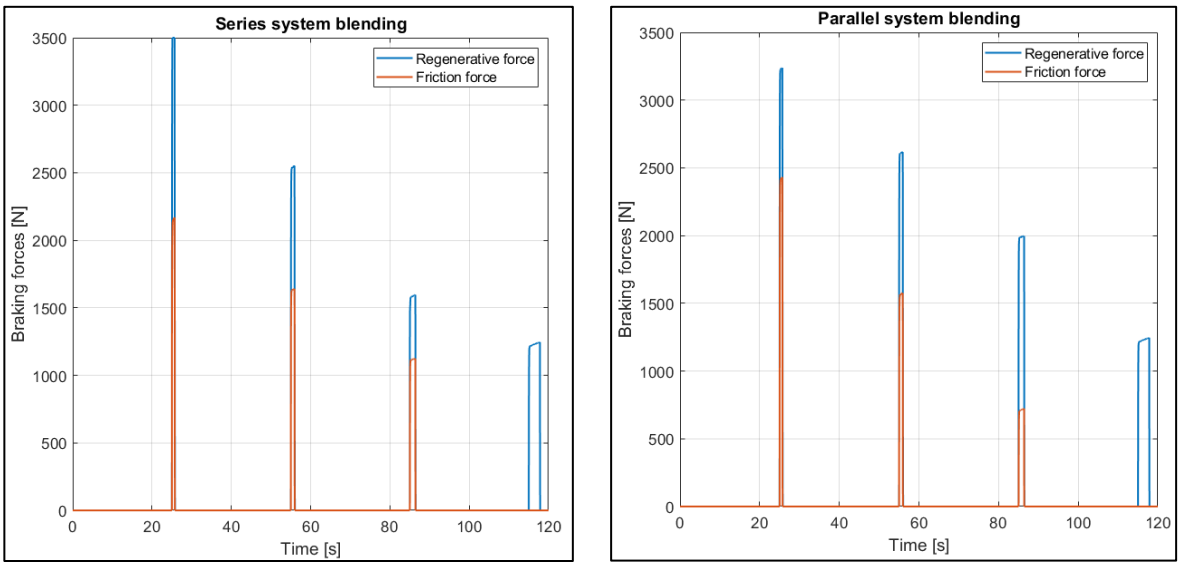

Figure 4.2 Torque amount at different accelerations- Series(left) Parallel(right)

At low accelerations, below or equal to -0.1 g, the two systems are made to behave in the same manner if the powertrain is a FWD one. This allows to have complete coverage by the electric motor on the total braking force. With accelerations greater than -0.1g the first difference appears. Series systems, following the ideal line will give part of the total force to rear wheels that are not regenerating energy.

On the contrary, at accelerations over -3g, series systems will have more electric force than parallel systems that are forced to split it also to the friction/parallel line.

If we use the regenerative efficiency parameter defined before, is possible to compare the results of the two logics as in Figure 4.3. Both series and parallel system can reach 50-60% of braking efficiency and recover energy otherwise lost in braking. Whenever accelerations are higher than -0.3 g series braking regenerates more and brakes at ideal braking limits with less risk of locking the front wheels.

For the parallel system (see Section 2.6.1), braking forces due to regenerative are higher for lower accelerations even though they bring the risk of near to the limit of sliding front forces and eventual lack of direction control in limit conditions.

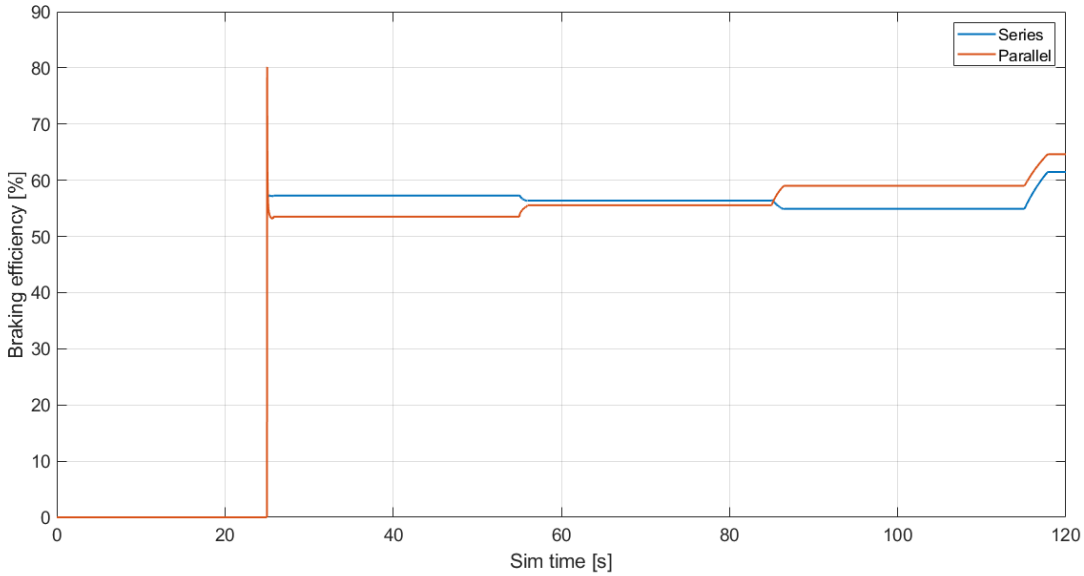

Figure 4.3 Regenerative efficiency comparison- Series(blue) Parallel(red)

4.2.1 Parentheses on the results without maximization of regenerative forces on parallel systems

In absence of maximization in regenerative curve for parallel braking (see Section 2.6.1.2), the results would be completely different. If the case represented in Figure 4.4, the regenerative part does not stop alone the vehicle for acceleration under -0.1g. The parallel system is designed to have still good regeneration since in case of the example 3000 N total force, the amount of regenerative force will be

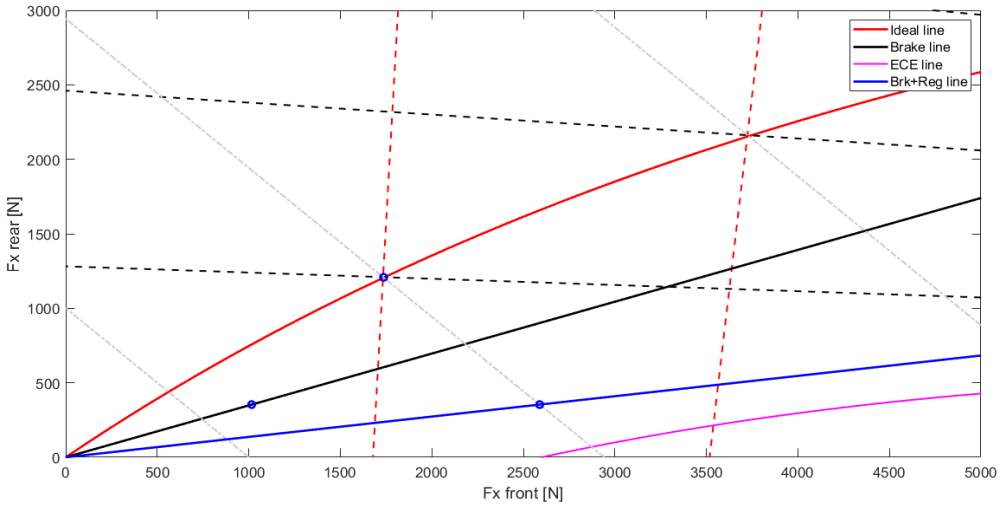

Figure 4.4 Example of parallel system without maximization of regenerative forces

the 2589-1016=1573N that consists of the 52% of total force. In the case of series system following the ideal line, the front axle forces will be 1740N because there is no need to apply the hydraulic system.

It is straightforward that in this represented case and in all the range covered by urban drive cycles, the series system will perform better both from energy efficiency point of view and performance in braking with respect to non-optimized parallel systems and as highlighted on Figure 4.5 in the last part of the simulation where series system gets better performances.

On the other side, the series system will have less regenerated force by following the ideal line in ideal conditions when accelerations involved will be higher. This last situation represents the first 80 seconds of the simulation in Figure 4.5, but these are not cases involving normal urban mobility and they also bring the parallel system to behave in less convenient zones of brake balance.

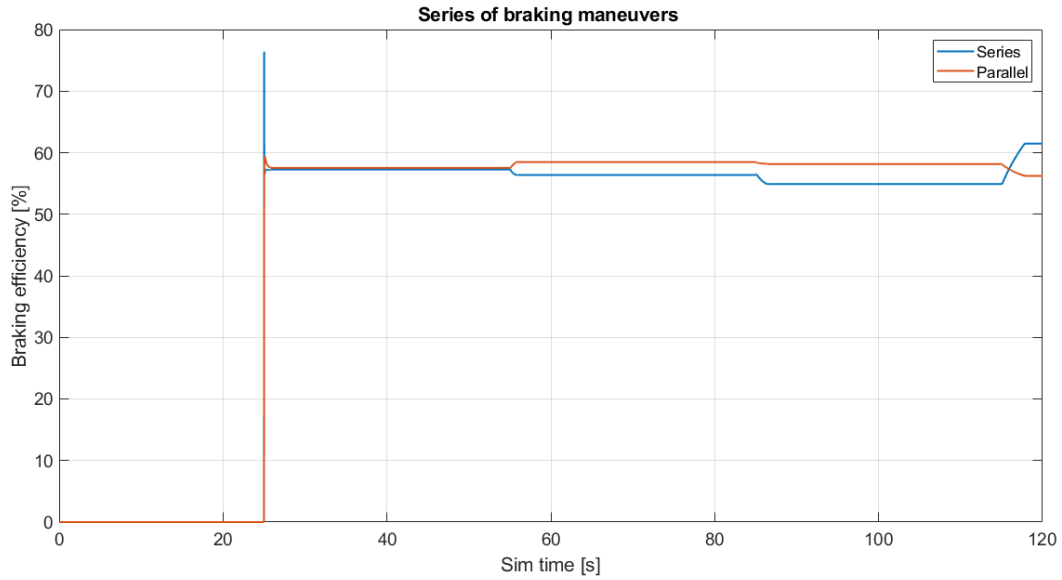

Figure 4.5 Regenerative efficiency comparison without maximization for parallel system- Series(blue) Parallel(red)

4.3 Results for WLTP and NEDC

In the following paragraph, parallel and series systems are compared giving more space to WLTP cycle since it represents conditions closer to reality. The final performance seems to be similar by SoC

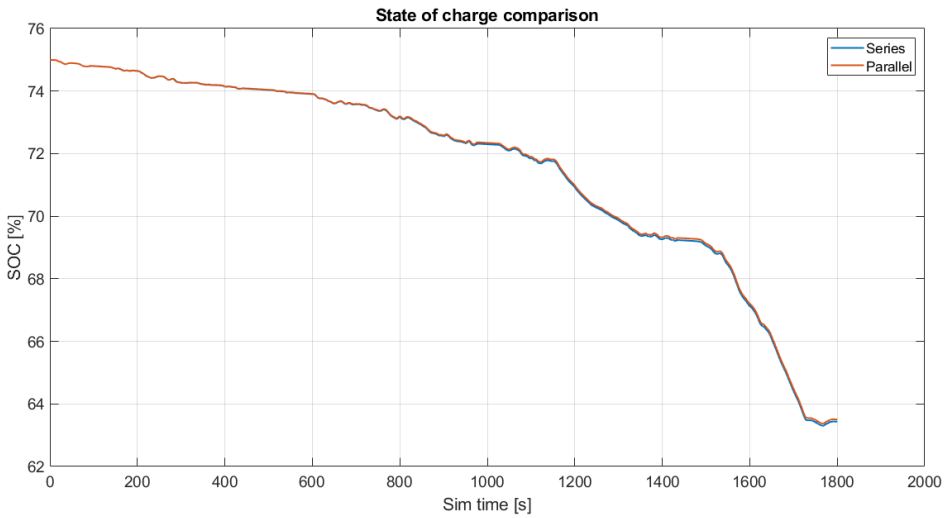

Figure 4.6 SoC levels over the WLTP cycle comparison

comparison in Figure 4.6. Moreover, in Figure 4.6 is possible to notice that all simulations are started with SoC value equal to 75% to avoid the limits set for overvoltage of battery cells.

As from Figure 4.7, the behaviour demonstrated in WLTP cycle between the two logics is very close. In the first part, where accelerations are closer to -0.1g they behave in the same way. When accelerations are closer to -0.15g, parallel systems regenerate more; this is the result of the optimization work for the parallel system.

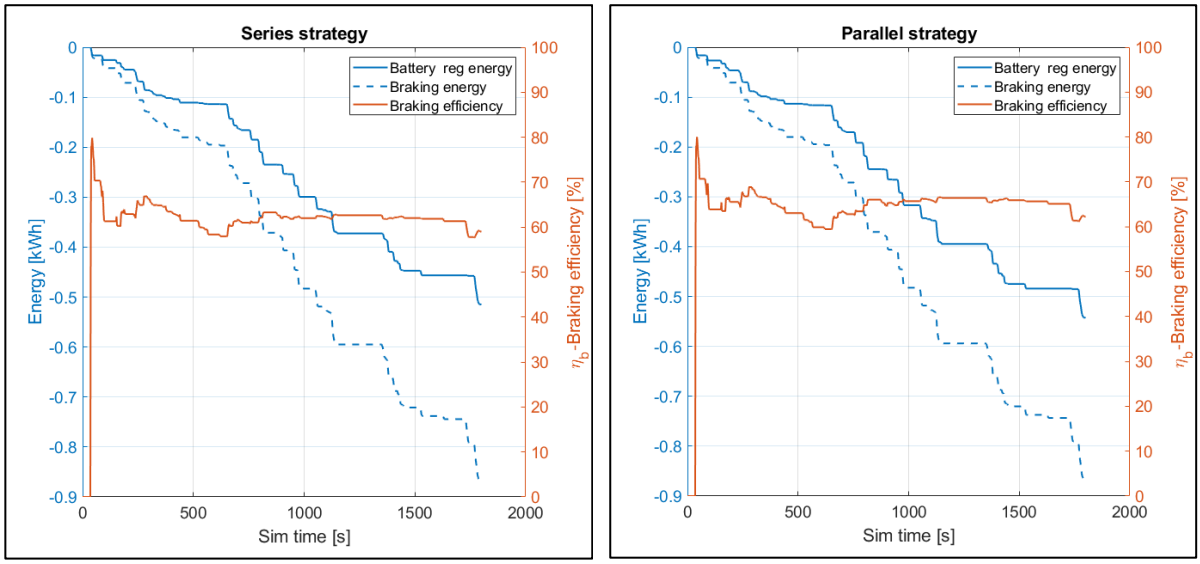

Figure 4.7 Braking energy and regenerative energy over WLTP cycle. Series(left) Parallel(right)

Even if the SoC levels are really close, the difference in energy entering the battery is greater. The plot in Figure 4.7 makes the comparison head to head including the total braking energy and the regenerated one along with the ratio between them. In Figure 4.8 is present their direct comparison for both WLTP and NEDC.

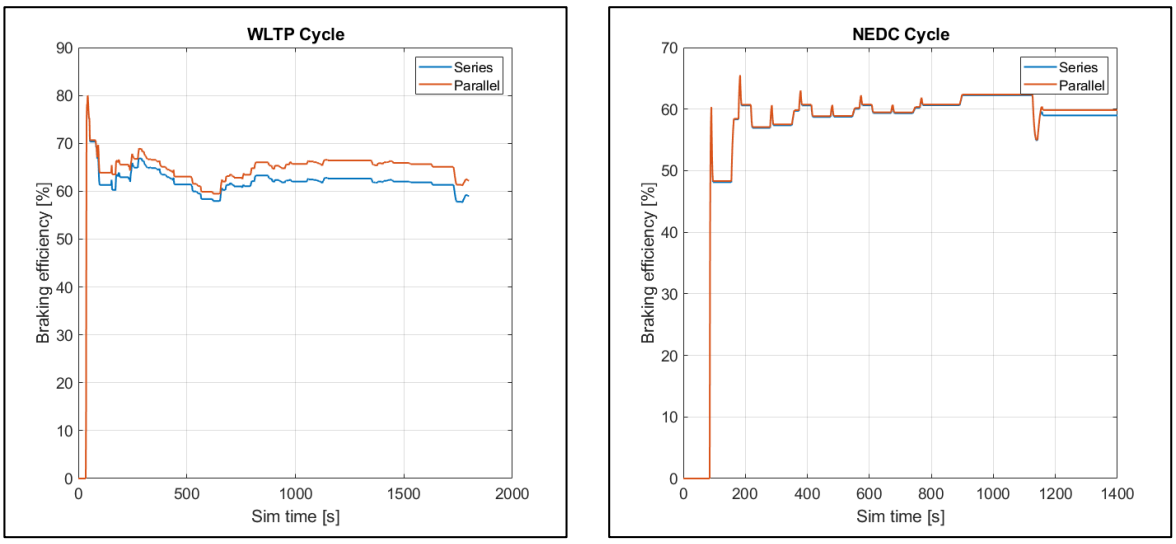

Figure 4.8 Braking efficiency comparison for WLTP (left) and NEDC (right)

The difference between the cycles is again due to their accelerations. In NEDC decelerations are present less frequently and with lower intensity, always under 0.1g for the first part that in ICE world is the cold start phase and of 0.15g in the last part. As predicted and occurring in other cases, the two systems are

practically identical under 0.1g. This plot also demonstrated that the NEDC does not give enough information for city driving.

4.3.1 Parentheses on the results without maximization of regenerative forces on parallel systems

A short parenthesis should be opened to prove what already written in Section 4.2.1 about the parallel system without maximum energy recovery. In Figure 4.9 a series system is compared to the non-optimized parallel system and the results are a lot different from what just reported in Figure 4.8. Now, the series system has a 20% higher braking efficiency with respect to the parallel system. Thus, the parallel system lost more than 25% braking efficiency without the maximization of regenerative effect that has been designed in this work. This is to mark the importance of analysis on the drive cycle and on the parameters of the system used.

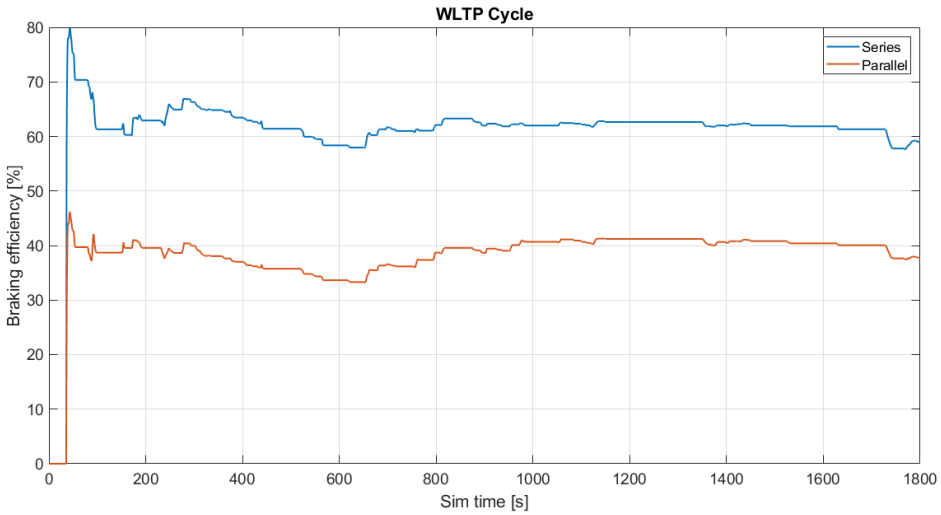

Figure 4.9 Comparison on WLTP cycle between optimized series and non-optimized parallel system

4.4 Comparison with series systems for maximum energy recovery

A third strategy was introduced in Section 2.6.2.2 as a logic to maximize the energy recovery in series systems. This strategy prioritizes the regenerative in all conditions and the results will be demonstrated in Figure 4.10 and 4.11 with respect to the series system used and the reference parallel system.

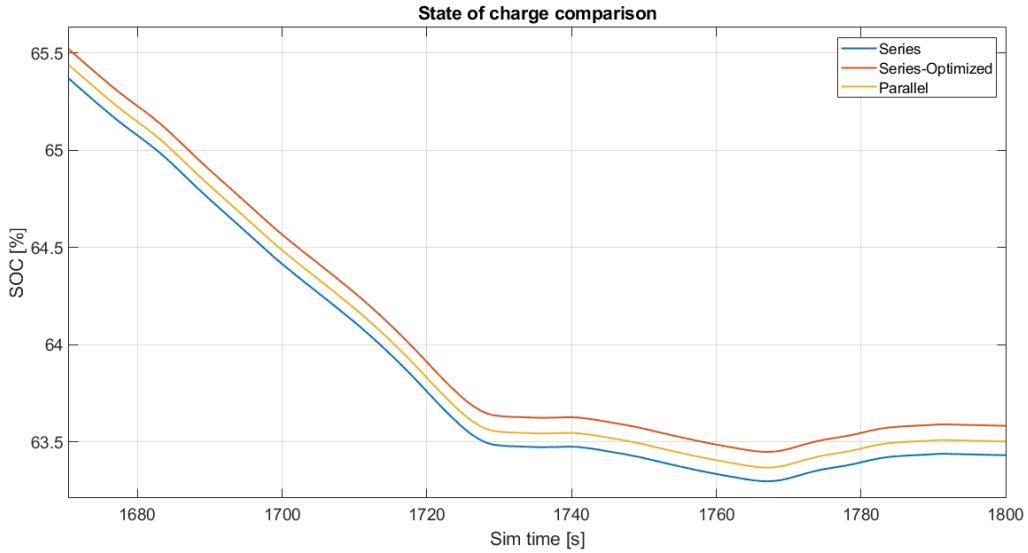

Figure 4.10 WLTP- SoC comparison among all systems

The optimization of the series system to always get the maximum recovery, and acting as described in Section 2.6.2.2, has always greater braking efficiency as in Figure 4.11 because it has no limits on the maximum regenerative braking with no-friction (0.1 for the series and parallel systems used before) and it can get closer to ECE regulation line. In this way it will result to have always higher SoC at the end of the cycle (see Figure 4.10).

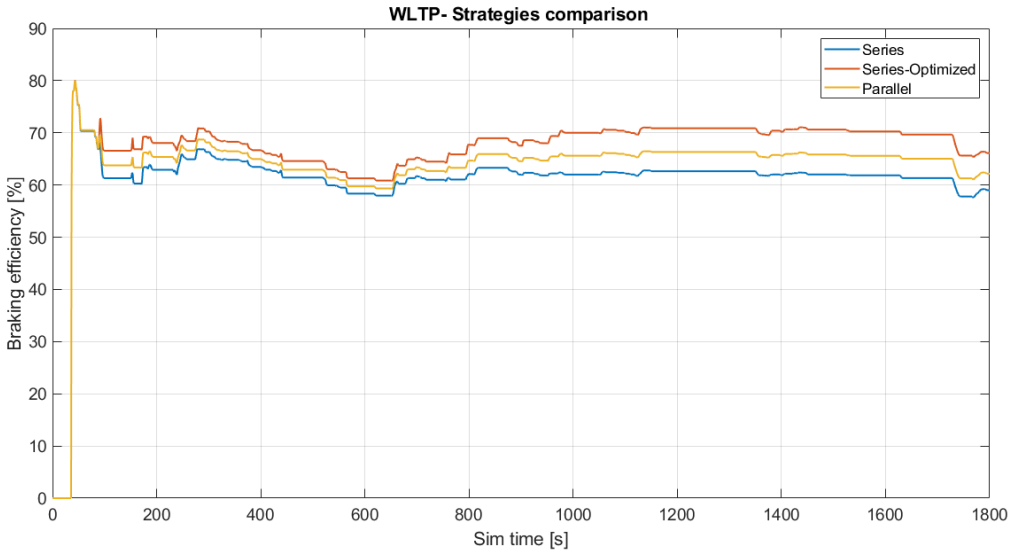

Figure 4.11 WLTP- Braking efficiency comparison among all systems

4.5 Final considerations

The results of the studies have been collected in Table 4.1. It is possible to see that the percentage of regenerated energy over the expended energy of the battery is consistent for the two different cycles taken into consideration and accounting for a good 12%. This is possible because almost 60% percent of the braking energy is covered by the power of the electric powertrain and the higher efficiency of electric powertrains with respect to ICE engines. The series optimized system is always the best, but results are really close in an urban drive cycle like the final range extension computed according (4.1) demonstrates.

Table 4.1 Summary on different strategies results

	NEDC			**WLTP**		
	Series	Series Optimized	Parallel	Series	Series Optimized	Parallel
Percentage of braking energy over traction energy- K_{dc} [%]	29.1	29.1	29.1	27.1	27.1	27.1
Achievable Braking efficiency- η_b [%]	58.98	60.8	59.84	59.01	66.12	62.23
Traveling distance per cycle [km]	11	11	11	23	23	23
Range extension [km]	1.28	1.39	1.31	2.62	2.99	2.78
Percentage of regenerated energy -ξ_{reg} [%]	11.7	12.64	11.95	11.4	13	12.1

Where:

$$Range\ extension = Tot.distance * (\xi_{reg}) \quad (4.1)$$

Moreover, throughout the chapter has been demonstrated that by using a less sophisticated system like parallel ones but optimized in its performance with respect to city driving, it can be achieved very good results. As seen, this implies the system to work in less balanced braking conditions to increase the portion of regenerative braking with respect to friction.

Series systems allowed to change the characteristics by means of a switch in the logic that allows to have balanced braking (by following ideal line) or reach greater efficiency (by maximizing the regenerative effect on the right axle) and thus, be more versatile. Even if this would require more sophisticated systems with enhanced electronics, it is safe to say that this requirement does not represents a problem for newer vehicles and electric powertrains and thus they represent the best choice.

Another difference between parallel and series systems has been already highlighted in Chapter 2 and is about the sensations for drivers. Series systems do need brake by wire systems and the feedback on the pedal is certainly different from the one of friction brakes. Parallel systems, on the other side, need a more complicated brake pedal that must activate the friction brakes and at same time function as position sensor for the electric brake system. Moreover, the feedback on the pedal will be always connected also to the pressure in the hydraulic line and as seen, pressure in parallel is usually much lower than expected affecting and misleading the driver about how much he is braking and in case of fade from motor torque, it is required an action directly from the driver with consecutive uncomfortable feelings.

5 Formula student vehicle analysis

5.1 Formula student presentation

Formula SAE is a student design competition which involves the departments of engineering of the Universities worldwide organized by SAE International (previously known as the Society of Automotive Engineers, SAE). The concept behind Formula SAE is that a fictional manufacturing company has contracted a student design team to develop a small Formula-style race car. The prototype race car is to be evaluated for its potential as a production item. The student team designs, builds and tests a prototype based on a series of rules, whose purpose is both ensuring on-track safety (the cars are driven by the students themselves) and promoting clever problem solving [19]. First competition in Europe took place in 1998, based on the American model which made its debut with the first edition in 1981 with only combustion engines (FSC), while in 2010, following the increasing interest for electric vehicles, an electric class of competitions was started with acronym FSE. The third and newest category to be opened is the Formula Student Driverless (FSD), for autonomous vehicles, continuing to follow the most important trends in automotive industry.

During the competition, teams deal with few challenges divided in two big categories:

Static events:

Design Event: presentation of the complete project of the car.

Business Event: simulation of the presentation of their project by each team in front of potential investors.

Cost Event: analysis of the cost report drafted by each team where are included quantities of materials and components used.

Dynamic events:

Acceleration: Acceleration race on 75 m straight.

Skid Pad: The skid pad track consists of two pairs of concentric circles in a figure of eight pattern where four full circles will be computed by the driver; two on the left turn and two on the right. Only the respective second turn in timed and contribute to the overall score based on mean time between left and right turn.

Autocross: It is a time attack race on a relative short circuit of maximum 1.5 km where the fastest time out of 4 trails is considered on the final scores.

Endurance and Efficiency is the main discipline, providing the highest number of points. Over a distance of 22 kilometres the cars have to prove their durability under long-term conditions. Acceleration, speed, handling, dynamics, fuel economy, reliability are all characteristics that the vehicles have to show. The Endurance also demands handling skills of the driver because there can be up to four cars on the track at the same time.

During the endurance race (FSC, FSE) and track drive event (FSD), fuel consumption (combustion cars) or energy consumption (electric cars) is precisely recorded. However, the absolute fuel and energy consumption is not what is used to calculate the efficiency score, but rather the consumption relative to speed. This is to prevent teams from driving particularly slowly in the endurance competition in order to score as highly as possible in the **efficiency** category that assigns a good number of points as pointed out in Figure 5.1 that presents and divides all points available in a formula student event for FSC and FSE categories.

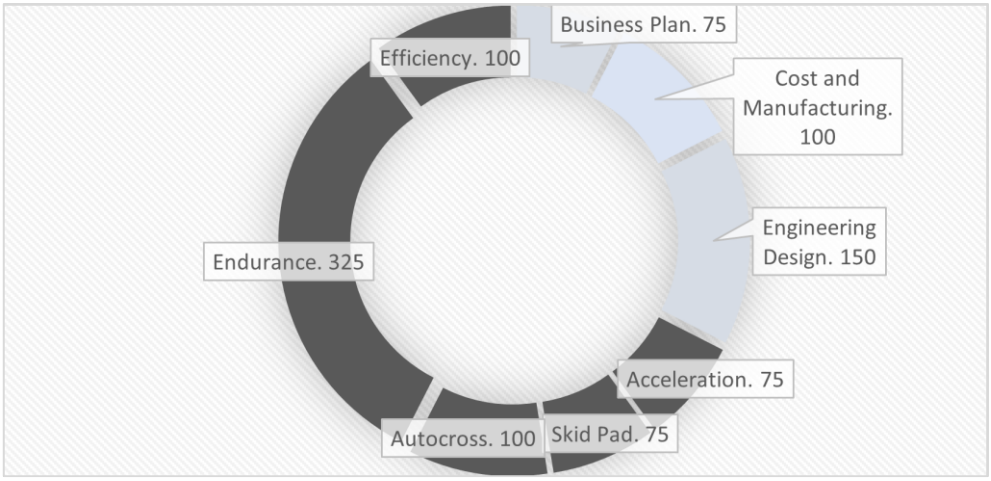

Figure 5.1 FSAE scores division

The challenge the teams face is to compose a complete package consisting of a well-constructed race car and a sales plan that best matches these given criteria. The decision is made by a jury of experts from the motorsport, automotive and supplier industries. The jury will judge every team's car and sales plan based on construction, cost planning and sales presentation. The rest of the judging will be done out on the track, where the students demonstrate in a number of performance tests how well their self-built race cars fare in their true environment.

5.2 Squadra Corse PoliTO

Squadra Corse (**SC**) PoliTO was born in 2005 to compete in Formula SAE events representing Politecnico di Torino [20]. Since 2012 is developing fully electric cars and obtaining very good results in the Italian and international stages, reaching its peak in electric category with 2017 podium in Italy and winning the 2019 Italian stage with its prototype, SC19 (alias Lucia) and consolidating its position in the top 30 of world ranking.

Due to convid-19 pandemic it has not been possible to conclude the production of the 2020 car so all the following work will be mainly developed on data coming from the previous car of 2019 year (in the following work eventually called **SC19**) where I personally took place in the design, production and testing.

5.2.1 SC19 Characteristics

The characteristics of the vehicle are summarized in table 5.1 and represented in Figure 5.2, representing the main sizes of SC19 prototype that will be used in the following work.

Table 5.1 Vehicle data

	Symbol	Value
Vehicle mass	M_tot	253 kg (with 70kg driver)
Wheelbase	L	1525 mm
Track	t	1200 mm
Centre of gravity distance from ground	CG	295 mm
Distance from gravity centre to front wheels	a	838 mm
Aerodynamics drag*Frontal surface	Cd*S	0.96
Aerodynamic lift*Frontals surface	Cz*S	-2.72
Aerodynamic lift repartition front	K_f	0.5

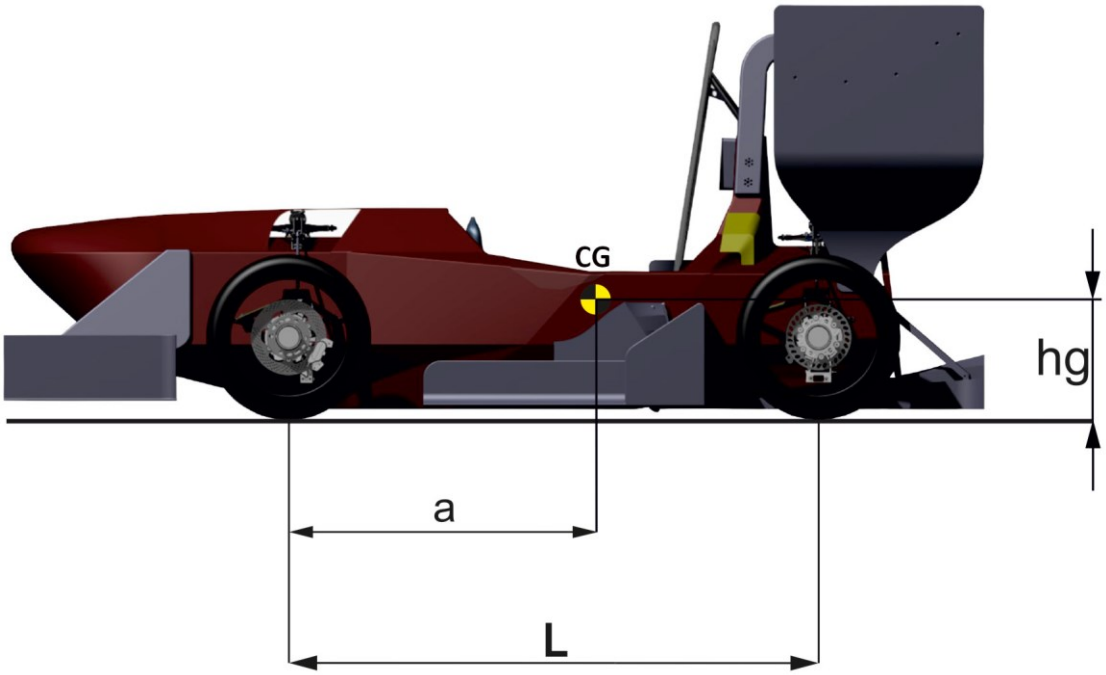

Figure 5.2 SC19 vehicle characteristics

The vehicle is a Formula-like prototype with important aerodynamic features. Its powertrain is composed of a 6 kWh Li-ion battery pack, a 4 in-wheel motors for a total, maximum power of 120 kW and planetary transmissions whose characteristics are listed in table 5.2 and 5.3.

Table 5.2 Motor and transmission data

	AMK-DD5-14-10-POW
Motor type	Brushless - Synchronous motor
Max torque	21 Nm
Rated torque	9.8 Nm
Rated power	12.3 kW
Rated speed	12000 rpm
Max speed limit	20000 rpm
Rated voltage	350 V
Rated current	41 A_{rms}
Maximum current	105 A_{rms}
Pole pair	5
Final transmission ratio	14.5

Table 5.3 Cell data

	Sony 18650 VTC6
Nominal capacity	3.12 Ah
Nominal voltage	3.60 V
Maximum voltage	4.25 V
Minimum voltage	2.60 V
Charge current (continuous)	5 A
Discharge current (continuous)	30 A
Internal resistance	12 mΩ
Operating range temperature	-20 ÷ 60 °C

5.2.2 Braking system used on SC19

The braking system of SC vehicles has a well-established layout, product of several years of development and data acquisition. This system is constrained by tough rules that forbid brake by wire systems [21]. Moreover, being a braking system of a performance vehicle, all design choices are done to comply with rules and to seek best performance and stability for the vehicle.

From the scheme represented in Figure 5.3, the brake lines are routed directly from the two master cylinders respectively to the front and rear callipers. The two master cylinders react to the force imposed by the balance bar that has the duty to divide the force coming from brake pedal to front and rear wheels and in this way separately changing the pressures inside the two separated circuits.

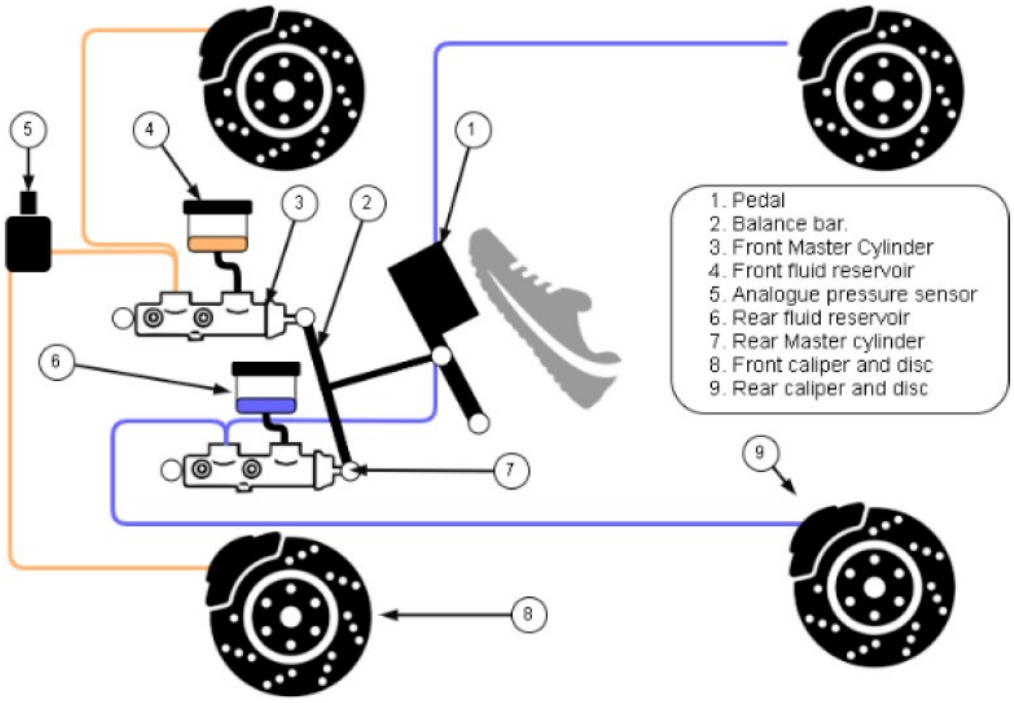

Figure 5.3 Brake line layout SC19-courtesy of Squadra Corse PoliTO

The response of 4 in-wheel motors is added in parallel to the hydraulic brake line. The starting point for this study is a **parallel system** that works like in Figure 5.6 where the first part of the braking phase is covered by only regenerative braking and after a certain brake pedal force, kicks out the friction system. This is possible because of the mechanical layout of the braking pedal that is represented in Figure 5.4. Springs are present to regulate the movement of the pedal and set the wanted preload that corresponds to the needed force to be applied to move the pedal and let the pressure build up inside the line.
Before the reaching of the preload for the movement of the pedal, the deformation on the rod, connecting the pedal to the rod of the master cylinder, is sensed by strain gauges that are then related to pedal

movement following the rule represented in Figure 5.5. The look-up table represented in Figure 5.5 is directly responsible for the driver sensibility and brake response of regenerative braking since it decides the amount of regenerative according to rod end deformation and it will be revisited during this work by means of more accurate studies.

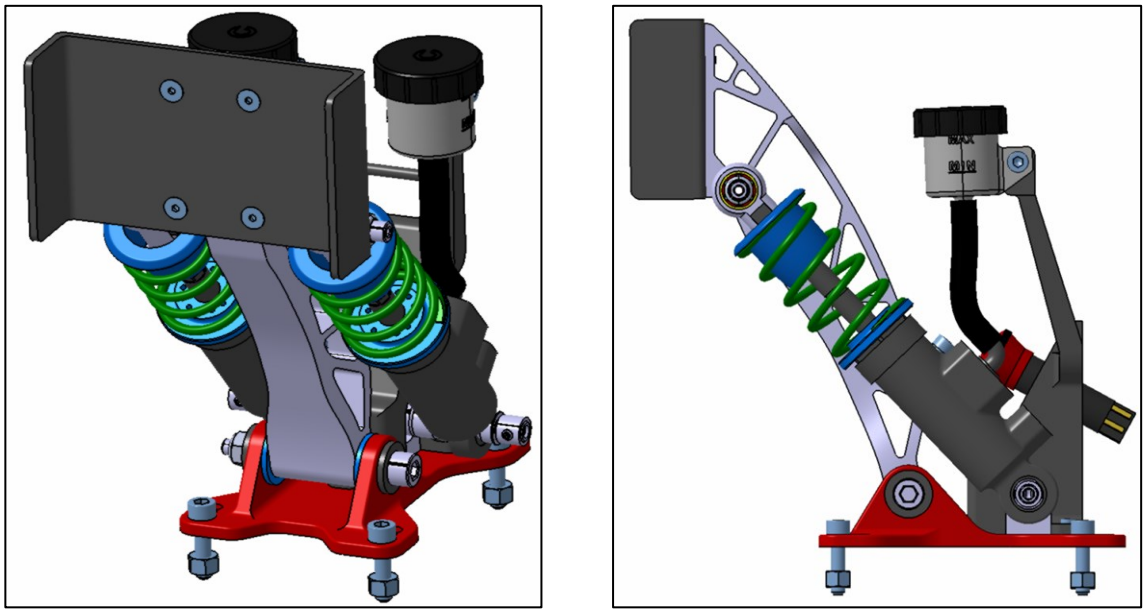

Figure 5.4 Brake pedal assembly for SC19 vehicle--courtesy of Squadra Corse PoliTO

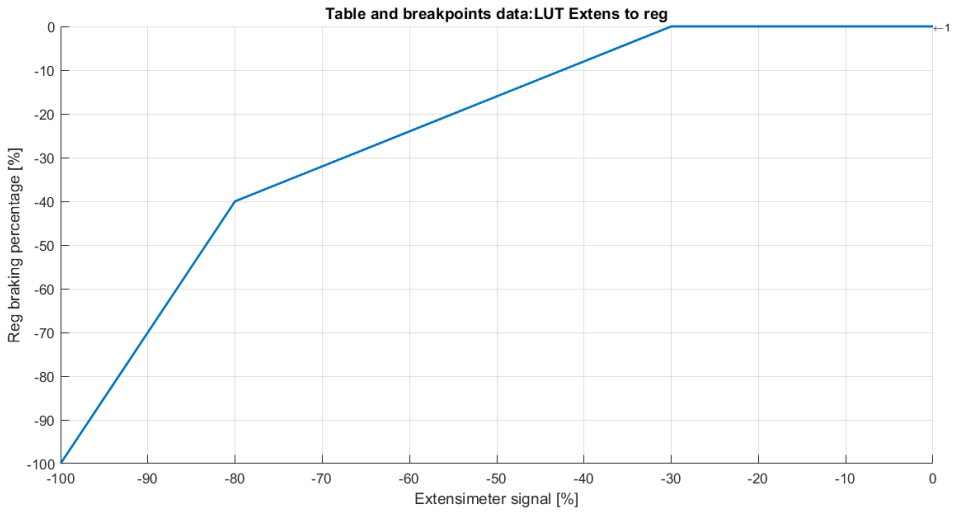

Figure 5.5 Pedal force and regenerative action-courtesy of Squadra Corse PoliTO

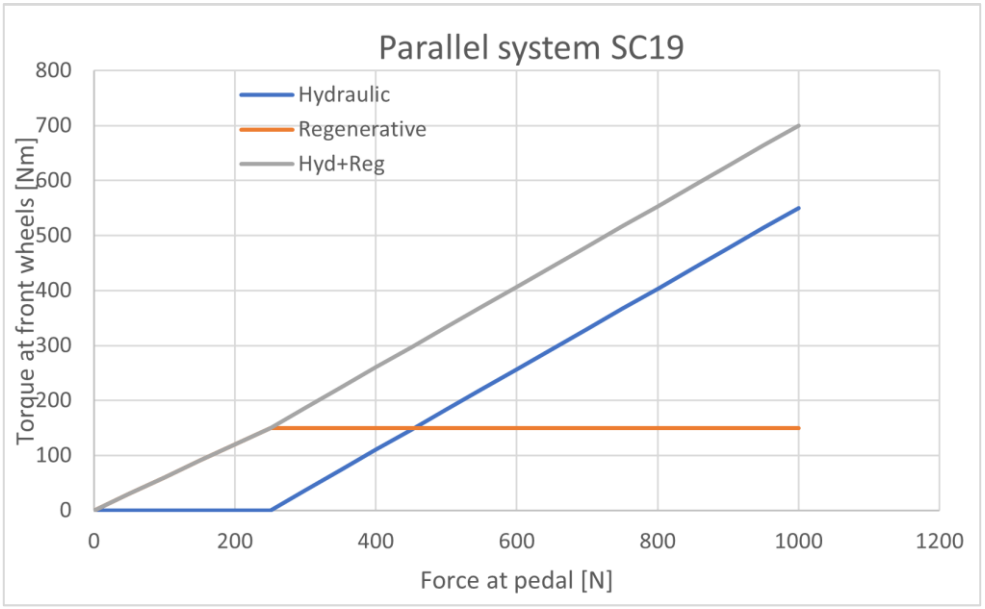

Figure 5.6 Parallel system, Regenerative and friction line response to input force on pedal-courtesy of Squadra Corse PoliTO

5.2.3 Master cylinder

A master cylinder, or master brake cylinder, is a device able to convert the pressure acting on the brake pedal surface into hydraulic pressure, sending the pressurized brake fluid into the braking lines and hence to the brake callipers.

As the piston inside the master cylinder moves along the bore due to pedal pressure, its motion is transferred through the hydraulic fluid to the slave cylinders (i.e. the calliper pistons). Varying the ratio between surface areas of master cylinder and slave cylinder, the amount of force and displacement applied to each slave cylinder can be varied respect to the amount of force and displacement on the master cylinder.

In SC19 hydraulic circuit there are two master cylinders, one for pressurizing the front brake line (going to the front wheels callipers) and one for the rear one (going to rear wheels callipers). This configuration comes to be very useful in the event of one braking circuit failure: in this case, the pressure builds up on the other circuit would not be affected, and the vehicle would still have some braking capability.

The front and rear master cylinders are of the same dimensions (16mm diameter) to have an initial repartition at 50:50.

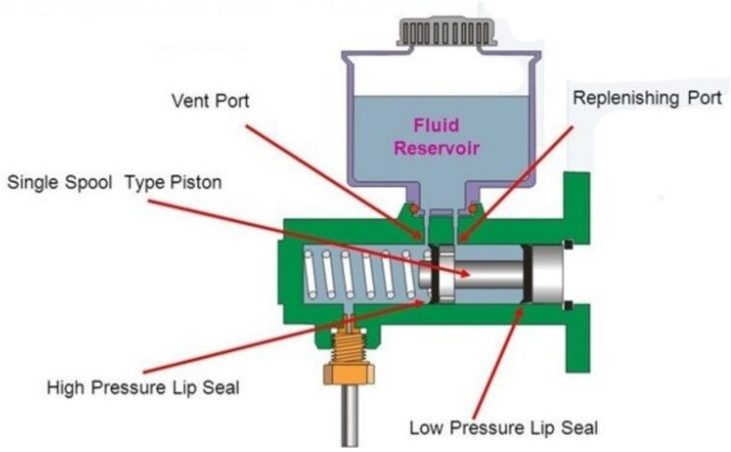

Figure 5.7 Master cylinder with single chamber section

5.2.4 Balance bar

A balance bar is a device designed to divide the force applied on the pedal by the driver between the two master cylinders, physically divided, as in Figure 5.8. As evidenced in Figure 5.8, it is a rod which connects the two master cylinders, placed one on each end, and that has a pivot point that can be moved, changing the levers. Since the torque on one side of the pivot must balance the torque on the other side, the master cylinder that is closer to the pivot will receive a higher percentage of the total pedal force. Therefore, this device is very useful to adjust the repartition of forces and therefore pressures on the two different lines.

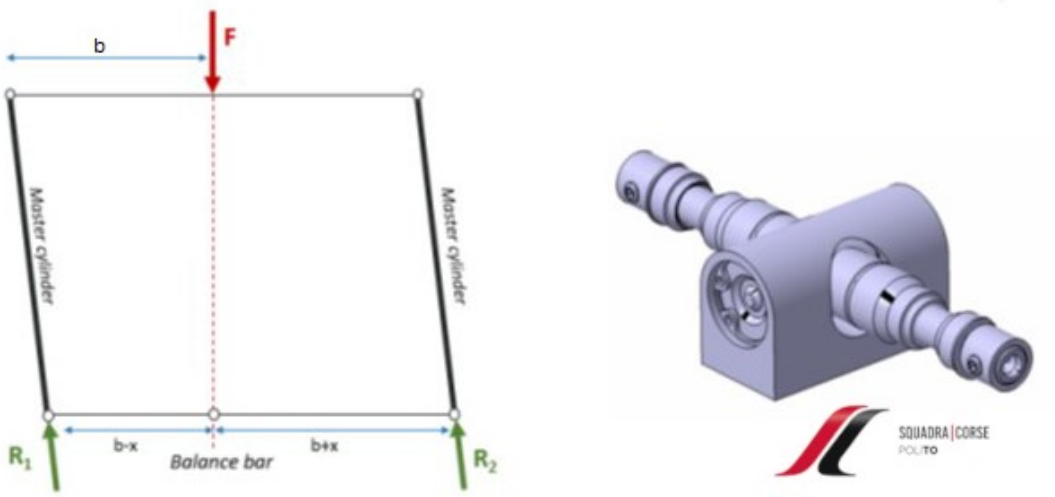

Figure 5.8 Balance bar schematics and CAD-courtesy of Squadra corse PoliTO

5.3 Brake analysis on FSAE vehicle

With data coming from SC19, listed in Table 5.1 it is possible to start a new analysis on ideal braking. In this case is worth to note that aerodynamics will play a non-marginal role and therefore will be considered in formulas (5.1), (5.2) and (5.3) that were presented in Chapter 1 in simplified form [1].

$$\frac{dV}{dt} = \frac{\mu_x(F_{z1} + F_{z2} + \frac{1}{2}\rho S C_z V^2) - \frac{1}{2}\rho V^2 S C_x}{m} \tag{5.1}$$

$$F_{z1} = mg\frac{b + \frac{1}{2}\frac{\rho S C_z}{m\,g}K_f\,V^2 \; - \dot{V}\frac{h_g}{g}}{l} \tag{5.2}$$

$$F_{z2} = mg\frac{a + \frac{1}{2}\frac{\rho S C_z}{m\,g}K_r\,V^2 + \dot{V}\frac{h_g}{g}}{l} \tag{5.3}$$

Thanks to equations 5.1, 5.2, 5.3 the ideal parabola is changing and represented for different speeds in Figure 5.12; the effect of speed is to move the ideal parabola according to the aerodynamics value. Drag forces tend to decelerate the vehicle and the higher the speed and drag, the greater the gain in F_{z1} with respect to F_{z2}. The lift coefficient (listed in Table 5.1) heavily influences the force on the axles, but it is also very important the distribution with respect to centre of gravity because with changes of K_f and K_r, aerodynamic lift distribution coefficients in 5.2 and 5.3, also vertical forces will dramatically change affecting the braking distribution, especially at higher speeds.

5.3.1 FSAE events analysis

The analysis should start, as in Chapter 2, by knowing the magnitude of braking power, energy and accelerations involved in a typical formula SAE event. In formula SAE, endurance is the most important event concerning regenerative braking and efficiency of the vehicle; in all other dynamic events, maximum performance and handling are primarily considered. Figure 5.9 is representing the analysis on endurance events of Spain 2019 (Circuit de Barcelona-Catalunya) and Italy 2018 (Autodromo di Varano) merged in order to have a broader idea and set of data that are related to a single track.

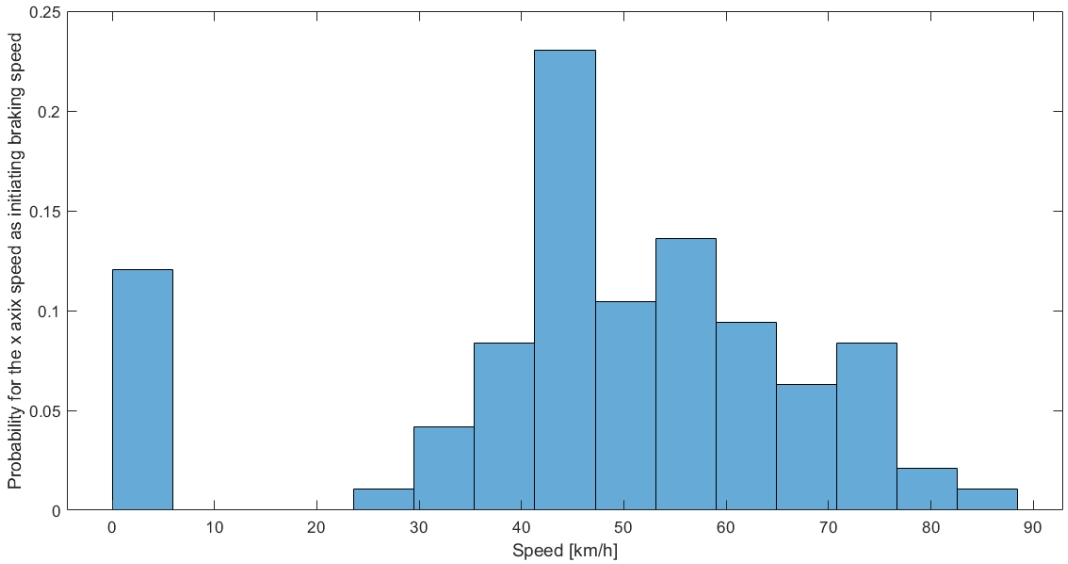

Figure 5.9 Probability distribution for the speed initiating braking

One useful piece of information is related to the vehicle speed distribution when initiating the braking manoeuvre, in order to focus the design of brake and regenerative line to optimize the performances. The most frequent range is between 40 to 75 km/h and such data have been used by Squadra Corse members to design the braking line.

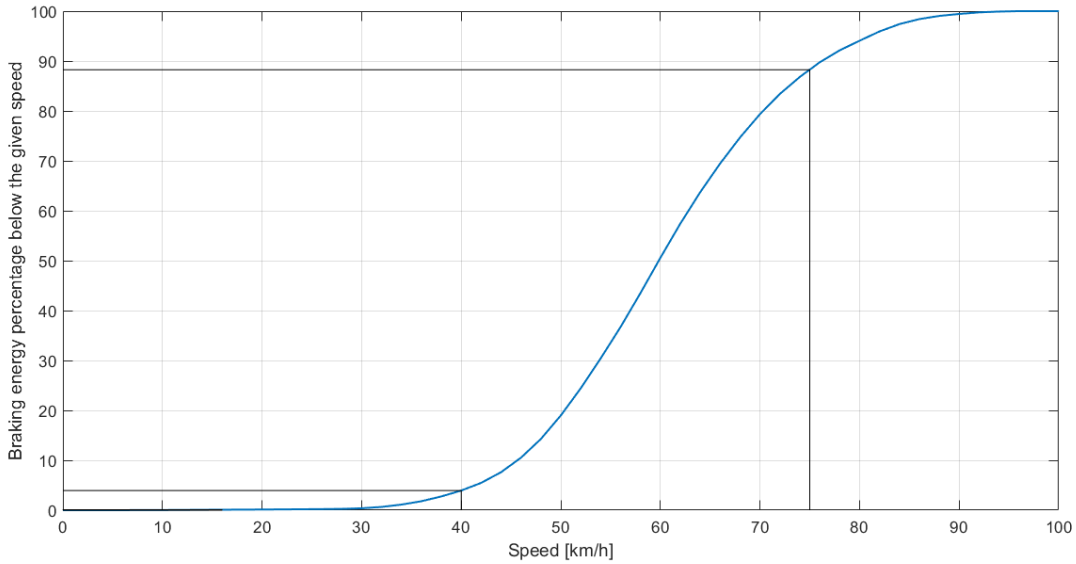

Figure 5.10 Braking energy percentage under a given speed

It is also possible to correlate the used braking energy with speed; in Figure 5.10 is represented the percentage of braking energy exploited under a given speed. For the vehicle analysed and the type of track that are usually seen in FSAE, the braking energy under 40 km/h is very low but the most frequent range of 40-75 km/h contains 83% of the total energy, piece of information that a quantitative idea over the importance on that range of speed.

Speed is only one half of the picture; the other half is represented by accelerations. In Figure 5.11 it is represented the amount of energy under a given deceleration and is very useful to understand and decide the amount of regenerative braking. In the case of a FSAE vehicle, a 0.15g deceleration in not good to regenerate since the braking anergy available is very low. A range of 0.6g with 50% of total braking energy to 0.9g of 78% is more reasonable and should be the target from which the feasibility has to be studied.

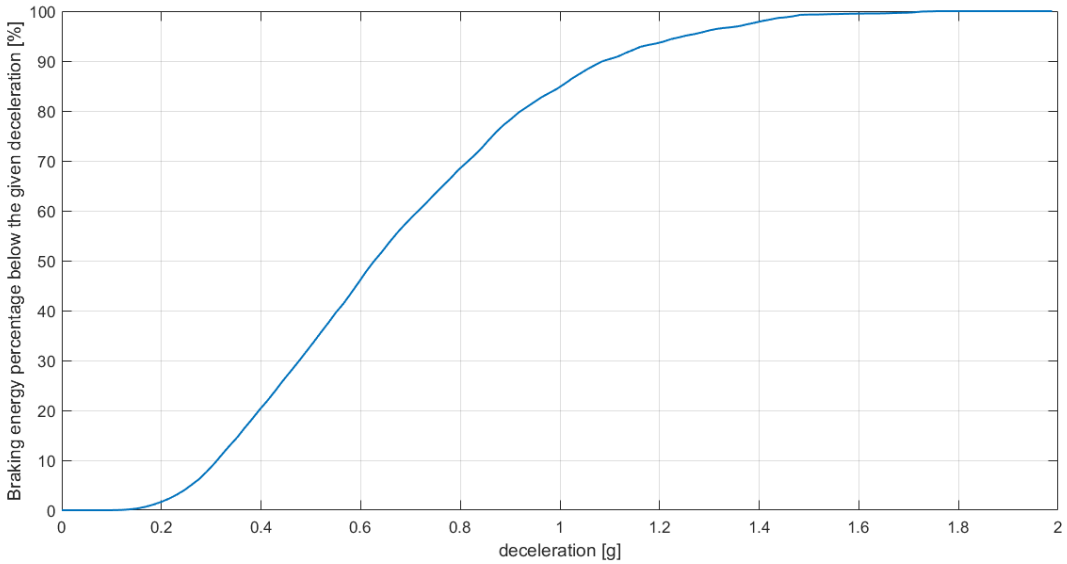

Figure 5.11 Braking energy percentage under a given deceleration

By combining the previous piece of information and the ideal braking line, considering aerodynamics, it is possible to choose the optimal braking line as presented in Chapter 2 and represented in Figure 5.12.

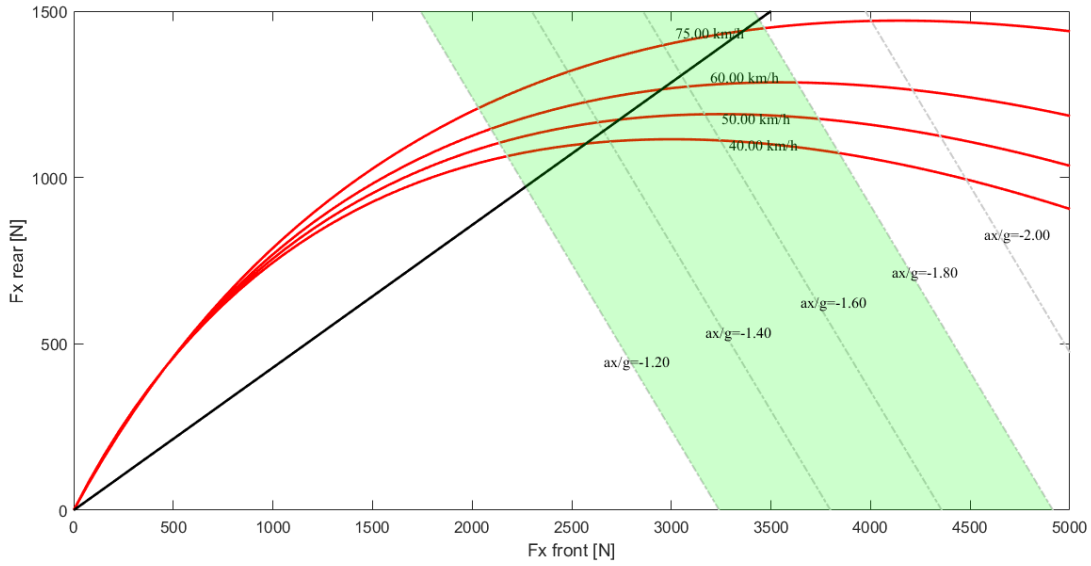

Figure 5.12 Friction braking system for SC19 and ideal braking lines function of speed

From Figure 5.12, the starting point of the friction braking repartition is 0.70 to front wheels, represented by the black line, that allows the vehicle to have brake up to 1.8 g under 70km/h and at least 1.4-1.6 g in the speed range of 50-60 km/h. This set-up would then be changed according to speed and ground conditions on a given circuit or driver preferences but taking into account that the tuning is limited by the movement of the balance bar.

5.4 Total braking torque, repartition and strategies

At control system level in SC19 vehicle, the amount of torque is decided according to the pedal actuation as anticipated earlier in this chapter. The amount of torque available at motors as seen in Chapter 2 and 3 and on the maximum amount of braking torque that is set by telemetry responsible. This last parameter is tuned according to the type of race, the driver and circuit. To help the reader understand the effect and the correlation with the parameters set within the control system, Table 5.4 sums up the different torque settings at motor level and correlates them with torque at axles and vehicle deceleration.

Table 5.4 Total motor torque, deceleration equivalent and axles torque

Total motor brake torque [Nm]	Motor torque front axle [Nm]	Motor torque rear axle [Nm]	Vehicle deceleration [g]	Torque at front axle [Nm]	Torque at rear axle [Nm]
5	3.5	1.5	**0.1240**	50.75	21.75
10	7	3	**0.2480**	101.5	43.5
15	10.5	4.5	**0.3720**	152.25	65.25
20	14	6	**0.4959**	203	87
25	17.5	7.5	**0.6199**	253.75	108.75
30	21	9	**0.7439**	304.5	130.5

Maximum values achieved during the years were of 28 Nm as total torque set at motors, distributed 70:30 to front. This value would result in 0.7 g of deceleration for SC19 vehicle.

As anticipated at the beginning of the chapter, the regenerative signal is depending on brake pedal load, computed by means of rod end strain gauges. This type of layout brings some limits with it. First the preload and the springs heavily influence the feedback to the drivers and their fatigue during driving. There should always be a compromise between a heavy and good feedback springs and light-no feedback ones and this trade-off mostly comes with the experience built year by year by members of Squadra Corse. Second limiting factor is the fact that regenerative braking modulation depends on the amount of force applied on the pedal with no movement of the brake pedal, making the modulation difficult. This means that the range between which the pilot can discretize the response of regenerative has to be limited. The limitation on 28 Nm value of torque, mentioned before, is set by driver feedbacks about too aggressive regenerative brake and low possibility to partialize the effect. Since this study has also the goal to maintain unaltered the features of driveable race car vehicle where driver feedback remains very important and since there is no possibility to change the hardware and construction design of the brake pedal, levels of 30 Nm will then be the upper limits for the coming analysis.

5.4.1 First action to improve brake control: Modulation on accelerator pedal

Lower decelerations that, from now on will be the ones under 0.4g, would represent a problem if low control on regenerative braking is present. This problem can be solved by means of the possibility to control and adjust electric motor response and the features of sensors and actuators. In fact, it is possible to apply a braking torque by modelling the output of the accelerator pedal with respect to pedal travel because, in this case, it is a by-wire hardware. This is going to follow what treated in [22] where the accelerator pedal travel is allocated 30% to negative torque, 5% to coasting and 65% to acceleration with respect to the corresponding maximum torque (that could be set differently from driving to braking) according to Figure 5.13.

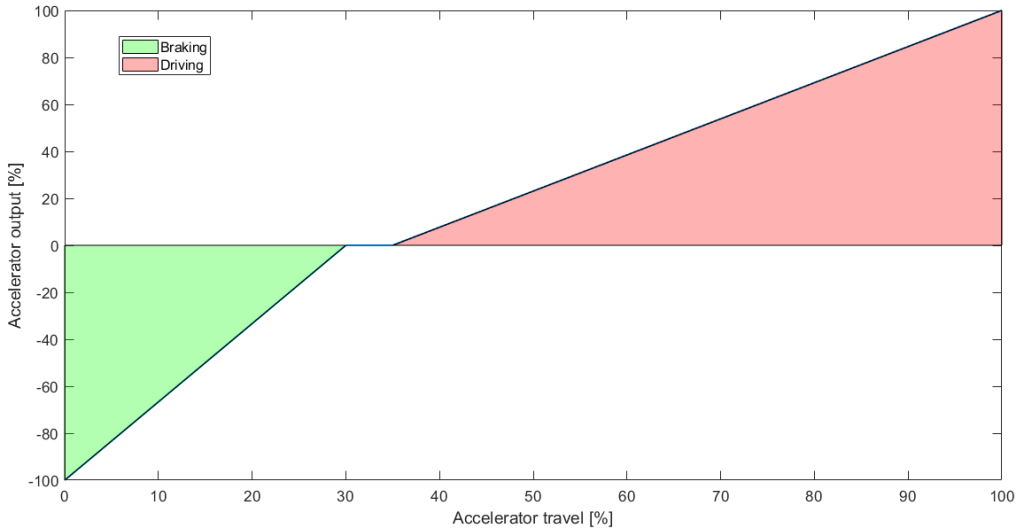

Figure 5.13 Single-pedal control for accelerator. Braking, coasting and driving division on accelerator travel

In addition to Figure 5.13, also Figure 5.14 must be considered to understand how the pedal travel is divided:

1. Acceleration (35-100% travel): the acceleration effect will be present only after 35% of pedal travel but only if the speed is higher than 7 km/h; set because that is also the limit on regenerative braking on brake pedals set on SC19. If the speed is lower than 7 km/h, the value is shifted leftward to avoid the case of low speed and high torque and also the standing start case where 30% of pedal travel is wasted as Figure 5.14 reports.
2. Coasting (30-35% travel): To let the vehicle decelerate only by inertia and to give a smoother transition to braking, the coasting range is set. Even this range will go towards 0 at lower speed and being eliminated at 0 km/h.
3. Braking (0-30% travel): When there is the need to brake, the driver can release the pedal and achieve the maximum braking torque at 30% of pedal travel. The pedal fully released (0%) corresponds to close to null braking torque. The way the values are shifted at lower speeds is represented in Figure 5.14.

	Vehicle speed km/h														
Pedal travel [%]	0	1	2	3	4	5	6	7	10	20	40	60	80	100	120
0	C	R	R	R	R	R	R	R	R	R	R	R	R	R	R
5	A	C	R	R	R	R	R	R	R	R	R	R	R	R	R
10	A	A	C	R	R	R	R	R	R	R	R	R	R	R	R
15	A	A	A	C	R	R	R	R	R	R	R	R	R	R	R
20	A	A	A	A	C	R	R	R	R	R	R	R	R	R	R
25	A	A	A	A	A	C	R	R	R	R	R	R	R	R	R
30	A	A	A	A	A	A	C	C	C	C	C	C	C	C	C
35	A	A	A	A	A	A	A	C	C	C	C	C	C	C	C
40	A	A	A	A	A	A	A	A	A	A	A	A	A	A	A
50	A	A	A	A	A	A	A	A	A	A	A	A	A	A	A
60	A	A	A	A	A	A	A	A	A	A	A	A	A	A	A
70	A	A	A	A	A	A	A	A	A	A	A	A	A	A	A
80	A	A	A	A	A	A	A	A	A	A	A	A	A	A	A
90	A	A	A	A	A	A	A	A	A	A	A	A	A	A	A
100	A	A	A	A	A	A	A	A	A	A	A	A	A	A	A

Regenerative Acceleration Coasting

Figure 5.14 Single-pedal travel allocation of braking, acceleration and coasting phases according to speed [22]

The negative values of accelerator will command the braking torque whose output can be set differently from maximum driving torque. The starting value for maximum braking torque is here set to 16 Nm that would result in 0.4 g deceleration. This value representing the most frequent deceleration at lowest speeds. Since no vehicle is available right now for the testing, the value will be taken as right but could be easily changed according to tests on track.

With this set up, when deceleration is required, the driver can adjust the accelerator pedal travel to within 0-30% to achieve different decelerations according to Figure 5.15 where every 5% of pedal travel there is an increase of about 0.07g. The maximum deceleration (0.4g) achieved when the pedal is at 30% and the minimum at 0% travel or fully released condition.

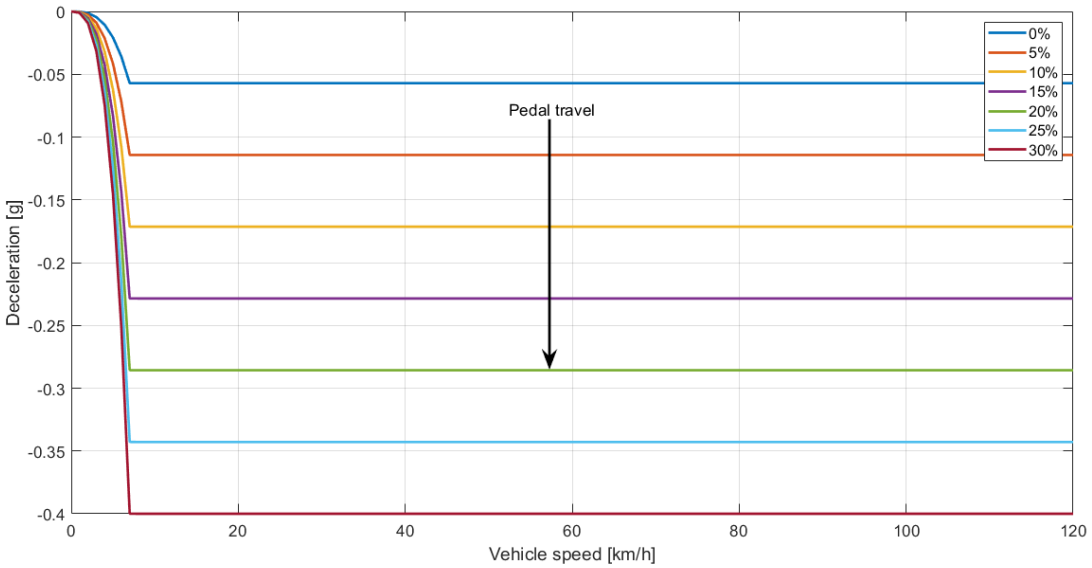

Figure 5.15 Vehicle deceleration at different accelerator pedal travel

5.4.2 Increased sensibility on brakes due to accelerator strategy

Thanks to the braking action on the accelerator, explained in last paragraph, is possible to increase the regenerative action also on the brakes because the problem of sensibility is partially solved. This is because in the first part of brake pedal action there is lower need to maintain linearity since deceleration up to 0.4g are covered by the accelerator pedal. In Figure 5.16, acceleration equivalent of total brake torque is represented as function of the strain gauge signal for the brake pedal and then, the same plot is represented with respect to the equivalent force to be applied on the brake pedal by the driver. If compared to a simple linear system and setting the maximum deceleration to 0.8g, the linear system would have a slope of 0.04 g/kg (g's of acceleration over kilogram of forces applied on brakes) and the newly implemented system will have 0.026 g/kg after 0.4g. Thus, the new system is 1.6 times less sensible to force change on the pedal and the driver can discretize better the force applied on the brakes in the more important range from 0.4 to 0.8g of deceleration.

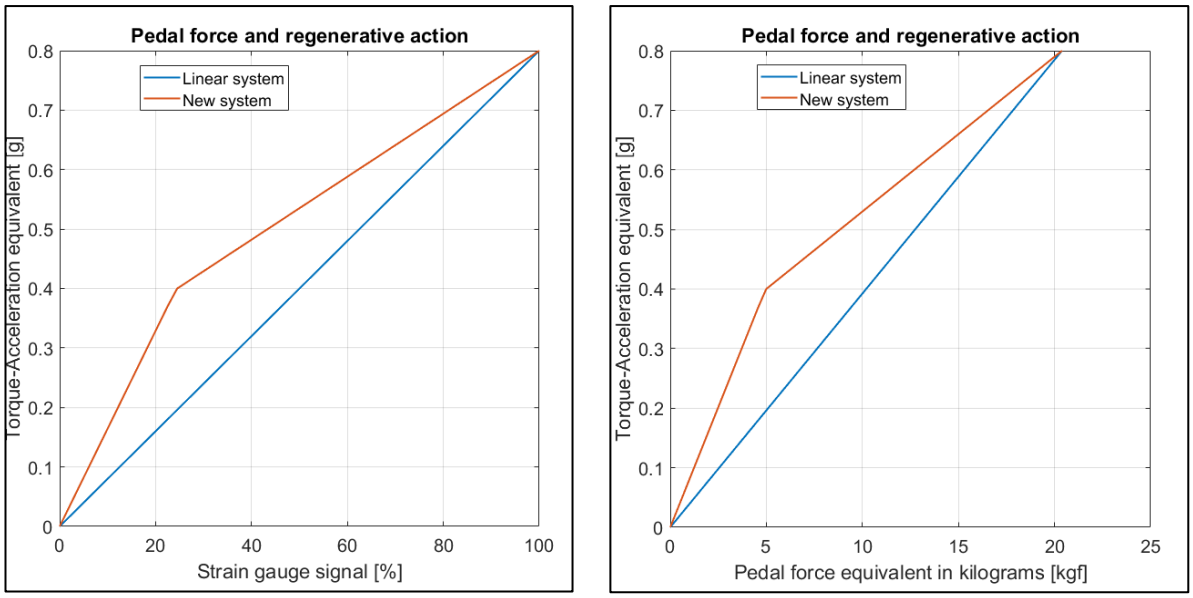

Figure 5.16 Regenerative action depending on strain gauge signal (left) and pedal force (right)

5.5 Parallel system design

From all the consideration done in previous sections, the new parallel braking system will be the one represented in Figure 5.17. Here the total system line, in blue, has three variations; the solid line represents the accelerator pedal strategy with regenerative braking up to 0.4 g then hitting the maximum value and staying constant and the dashed line is representing the system with regenerative braking up to 0.6 g. The repartition for the regenerative is different from friction line. In fact, it has been chosen to follow a 0.65 repartition to front wheels that helps to be closer to the ideal line exploiting better performances. The last variation is the line following 0.8g strategy that instead will follow the same repartition of the friction line (70:30) to be safer for higher accelerations and high speed. 0.8g system will be superimposed on the friction line, meaning following the same force build-up. In Figure 5.18 and 5.19 is represented the division between regenerative and brake line for each strategy.

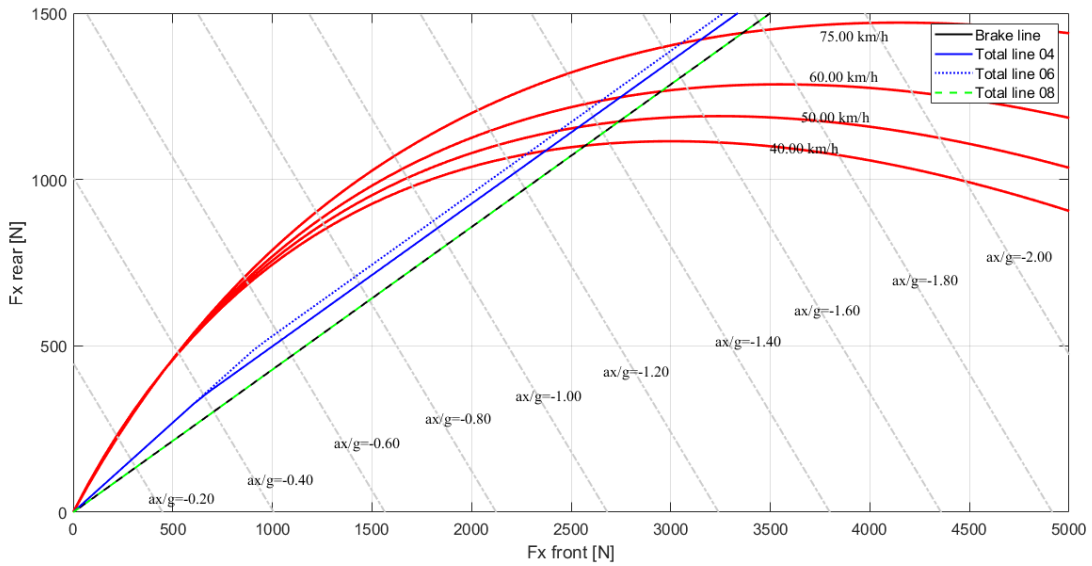

Figure 5.17 Parallel system design for different levels of regenerative actions

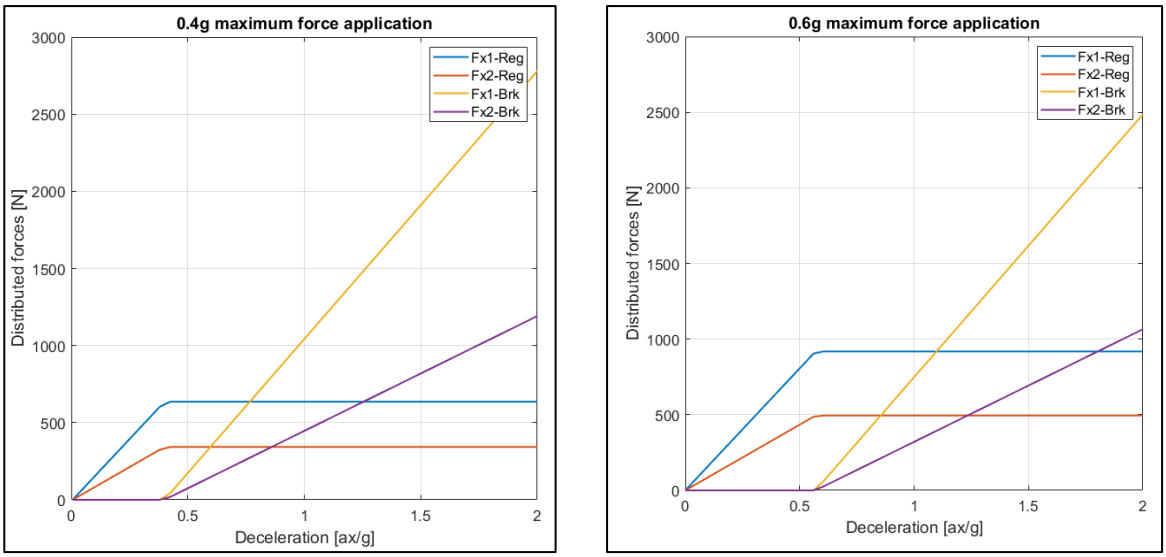

Figure 5.18 Force division between regenerative and friction braking for 0.4g (left) and 0.6g (right) strategy

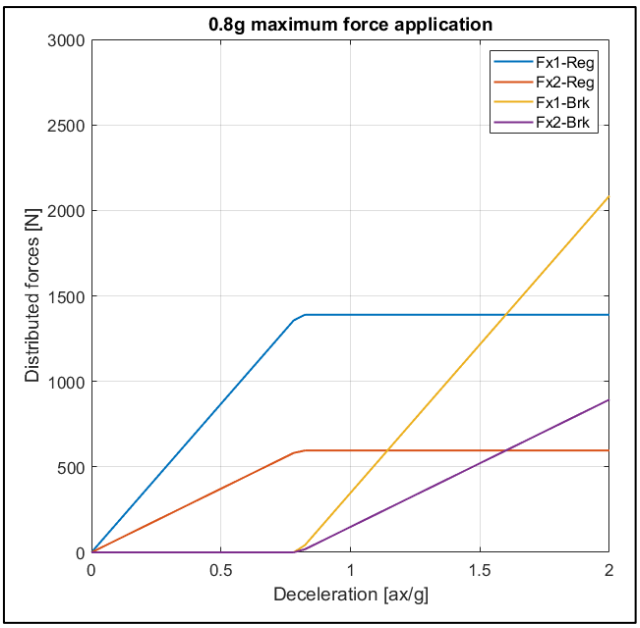

Figure 5.19 Force division between regenerative and friction braking for 0.8g strategy

5.5.1 Regenerative forces and speed

Another point into the analysis is that a constant and less changing braking behaviour is needed for performance vehicles like SC19 since accelerations and speed are greater than a road vehicle and the conditions are closer to limits of the ground and vehicle capability, this has been translated as leaving constant maximum regenerative forces. For this last point it is possible to consider the aerodynamic effect on braking torque because the acceleration experienced with same forces on the ground will change with speed. This effect makes the torque needed to brake the vehicle become higher for higher speeds because of drag and lift, like represented in Figure 5.20.

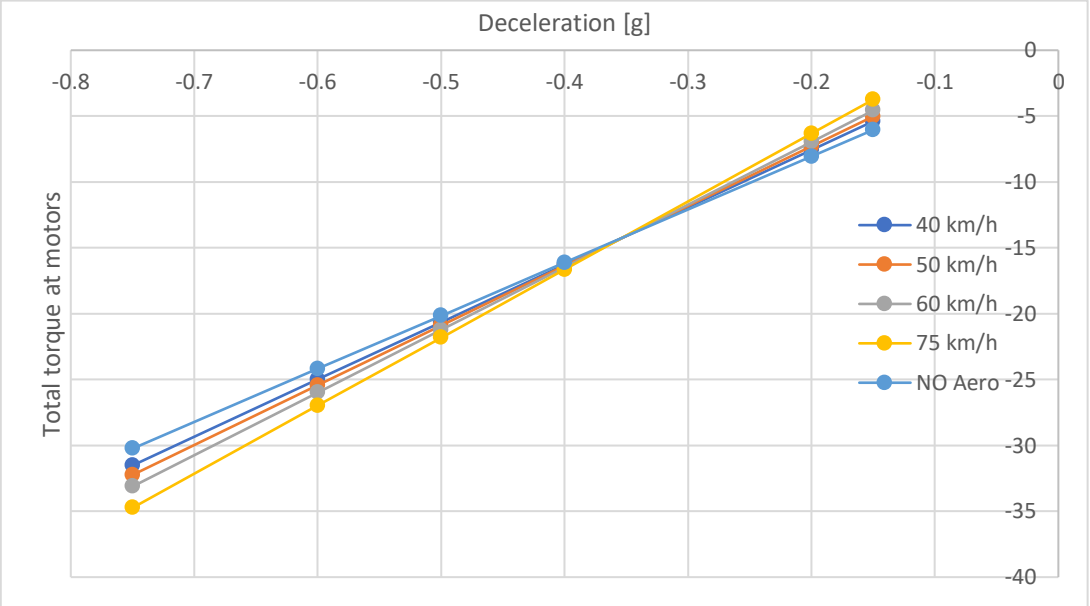

Figure 5.20 Torque correction based on vehicle speed

This will be useful when the control algorithm will be implemented because it will be possible to adjust the response of the vehicle to obtain the same performance and could be addressed by a simple look-up table depending on the speed and the strategy used as in Figure 5.21.

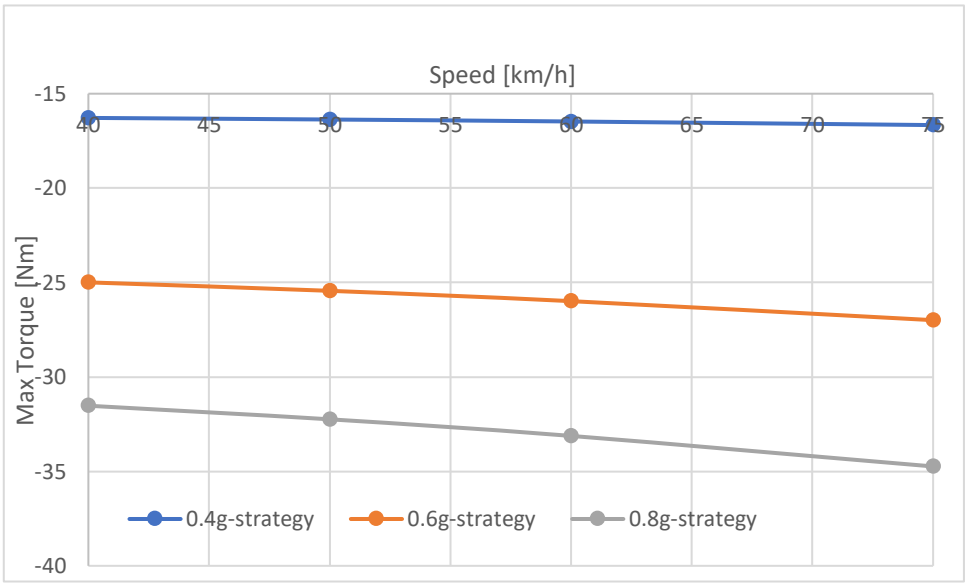

Figure 5.21 Look-up table for torque correction based on the speed and the strategy to follow

5.6 Results from the simulator

Changing the level of regenerative is thus possible to change the efficiency of the powertrain in recuperating the energy but it will also affect the performance of the vehicle and the still important feelings to the driver. In this paragraph the analysis concerning the different levels of regenerative braking will be performed but a comparison to real data and driver feelings will be still needed for the final choice.

The results will be presented following the theoretical studies and strategies explained in previous paragraph and by means of the simulator presented in Chapter 3 that has been modified with data of the SC19, here listed:

- Different parameters for braking line. This is because Squadra Corse vehicle uses custom made and self-designed components using different friction lines from urban vehicles.
- New Torque vs rpm characteristic and efficiencies for motors. Motor characteristics are listed in Table 5.2 and the new efficiency table is coming from datasheets provided by the manufacturing company. (Figure 5.22)
- New final ratio for the transmission and wheel radius. Final gear ratio designed to optimize performances for the motors in all competition events
- Power limits and level of SoC based on different battery cells and pack configuration relative to the Sony cell presented in Table 5.3
- New powertrain type with 4 in-wheel motors

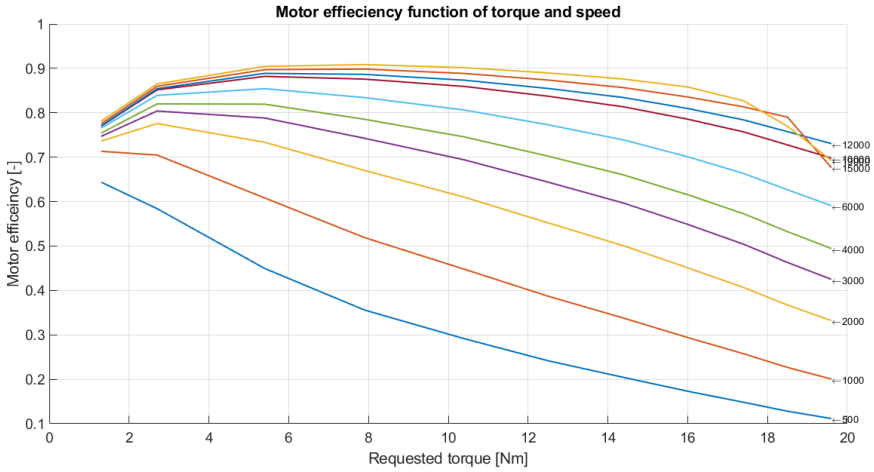

Figure 5.22 Motor efficiency function of torque (x axis) and rpm (different lines)

5.6.1 Drive cycle for FSAE event endurance

The drive cycle that is used in this case is the one represented by the acquired data coming from season 2019 endurance race held in Spain and represented in Figure 5.23 and 5.24. All signals coming from race events are far from straight line acceleration/braking dynamics so an analysis on the simulator, will carry some errors but it will also give a very good estimation on the factor influencing the regeneration of energy and help to understand the impact of the strategies used.

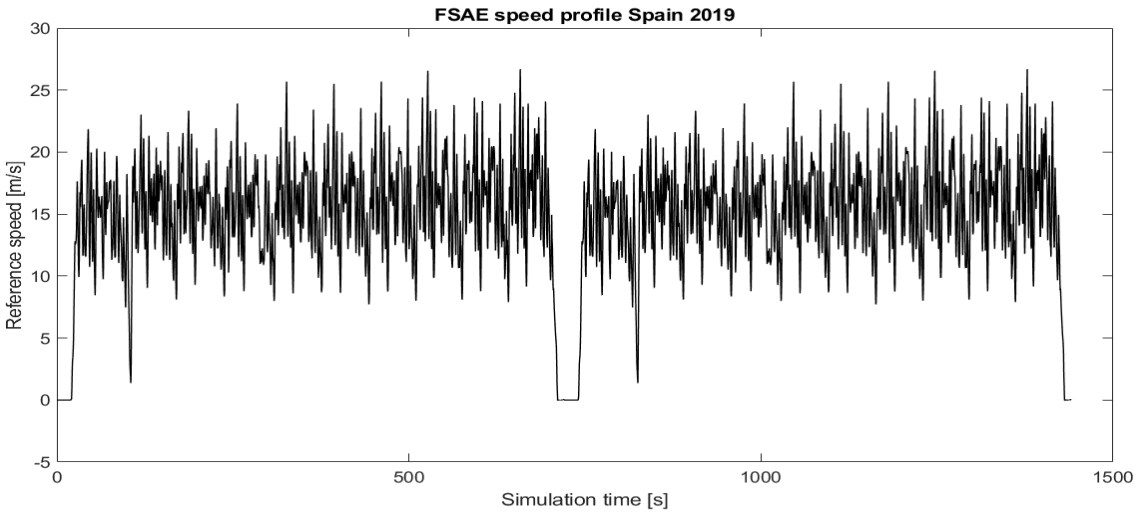

Figure 5.23 FSAE-endurance speed profile

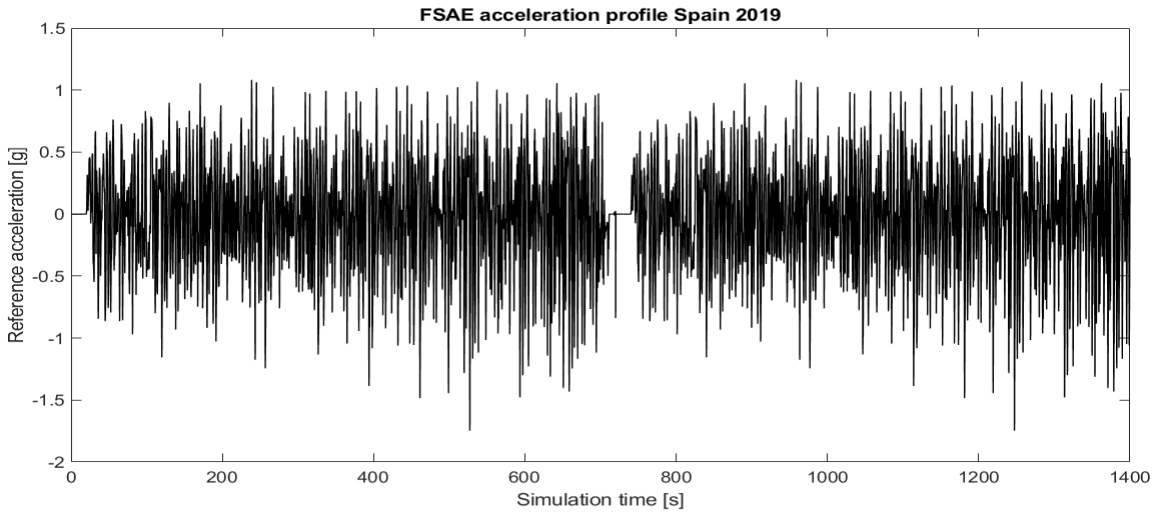

Figure 5.24 FSAE-endurance acceleration profile

5.6.2 Accelerator strategy effect

By the analysis of the results on the simulator, the effect of the implementation of the regenerative braking on the accelerator is presented. The strategy applies a maximum of 16 Nm as base torque as explained in Section 5.3.1 and eventually applies changes according to the speed of Figure 5.17. Figure 5.25 shows the effect on the run, and it is possible to see that by regenerating only on the accelerator it is possible to achieve and efficiency in braking as high as 40%. This is quantified by a total of 0.95 kWh of regenerated energy over an expresses braking energy of 2.37 kWh presented respectively as the full line and the dashed line in Figure 15.26.

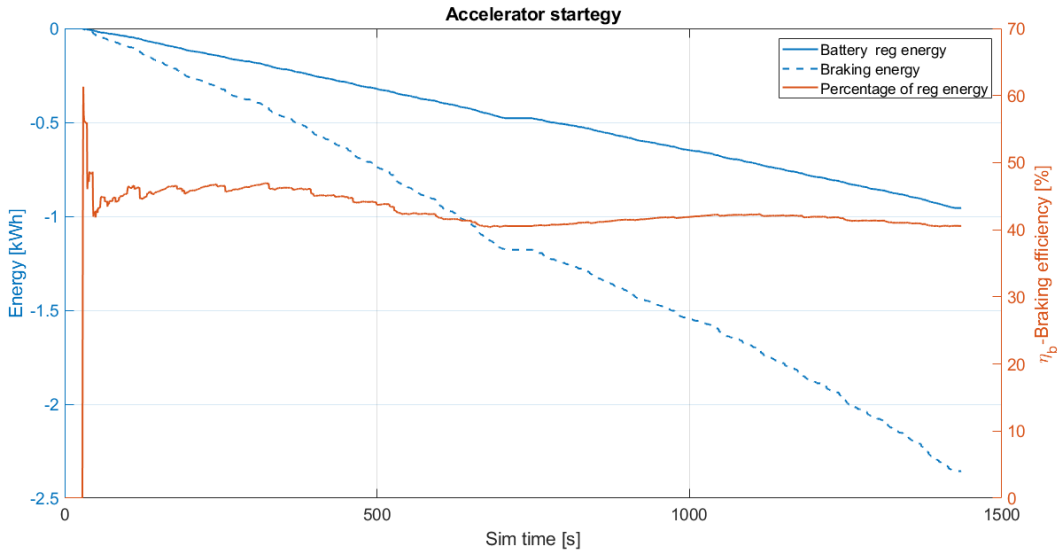

Figure 5.25 Accelerator strategy results-Braking efficiency

If the percentage of regenerated energy is taken into account as the amount of regenerated energy over the expended energy by the battery pack, this strategy can already achieve good values as high as 23 % (Figure 5.26).

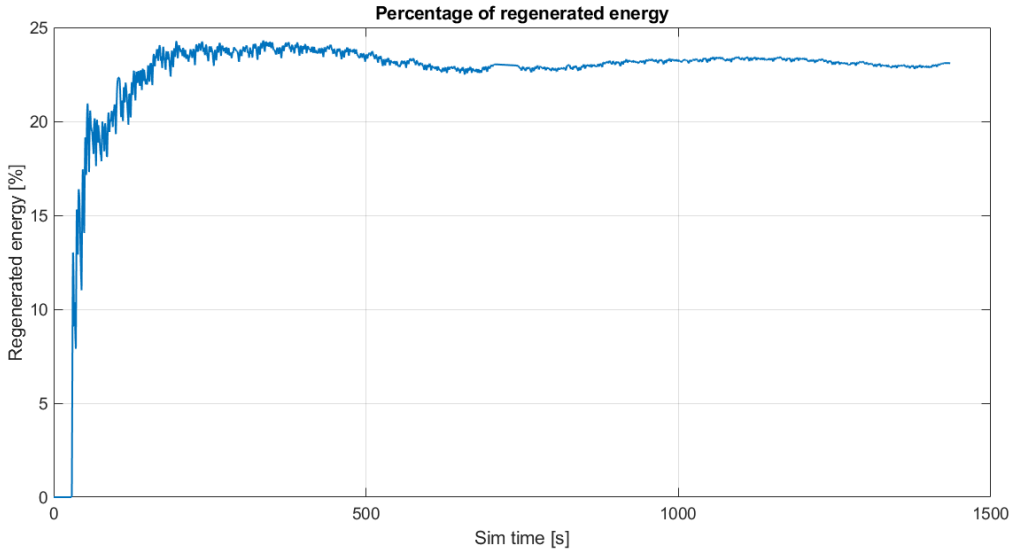

Figure 5.26 Accelerator strategy results-Regenerated energy percentage

5.6.3 Brake strategy effect

5.6.3.1 Effect of 0.6g strategy

The effect of the strategy named as 0.6g and represented in dotted, blue line in 5.17 is here presented. This strategy sets the maximum of 24 Nm of braking torque, distributed 65:35 to the front (the distribution of forces is represented in Figure 5.18 on the right plot). The braking efficiency, reported in Figure 5.27 reaches 50% and the percentage of regenerated energy reaches 30% with 1.19 kWh regenerated energy in braking.

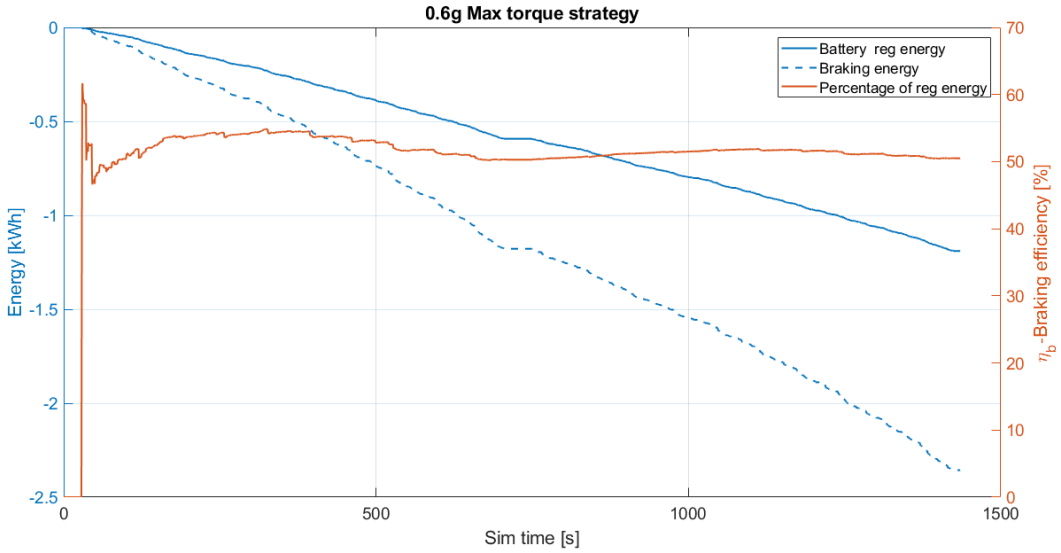

Figure 5.27 06g-Regenerative strategy results-Braking efficiency

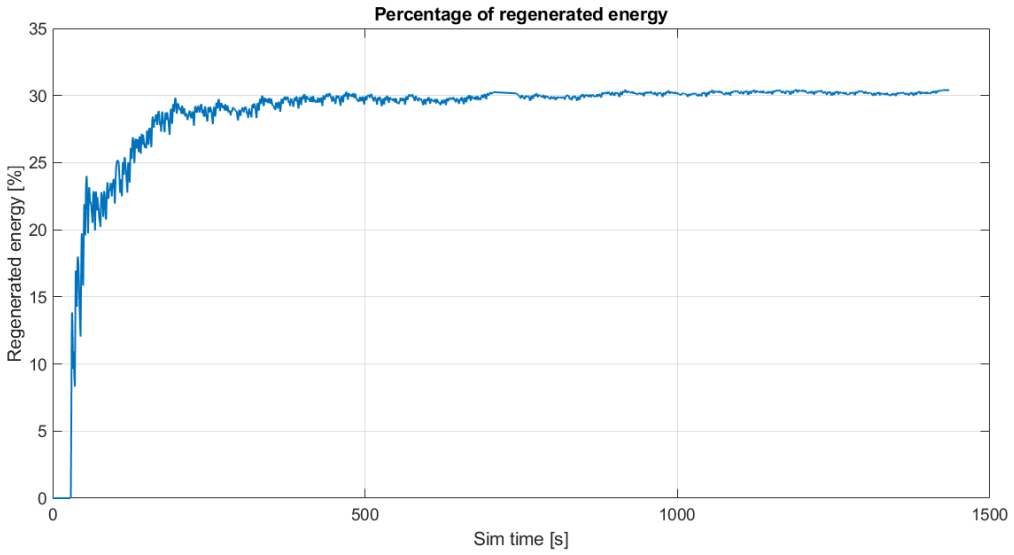

Figure 5.28 06g- Regenerative strategy results-Regenerated energy percentage

5.6.3.2 *Effect of 0.8g strategy*

The effect of the 0.8g strategy acting on the brake is reported in Figure 5.29 and 5.30 where the regenerative braking can apply 31 Nm as maximum and corresponding to the force that would be needed to brake the vehicle at 0.8g. The torque would be divided 70:30 to front as already represented in Figure 5.17. In this case it is possible to reach braking efficiency close to 58% (see Figure 5.29) since the braking torque developed by motors covers a greater extent of the needed force to brake; an improvement that is very important with respect to 18% coming from the regeneration on the accelerator pedal and 8% respect to 0.6 strategy.

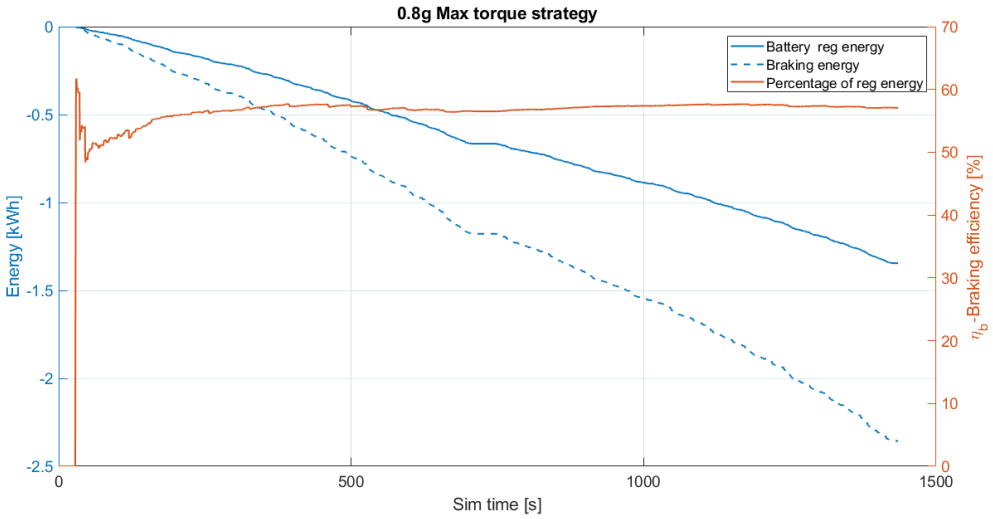

Figure 5.29 08g-Regenerative strategy results-Braking efficiency

The improvement on the braking efficiency is also supported by the improvement of the percentage of regenerated energy that is reaching 35% (Figure 5.30) when the simulation ends. By analysing the details of the used energy from the pack and the energy needed for braking that is also the ratio between the two presented quantities of braking efficiency and percentage of braking energy as in Formula (5.1) is possible to see that the overall efficiency of the powertrain is 65%. This last value seems to be realistic but could be too high for the vehicle that is considered in this study.

$$\frac{\xi_{reg}}{\eta_b} = \frac{\frac{Regenerated\ energy(E_b)}{Total\ used\ energy(E_{tot})}}{\frac{Regenerated\ energy(E_b)}{Total\ braking\ energy(E_k)}} = \frac{Total\ braking\ energy(E_k)}{Total\ used\ energy(E_{tot})} \tag{5.1}$$

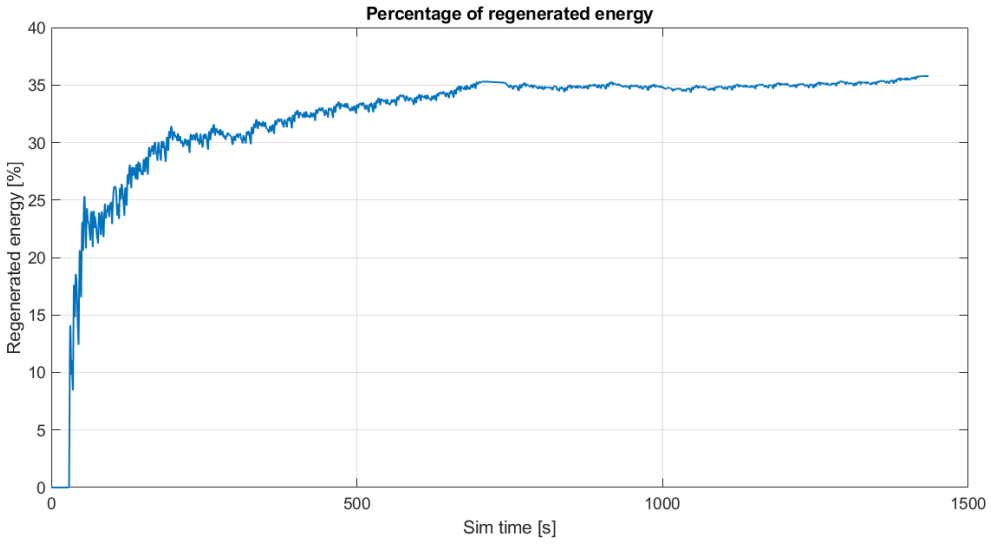

Figure 5.30 08g-Regenerative strategy results-Regenerated energy percentage

5.6.4 Comparison with real data

The obtained results are very good and should be compared to real data coming from the vehicle and drive cycle considered. 35% saving would allow the battery pack energy to pass from the available 5.2 kWh to 7 kWh. Logged data during the race have been analysed and the regenerated percentage has been shown in Figure 5.31.

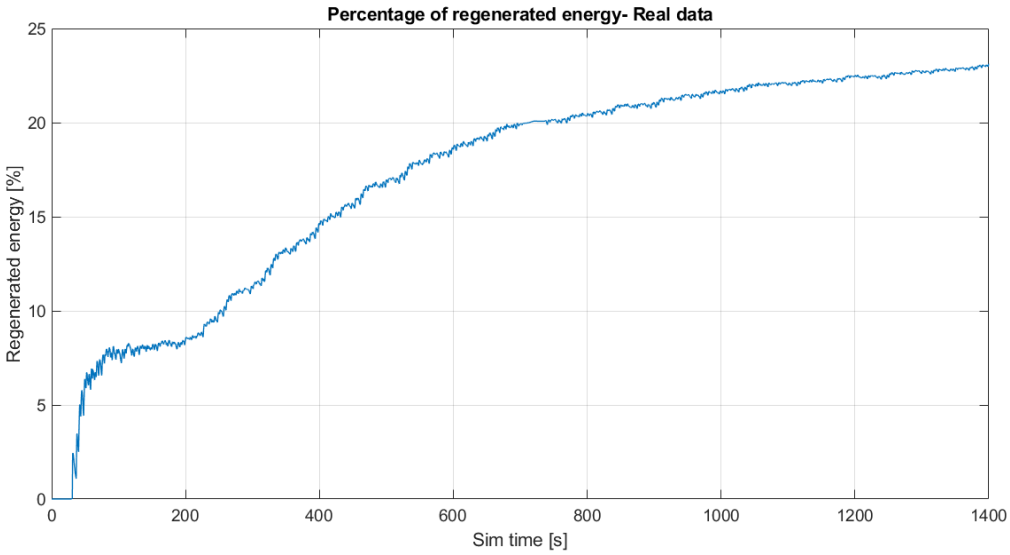

Figure 5.31 Regenerative strategy real data-Regenerated energy percentage

The final values reach 23% but the gap between real and simulated values can be attributed to the following reasons:

- Idealized behaviour of the simulator, being not suitable to simulate very demanding and changing scenario like a race vehicle car during a race where high accelerations and cornering along with fast response on the brake/accelerator pedal and fast transient demand to energy storage systems
- Dynamic controls and manually tuned parameters during the race that changed according to experience on test. This last part can be seen in Figure 5.31 where for the time interval between 0 and 200 s the regenerative settings were at minimum for problems on overvoltage on battery pack because limits on the control systems were not enough.
- Different condition for the battery pack and most importantly on temperature that change the system behaviour and that are not considered inside the used simulator.

Another difference is explained by means of Figure 5.32 where is presented the comparison between the simulator and real data braking forces calculated at wheels. The first observation that can be done is that the distribution between regenerative and friction brake forces is different; this is mainly due to the control system inside the vehicle being much more complicated than the one inside the simulator and being a dynamic situation, it could be less effective to reach the target. This is also demonstrated by the ripple observable in Figure 5.32 inside the red circles and by the fact that the effective torque reached by the vehicle is lower than the target. This last effect is due to the way the target is set. Inside the real system, the target is a fraction on maximum traction torque and thus is varying. Inside the simulated values, braking torque is set separately according to the studied values and only changing following the LUT in Figure 5.18.

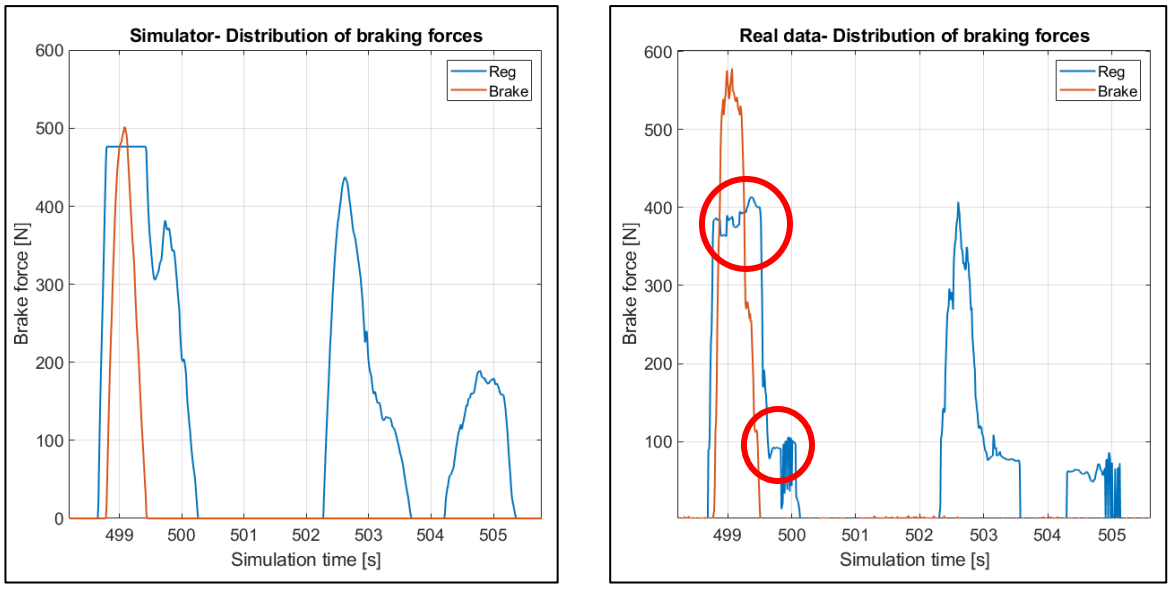

Figure 5.32 Brake force distribution for simulated data (left) and real data (right)

These simulations suggest us that even without a quantitative value, it is clear that there is a good margin for improvement. One improvement could come from driver action on brakes. Figure 5.33 shows the comparison between the real system braking forces as logged from the vehicle and the actuation on the simulator. The simulator is acting as ideal pilot, perfectly dosing the brakes, and actuating in the right position according to the needs; this gives possibility to release brakes in different way and give priority to regenerative. The simulator can decrease more smoothly the pressure where the driver released the brake pedal to leave only the effect of the accelerator as can be seen also in Figure 5.32, on the right, around 500s where the braking force is lower. This behaviour is also part of the greater effect on regenerative on the simulator and the main reason for the analysis on accelerator pedal and increase of virtual sensibility on the brakes to dose regenerative.

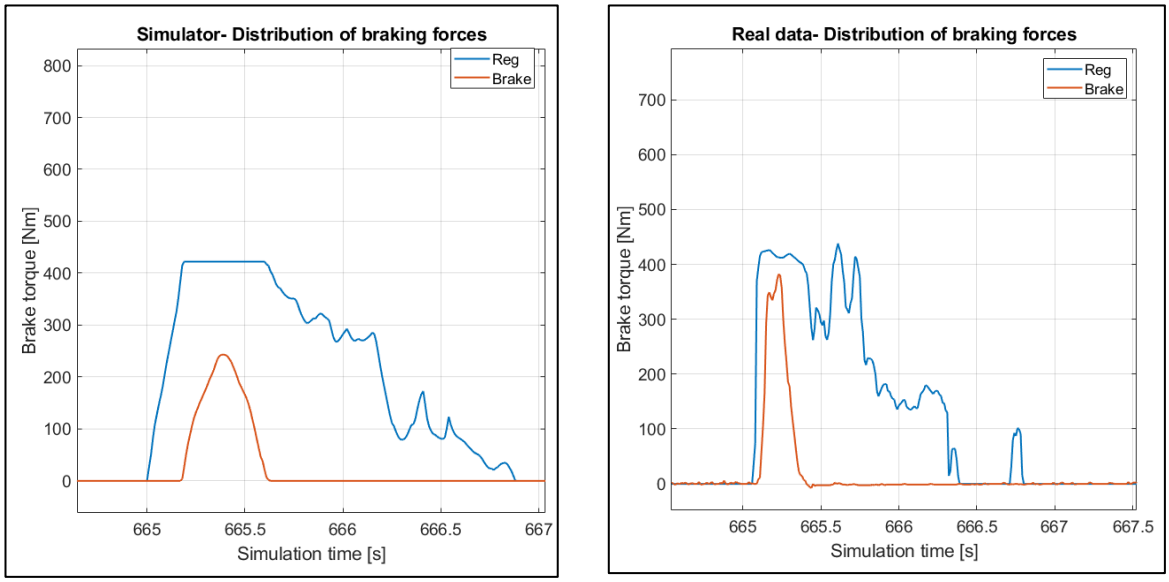

Figure 5.33 Regenerative action comparison for simulated data (left) and real data (right)

5.7 Conclusions

The study done on speed distribution and decelerations has been performed to detect most frequent speed and acceleration ranges in braking during a FSAE event in order to set the strategy and blending between regenerative and friction braking on a race vehicle. The original system had some limits on regenerative sensibility over friction brakes due to design and rule restrictions. A study on the amount of force allocation on accelerator pedal has been done to mitigate the problem. Finally, the effect and weight of the different designed strategies has been analysed and presented in Table 5.5.

Table 5.5 Comparison of obtained results on FSAE vehicle

	Accelerator contribution	**0.6g strategy**	**0.8g strategy**
Percentage of braking energy over traction energy-K_{dc} [%]	48	48	48
Achievable Braking efficiency-η_b [%]	40	50	58
Traveling distance per cycle [km]	22	22	22
Range extension [km]	5.06 km ~ 5 laps	6.6 km ~ 6/7 laps	7.7 km ~ 7/8 laps
Percentage of regenerated energy -ξ_{reg} [%]	23	30	35

From Table 5.5 is possible to say that the accelerator pedal alone improves efficiency of the vehicle to a non-negligible extent that covers the estimation of about 5 laps. 0.6g-strategy on the brakes increases the efficiency to roughly 30%. 0.8g-strategy increases of 5% the percentage of regenerated energy with respect to 0.6g that represents a non-negligible amount, being 1 km(~ 1 lap) a 4.5% of the total race distance (22km). Following on from what just written, the 0.6g strategy gives good results but a 5% increase on regenerated energy due to the use of 0.8g makes this last strategy more appealing and thus the one indicated to be used on the new vehicles. Moreover, allocating all braking manoeuvres up to 0.4g to the accelerator pedal strategy, 0.8g-startegy becomes easier to be used by the driver since the problem with brake sensibility is solved.

Finally, these theoretical values should be tested on the real vehicle and drivers because they behave dramatically different from models and simulators and all strategies would be effective only if the driver will learn to better use the regenerative effect.

References

[1] Genta G., Morello L., *The Automotive Chassis Vol.2*, Springer, 2009

[2] Bosch Professional Automotive Information, *Brakes, Brake Control and Driver Assistance Systems: Function, Regulation and Components*. Konrad Reif, Springer Vieweg, Wiesbaden, Reif, Konrad. (2014). DOI: 10.1007/978-3-658-03978-3.

[3] ECE Regulation. Addendum 12-H: Regulation No. 13-H, Revision 8, October 2014

[4] Pacejka Hans B. *Tire and Vehicle Dynamics, second edition,* Butterworth-Heinemann, 2006

[5] Giuggiani M., *The Science of Vehicle Dynamics*, Springer, 2014

[6] M. M. Kabir, D. E. Demirocak, *Degradation mechanisms in Li-ion batteries: a state-of-the-art review*, Int. J. Energy Res., 2017

[7] Shuai Ma, Modi Jiang, Peng Tao, Chengyi Song, Jianbo Wu, Jun Wang, Tao Deng, Wen Shang, Temperature effect and thermal impact in lithium-ion batteries: A review, Progress in Natural Science: Materials International, 2018

[8] M. Dubarry, C. Truchot, M. Cugnet, B. Y. Liaw, K. Gering, S. Sazhin, D. Jamison, C. Michelbacher, *Evaluation of commercial lithium-ion cells based on composite positive electrode for plug-in hybrid electric vehicle applications*. Part I: Initial characterizations, Journal of Power Sources, 2011

[9] M. Elsied et al., *Efficient Power-Electronic Converters for Electric Vehicle Applications*, IEEE Vehicle Power and Propulsion Conference (VPPC), 2015, pp. 1-6

[10] Institute for Power Electronics and Electrical Drives, RWTH Aachen University, F. Qi, D. Scharfenstein, C. Weiss, *Motor Handbook*, 2019

[11] ECE/TRANS/180/Add.15, *Global technical regulation on Worldwide harmonized Light vehicles Test Procedure,* March 2014

[12] Ehsani M., Gao Y., Longo S., Ebrahimi K., *Modern Electric, Hybrid Electric, and Fuel Cell Vehicles*, Third Edition, CRC Press, 2018

[13] Gao Y., Chen L., and Ehsani M., "Investigation of the Effectiveness of Regenerative Braking for EV and HEV," SAE Technical Paper 1999-01-2910, 1999

[14] Statistical Release – Department for transport, Annual Road Traffic Estimates: Great Britain 2019

[15] Official Journal of the European Communities REGULATION (EC) No 661/2009 OF THE EUROPEAN PARLIAMENT AND OF THE COUNCIL of 13 July 2009

[16] Bosch Engineering GmbH, https://www.bosch-motorsport.com/content/downloads/

[17] The MathWorks, Inc., 1994-2021, https://it.mathworks.com/matlabcentral/

[18] Yuantao Sun *et al*., *Study on the Control Strategy of Regenerative Braking for the HybridElectric Vehicle under Typical Braking Condition*, 2018 IOP Conf. Ser.: Mater. Sci. Eng. 452 032092

[19] Formula SAE International, https://www.fsaeonline.com/

[20] Squadra Corse PoliTO, https://www.squadracorsepolito.com/

[21] Formula student Germany, https://www.formulastudent.de/fsg/rules/, Rules for FSG, Section T6, 2021

[22] Liu, W., Qi, H., Liu, X. *et al. Evaluation of regenerative braking based on single-pedal control for electric vehicles,* Front. Mech. Eng. **15,** 166–179, 2020